1988

High resolution electronic spectroscopy of para-alkyl substituted phenols and tetramethyl cyclobutane-1,3-dione

Kyuseok Song
Iowa State University

Order Number 8825451

High resolution electronic spectroscopy of para-alkyl substituted phenols and tetramethyl cyclobutane-1,3-dione

Song, Kyuseok, Ph.D.

Iowa State University, 1988

U·M·I
300 N. Zeeb Rd.
Ann Arbor, MI 48106

High resolution electronic spectroscopy of para-alkyl substituted phenols and tetramethyl cyclobutane-1,3-dione

by

Kyuseok Song

A Dissertation Submitted to the
Graduate Faculty in Partial Fulfillment of the
Requirements for the Degree of
DOCTOR OF PHILOSOPHY

Department: Chemistry
Major: Physical Chemistry

Approved:

Signature was redacted for privacy.
In Charge of Major Work

Signature was redacted for privacy.
For the Major Department

Signature was redacted for privacy.
For the Graduate College

Iowa State University
Ames, Iowa

1988

TABLE OF CONTENTS

GENERAL INTRODUCTION	1
SECTION I. ELECTRONIC STRUCTURE OF PARA-ALKYL SUBSTITUTED PHENOLS IN A SUPERSONIC JET	6
ABSTRACT	7
INTRODUCTION	8
PRINCIPLES OF SUPERSONIC EXPANSION	12
EXPERIMENTAL SECTION	16
RESULTS	21
DISCUSSIONS	93
CONCLUSION	124
REFERENCES	126
SECTION II. SINGLE CRYSTAL FLUORESCENCE AND POLARIZED ABSORPTION STUDIES OF THE $S_1(^1A_u) \leftrightarrow S_0(^1A_g)$ TRANSITIONS OF 2,2,4,4-TETRAMETHYL CYCLOBUTANE-1,3-DIONE AT 4.2 K	130
ABSTRACT	131
INTRODUCTION	132
CRYSTAL STRUCTURE OF TMCBD	144
EXPERIMENTAL SECTION	145
RESULTS	150
DISCUSSIONS	170
CONCLUSION	192
REFERENCES	195
SUMMRY AND CONCLUSION	198
REFERENCES FOR GENERAL INTRODUCTION	201
ACKNOWLEDGEMENT	203
APPENDIX	204

GENERAL INTRODUCTION

Electronic spectroscopy has been used as a general technique to investigate the ground and excited state vibrational structures of polyatomic molecules. Information about the excited state vibrational structure can be obtained from absorption spectra, whereas, fluorescence emission spectra reveal the structure of the ground state. In general, however, absorption spectra are very complicated due to spectral congestion arising from hot and sequence bands. Spectral congestion prevents a clear understanding of the excited state vibrational structure, and therefore, several methods have been developed to avoid, or at least minimize, spectral congestion. Among these methods, two will be presented in this dissertation. The first is laser induced fluorescence (LIF) in a supersonic jet, and the second is low temperature polarized single crystal absorption and fluorescence spectroscopy.

Supersonic jet spectroscopy has been regarded as an ideal technique for the investigation of the electronic and vibrational structure of polyatomic molecules in the gas phase for the past several years. This arises from the fact that a supersonic jet provides an ideal spectroscopic medium, i.e., isolated molecules, vibrationally and rotationally cold molecules, and a medium free of any matrix or collisional perturbations (1). The supersonic expansion was first proposed in 1951 by Kantrowitz and Grey (2) and demonstrated by Kiastakowsky and Slichter (3). Their results demonstrated that the intensity of the molecular beam can be increased by ~2 orders of

magnitude in the supersonic expansion compared to the effusive nozzle beam and that the population of the lower energy rotational levels can be increased at the expense of higher levels.

In 1974, Smalley et al. (4) published the laser induced fluorescence spectra of NO_2 in a supersonic jet for the first time. They were able to demonstrate the dramatic cooling effect of a nozzle expansion. Since then, many researchers have used supersonic jets and hundreds of papers have been published. The supersonic jet technique has opened new fields of spectroscopy. For example, a supersonic jet has been used to study van der Waals complexes (5,6), since the supersonic expansion can provide desirable complexes in the gas phase by adjusting experimental conditions. The supersonic nozzle beam has also provided a high resolution tool for the study of biologically important molecules (7-10).

The supersonic jet technique has been coupled mainly to laser induced fluorescence (LIF) (11-13) and to multiphoton ionization spectroscopy (MPI) (14-16). The combination of these spectroscopic techniques with the supersonic nozzle expansion provides two of the most popular techniques in gas phase electronic spectroscopy. However, these techniques coupled with the supersonic jet demand several requirements, not all of which are amenable to supersonic jet experiments. First, a reasonable sample vapor pressure is required to apply these techniques (MPI and LIF) in a supersonic jet. Reasonable sample vapor pressure can be achieved by heating, however, thermally unstable and nonvolatile molecules cannot be vaporized by heating methods. Furthermore, in most pulsed valve experimental setups, samples cannot be heated to high

temperatures due to limited valve operation temperatures. For example, the valve used for this work could not be used above 100 °C. The recently developed laser desorption technique (17,18), in which a laser is used to vaporize samples, can be applied in these cases. Laser desorption has been a very successful technique for the vaporization of thermally unstable or nonvolatile molecules in mass spectroscopy. However, this technique needs improvement to minimize sample fragmentation, if it is to be used generally.

Second, a reasonable fluorescence quantum yield is needed for the molecules to be investigated if LIF is to be used. For some molecules which have very low fluorescence quantum yields and have low ionization potentials, MPI can be used to detect ions instead of fluorescence. However, some molecules, such as 2,2,4,4-tetramethyl cyclobutane-1,3-dione (TMCBD) which will be discussed later, have a reasonable vapor pressure, but possess a very low fluorescence quantum yield (lower than 10^{-3}) and a high ionization potential (8.8 eV = 70974 cm^{-1}) (19). These molecules do not lend themselves to any of the above mentioned techniques. Although 8.8 eV is not a particularly high ionization potential, the energy gap between the ground state (S_0) and the first excited singlet state (S_1) is ~ 27000 cm^{-1}, and therefore, at least three photons are required to ionize this molecule when using resonance excitation of the first excited singlet state. Originally, the study of TMCBD was intended to proceed through the use of LIF or MPI in a supersonic jet. However, no useful results have been obtained for TMCBD in the jet experiment due to the reasons mentioned above.

This manuscript is composed of two sections which represent two separate papers. In Section I, the study of para-alkyl substituted phenols (p-cresol, p-ethylphenol, p-isopropylphenol, p-sec-butylphenol, p-propylphenol, p-tert-butylphenol, p-pentylphenol) by LIF in a supersonic jet is discussed. The p-alkyl substituted phenols are analogous to tyrosine which is one of the near ultraviolet fluorescence chromophores in proteins. There have been many studies dealing with tyrosine and its derivatives due to the biological and photophysically interesting aspects of these molecules. However, since almost all studies have been performed in solution, many details about the energy structure of tyrosine and its derivatives have not been obtained due to spectral congestion. As an initial step towards the study of amino acids, p-alkyl substituted phenols, which have been rarely studied, were studied by observing the fluorescence excitation and dispersed fluorescence spectra. Several molecules presented here show transitions from different isomers upon excitation. These isomers can be understood by assuming the rotation of alkyl substituents.

In Section II, the vibronic structures of TMCBD are discussed. TMCBD, which has two carbonyl groups, and therefore, four possible $n\pi^*$ transitions, has been studied by several groups because of spectroscopic and photochemically interesting aspects of this compound (20,21). Among the studies performed by various workers on TMCBD, two studies were done by single crystal absorption spectroscopy. There are discrepancies between these two studies concerning the interpretation of the vibrational structures of TMCBD. As a first step in the study of TMCBD, the gas phase absorption spectrum and xy- and z-polarized low

temperature single crystal absorption spectra in the (001) crystal face were obtained. The observed polarized single crystal absorption spectra yielded more detail about the vibronic origins and the progression forming mechanism than the previously mentioned studies (20,21). Gas phase experiments performed by this researcher in a supersonic jet were not as fruitful as the single crystal absorption studies due to the reasons mentioned previously. Therefore, more studies were done on other crystal faces of TMCBD with different polarizations and the single crystal fluorescence spectrum was obtained, for the first time, at low temperature (4.2 K). These studies revealed more vibronic origins than previously observed and more detail concerning vibronic coupling in the ground state as well as the excited state. Therefore, conflicting interpretations between two previous studies on TMCBD have been resolved through this work.

SECTION I. ELECTRONIC STRUCTURE OF PARA-ALKYL SUBSTITUTED PHENOLS IN A SUPERSONIC JET

ABSTRACT

Fluorescence excitation spectra and dispersed fluorescence spectra are measured for the $S_1 \leftarrow S_0$ transition of a series of the para-alkyl substituted phenols cooled in a supersonic jet. The series consists of p-cresol, p-ethylphenol, p-propylphenol, p-isopropylphenol, p-sec-butylphenol, p-tert-butylphenol, p-pentylphenol. The p-cresol and p-ethylphenol show a single origin band in the excitation spectra and no isomers can be seen. The p-isopropylphenol, p-sec-butylphenol and p-tert-butylphenol show two origin bands in the excitation spectra and the doublets are assigned as origin bands of different isomers (cis- and trans-isomer). The p-propylphenol and p-pentylphenol show multiple origin bands (more than two) which are assigned as origin bands of several conformers. The energy separations among origin bands of isomers range from 13 cm^{-1} for p-sec-butylphenol to 82 cm^{-1} for p-pentylphenol. For p-propylphenol, the energy separations range from 9 cm^{-1} to 58 cm^{-1} among five origin bands of the isomers. The conformations of isomers for all molecules studied here are understood by assuming the rotation of alkyl substituents. For all molecules studied, hydrogen bonded structures with water are observed at ~ 350 cm^{-1} lower in energy from the electronic origin bands of the monomer.

INTRODUCTION

The electronic spectroscopy and photophysics of amino acids and their derivatives has been the subject of numerous investigations due to the photobiological and photophysically interesting properties of these molecules (1-7). Proteins contain three amino acid residues which may contribute to their near ultraviolet absorption and fluorescence (tyrosine, tryptophan and phenylalanine). Since tryptophan is believed to be most responsible for the absorption and fluorescence of the near ultraviolet radiation by proteins, many investigations have been performed to understand why the fluorescence of tyrosine has such a small contribution to the overall fluorescence of proteins. It has been suggested, by many authors, that the main reason for the weak fluorescence of tyrosine, in proteins, is due to energy transfer from tyrosine to tryptophan residues or self quenching of tyrosine by a variety of pathways (2,3). Because the fluorescence quantum yield of phenylalanine is low (~ 0.04 in water) relative to that of tyrosine and tryptophan, significant phenylalanine emission is not observed in proteins containing tryptophan and/or tyrosine. Therefore, interest in the fluorescence of phenylalanine has lagged behind that of the other aromatic amino acids (1,2).

So far, most research has been performed in solution where the spectra may be complicated by solvent interactions. If the electronic states of tyrosine and its derivatives are observed under isolated molecule conditions, the effects of solvents can be understood by adding solvents to the tyrosine and its derivatives. An isolated molecular

condition can be achieved in a supersonic jet expansion (8,9). To understand the electronic energy structures of tyrosine, the study of its model molecules, i.e., phenol and p-substituted phenols, is required first.

Phenol and the substituted phenols have been previously investigated by many research groups (10-15). Fluorescence excitation spectra, dispersed fluorescence spectra and multiphoton ionization spectra of phenol and hydrogen-bonded phenols have been measured in a supersonic jet expansion (16-20). Although there has been considerable research on substituted phenols, there has not been corresponding amount of research performed on the p-alkyl substituted phenols compared to the ortho- and meta-derivatives. The absorption spectra of p-ethylphenol was studied by Methrotra (21) and Shashidhar and Rao (22) at room temperature in the gas phase, and some vibrational band assignments were made. P-cresol has been studied by Tembreull and coworkers (23) by two photon ionization in a supersonic jet and vibronic band assignments were made for the excited state based on the vibrational modes of the benzene ring.

Meanwhile, there have been several studies on the isomer structures of substituted benzenes. Hopkins et al. (25) have studied a series of alkyl substituted benzenes in a supersonic jet and have shown the existence of isomers when alkyl substituents have carbon chains greater than two (e.g., n-propylbenzene, n-butylbenzene etc.). They explained these isomers as trans- or gauche- (or eclipsed) isomers due to interactions between the π electrons of the benzene ring and the hydrogen of the alkyl substituents. The energy separation between the

origin bands of the two isomers ranged from 49 cm^{-1} for n-propylbenzene to 67 cm^{-1} for n-hexylbenzene. Breen et al. (26-28) have also reported the observation of isomer structures for di-substituted benzenes. For p-propyltoluene, they observed two intense origin features using time-of-flight mass spectroscopy (TOFMS) and these bands were assigned as origin bands of anti- and gauche- conformers. The energy separation between these two origin bands was reported as 49 cm^{-1} which is similar to that of n-propylbenzene. They also observed only one origin band for p-ethyltoluene. Okuyama et al. and Ito and coworkers have studied several m-substituted phenols, β-naphthol and p-dimethoxy benzene and observed isomer structures in supersonic jet experiments (29-31). In the study of p-dimethoxy benzene, they observed via multiphoton ionization in a supersonic jet two bands which were assigned as origin bands of cis- and trans- isomers depending on the symmetry of the molecules (C_{2v} for cis-isomer and C_{2h} for trans-isomer). Although there have been several reports of isomers of other phenol derivatives, no studies have been done on isomers of para-alkyl substituted phenols. This lack of information about the excited state or ground state of p-substituted phenols and their isomer structures motivated us to study the p-alkyl substituted phenols.

It is well established that electronic spectroscopy is a powerful tool for the resolution of rotational isomers (32,33). It is also known that the supersonic jet technique can eliminate hot bands and sequence bands observed in room temperature absorption and emission spectra by cooling the vibrational and rotational temperature of the molecules to very low temperatures (8,9). Here we present fluorescence excitation

spectra and dispersed fluorescence spectra of p-alkyl substituted phenols (p-cresol, p-ethylphenol, p-propylphenol, p-isopropylphenol, p-sec-butylphenol, p-tert-butylphenol, and p-pentylphenol) for the $S_1 \leftarrow S_0$ transition in a supersonic jet. The origin band structures of these molecules observed in their fluorescence excitation spectra are different from those of p-propyltoluene and p-propylbenzene. These differences will be discussed in relation to the relative position of hydroxyl and alkyl substituents. The assignments of vibrational bands are made based on the vibrational modes of the benzene ring.

PRINCIPLES OF SUPERSONIC EXPANSION

The principles of supersonic jet expansion have been thoroughly reviewed in several articles during the past several years (34-37). Therefore, only a brief description and explanation of the supersonic expansion will be given here.

When a pure gas with an initial temperature T_0 and initial pressure P_0 in the reservoir is expanded through a nozzle, the velocity distribution of the expanded gas depends on the size of the nozzle. If the size of the nozzle is smaller than the mean free path of the expanded molecules, the molecular beam is called an effusive beam. In the effusive beam, the velocity distribution of the expanded gas resembles the Maxwell-Boltzman velocity distribution and the distribution has a peak at $V = \sqrt{(3kT/m)}$. Therefore, the potential of the internal energy states (rotational, vibrational) will be the same as in the reservoir and the velocity distribution is characteristic of the reservoir.

However, if the size of the nozzle is bigger than the mean free path of the molecules to be expanded, collisions can occur during the expansion inside the nozzle and also in the downstream region of the expansion. These collisions cause a narrowing of the velocity distribution of the expanded gas, and therefore, cause cooling to a temperature which corresponds to the narrowed velocity distribution. Among pure gases, helium is regarded as an ideal gas for this cooling in a supersonic expansion. When a polyatomic molecule is present as an impurity in the supersonic expansion of helium, the collisions in the

early part of the expansion will accelerate the polyatomic molecules to roughly the same speed as the flowing helium. Then subsequent collisions begin to cool the internal molecular degrees of freedom.

In the supersonic expansion of a monatomic gas, the translational temperature decreases to a few degrees millikelvin according to the following equation

$$(T/T_0) = (P/P_0)^{(\gamma-1)/\gamma} = [1 + (\gamma-1)M^2/2]^{-1}$$

where, T : Temperature of molecules after expansion

T_0: Temperature of the sample chamber

P_0: Pressure of the sample chamber

P : Pressure of the expansion chamber

γ : C_p/C_v=5/3 for monatomic gas

M : Mach number

and

$$M = A(X/D)^{(\gamma-1)}$$

where A : Constant that depends on γ and equals to 3.26 for a monatomic gas

X : Distance downstream from orifice

D : Diameter of nozzle

assuming the expansion is isentropic.

When M>1, the expansion is called supersonic. The assumption that the expansion is isentropic is valid, at least for the initial part of the expansion. The isentropic state implies that there is an equilibrium

between the translational and the internal degrees of freedom. The low translational temperature transfers to the other degrees of freedom (rotational, vibrational) by binary collisions. In usual experimental conditions, the translational temperature can be decreased to lower than 1 K, the rotational temperature to ~few degrees K, and the vibrational temperature to ~ 30 - 50 K for a polyatomic gas.

The practical limit to the cooling of a supersonic expansion is the requirement of a large pumping capacity to handle the gas discharge through the nozzle. The earliest attempt to realize the Kantrowitz-Grey type of expansion utilized systems originally designed for an effusive source by replacing the oven with a skimmed nozzle source. This type of system, which is called a Fenn type expansion, requires very low-background pressure, i.e., large pumping capacity and usually consists of at least two large vacuum chambers. In this type of expansion, the nozzle output is usually skimmed relatively close to the nozzle (36). There are two ways to increase the performance of the system while minimizing the pumping requirement. The first method is pumping at relatively high pressure, as reported by Campargue (35). In Campargue's method, the pressure of the expansion chamber is much higher (10^{-1} to 1 torr) than the Fenn type nozzle (36). At this high pressure, the jet is inside the shock wave and this shock wave is thick enough to prevent penetration to the core of the jet by the warm background. The effect of this shock wave is to develop a region around the beam protected from intrusion by warm background gas in the vacuum pump. The components of the shock wave are referred to as the barrel shock which extends outward from the orifice to the Mach disc, which is a circular shaped area

perpendicular to the flow direction (36). All spectroscopic measurement must be done inside the shock wave which is called the 'zone of silence' by Campargue. A second method to overcome the large pumping requirement is to use a pulsed valve instead of a continuous valve. By using a pulsed valve and by synchronizing the valve operation with the excitation laser pulse, the valve only needs to be open for a short period of time. Therefore, it will substantially decrease the pumping requirement. The pulsed valve can give better cooling compared to the continuous nozzle, since the pulsed valve can use a bigger diameter nozzle compared to the continuous valve without increasing the pumping requirement to any great extent.

In our present system, the pulsed valve (Quanta-ray Model PSV-2) is operated at a repetition rate of 10 Hz and is synchronized with the excitation source (Quanta-Ray model DCR-1 Nd:YAG laser pumped PDL-1 dye laser). The nozzle size is 0.5 mm. The terminal Mach number for helium gas at 1 atmosphere is 26.5 cm and the free flow distance, which describes the starting point of the 'zone of silence', is calculated as 0.8 cm. Therefore, all the spectroscopic measurements can be done between 0.8 cm and 26.5 cm downstream from the nozzle. For the work discussed in this dissertation, the fluorescence excitation spectra and dispersed fluorescence spectra were done in a region 1.2 cm downstream from the nozzle.

EXPERIMENTAL SECTION

The fluorescence excitation spectra were taken with the supersonic jet apparatus shown schematically in Figure 1. The sample vapor was seeded into 1-5 atmospheres of a helium carrier gas and expanded through a nozzle with a 0.5 mm pinhole. The pulsed valve (Quanta-Ray Model PSV-2) has a 60 μsec pulse duration time and was operated at a repetition rate of 10 Hz and synchronized to the excitation laser. The operating temperature of the valve ranges from room temperature to 100 °C. The pressure of the expansion chamber was ~ $2x10^{-5}$ torr during valve operation. The vacuum system consists of a 6 inch diffusion pump (Varian Model 3352-K2977-302) with a 1740 L/S pumping rate and mechanical pump with a 50 L/S pumping rate.

The excitation source was a Nd:YAG laser (Quanta-Ray Model DCR-1) pumped dye laser (Quanta-Ray Model PDL-1). Ultraviolet radiation was generated by frequency doubling the dye laser output in a KDP crystal controlled with an autotracker (Inrad Model 5-12). The laser linewidth is specified as 0.7 cm^{-1} (FWHM). The excitation beam entered the apparatus through a Brewster angle window and a series of conical skimmers which decreased the amount of scattered light. This beam was focused to the excitation point with a 50 cm focalength convex lens. The sample was excited ~10 mm downstream from the pulsed nozzle.

The detection of total fluorescence was accomplished with an elliptical reflector, interference filter, and a photomultiplier tube (Amperex model 56 AVP). The elliptical mirror (Melles Griot model 02REM001) has two focal points, f_1=12.1 mm and f_2=102.8 mm with a

F number of 0.16. Two holes were drilled to accommodate the laser light path. The fluorescence was detected at right angles to the jet propagation direction and also at right angles to the laser light path. Although scattered light was well skimmed by the light baffles, scattering was detected when the elliptical reflector was used. Therefore, an interference filter which has a transmittance maximum at 310 nm with a bandwidth of 10 nm (FWHM) was placed in front of the photomultiplier tube (PMT) to further reduce scattered light contributions to the signal. The PMT was placed at the focal point (f_2) of the elliptical reflector. By using this detection system, fluorescence detection efficiency was increased about fifty times compared to the system using a monochromator and a PMT which was used for the dispersed fluorescence experiments. Signals detected by the PMT were sent to a dual gated amplifier (Quanta-Ray model DGA-1), which has fixed gate widths of 4.5 μsec or 100 μsec. The output of the gated amplifier was digitized by the computer and stored for data analysis. High resolution experiments were performed by using a pressure tuned etalon scan.

Dispersed fluorescence spectra were measured with an Instruments SA model 320 monochromator (0.32 m, holographic grating) with variable slit widths. The resolution of the monochromator was 14 cm^{-1} for the dispersed fluorescence experiments. The fluorescence was collimated by a 5cm focalength convex lens and a 5cm focalength concave mirror, and the collimated beam was then focused onto the entrance slit of the monochromator by a 20cm focalength convex lens. The focused beam was detected by a PMT (Hamamatsu model R-106UH), and another PMT (RCA model

1P-28) was used as a reference PMT for nomalization of the signal. Dispersed fluorescence spectra were obtained via computer control. Averaging was used (50 - 200 shots per data point) to increase the S/N ratio. Even with this averaging, it was difficult to detect the signal from some molecules due to low fluorescence quantum yields.

P-isopropylphenol was obtained from Chemical Intermediates & Research Laboratories and was purified by vacuum sublimation before using. P-tert-butylphenol was purchased from Kodak Chemical Co. and was purified twice by vacuum sublimation. P-cresol, p-ethylphenol, p-propylphenol, p-pentylphenol, and p-sec-butylphenol were purchased from Aldrich Chemical Co. and were used without further purification. All samples except p-isopropylphenol were at least 98 % purity when they were purchased.

The experimental system was tested by seeding aniline into the helium carrier gas, and the vibrational temperature of aniline was measured as less than 10 K.

Figure 1. Schematic diagram of the experimental setup for the fluorescence excitation experiments.

L: Lens M: Mirrors E: Elliptical mirror

DGA-1: Dual gated amplifier

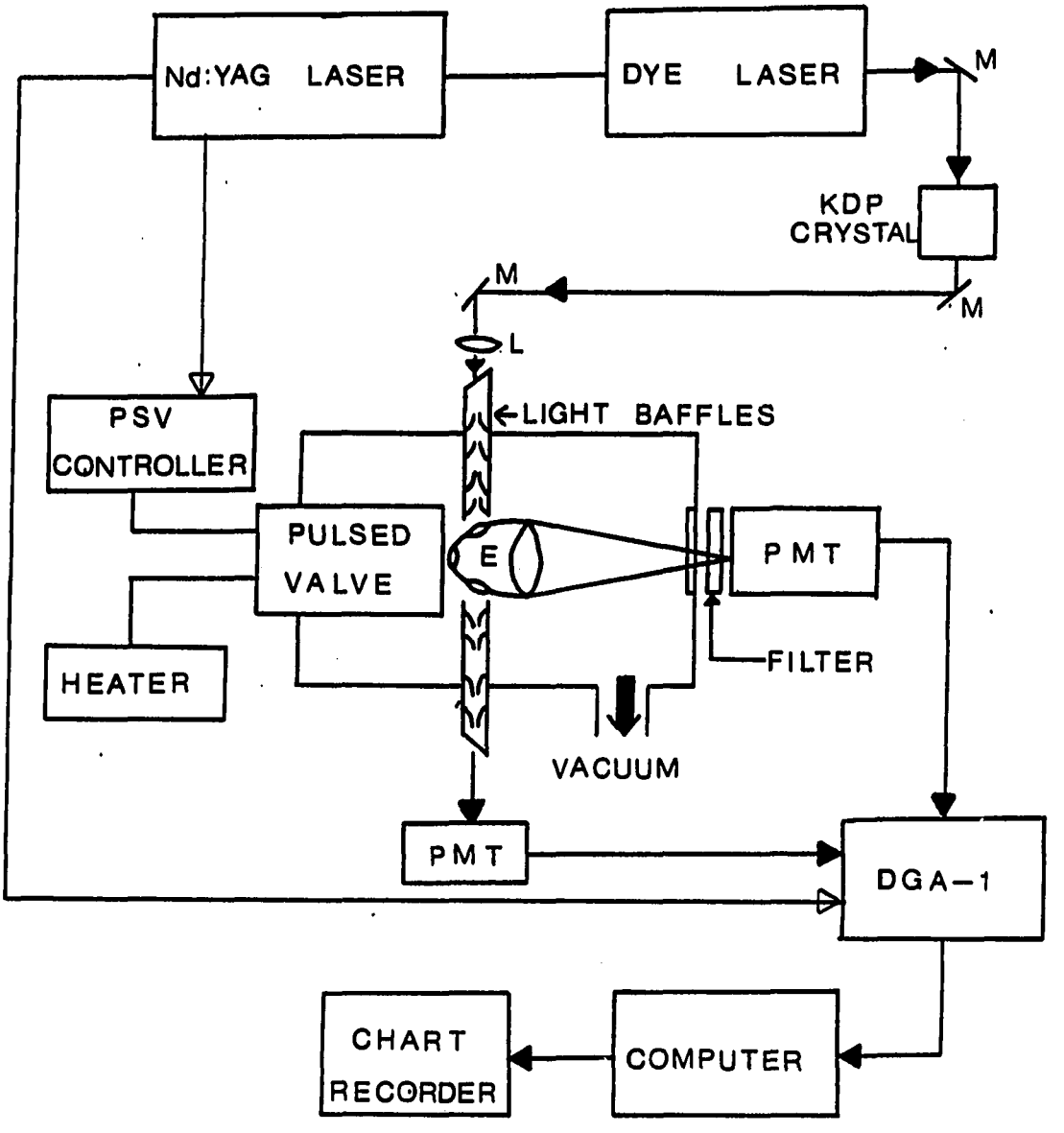
Nd:YAG LASER
DYE LASER
M
KDP CRYSTAL
M
M
L
PSV CONTROLLER
LIGHT BAFFLES
PULSED VALVE
E
PMT
FILTER
HEATER
VACUUM
PMT
DGA-1
CHART RECORDER
COMPUTER

RESULTS

It has been previously suggested that the point groups of p-cresol and p-ethylphenol are C_{2v} by assuming the substituents to be mass points (22,23). In the present study, we also assume the point symmetry group of the molecules studied here to be C_{2v} in the ground state. However, several vibrational modes which are not allowed in the C_{2v} point symmetry group are observed and show moderate intensity in the fluorescence excitation spectra of all the p-alkyl substituted phenols studied here. Therefore, the possible change of the point symmetry group upon excitation to the first excited singlet state (S_1) should be considered. Methrotra (21) suggested the possible change of the point symmetry group from C_{2v} to C_s upon excitation to the S_1 state in the study of p-ethylphenol. Similarly, Bist and coworkers (31) suggested the point symmetry group change upon excitation to the S_1 state in the study of phenol. Considering the fact that several forbidden vibrational modes (in the C_{2v} symmetry) become allowed and in light of the suggestions proposed in the previous studies (21,31), we conclude that the point symmetry group in the S_1 state of p-ethylphenol and p-cresol is distorted from C_{2v} to C_s.

It may be important to note that, however, as the size of the alkyl substituents in the para position of phenol become larger, it may be no longer reasonable to assume the alkyl substituents as mass points. If these alkyl substituents are not regarded as mass points, the symmetry of molecule will be further reduced from C_{2v}. Hence, the effective

point symmetry group will be different for molecules with different alkyl substituents. In addition, molecules studied here except for p-cresol and p-ethylphenol have several conformational isomers in the S_1 state. Therefore, the point symmetry group will be different for the different conformers of a molecule. As the symmetries of molecules are reduced, more vibrational modes are expected to be observed in the fluorescence excitation spectra. Additionally, the totally symmetric modes in the reduced symmetry point group do not show intensity as high as in the higher point symmetry groups. We tentatively assume that the point symmetries of molecules studied here is C_s or further reduced symmetry in the S_1 state. The $S_1 \leftarrow S_0$ transition is allowed in C_s point group by the electric dipole transition selection rules. Therefore, the (0-0) origin bands for each compound should be very intense. In this manuscript assignments of vibrational modes are based on a standard notation scheme. Therefore, for example, the notation $6a^1$ denotes a vibrational band arising from a transition from the S_0 level with zero quantum to the S_1 level with one quantum in the 6a vibrational mode, while $6a_1$ denotes a vibrational band arising from a transition from the S_1 level with zero quantum to the S_0 level with one quantum in the 6a vibrational mode.

P-cresol

The fluorescence excitation spectrum of p-cresol is shown in Fig. 3 and the assignments of vibrational modes in the excited state are listed in Table 1. Vibrational assignments are confined to the ring

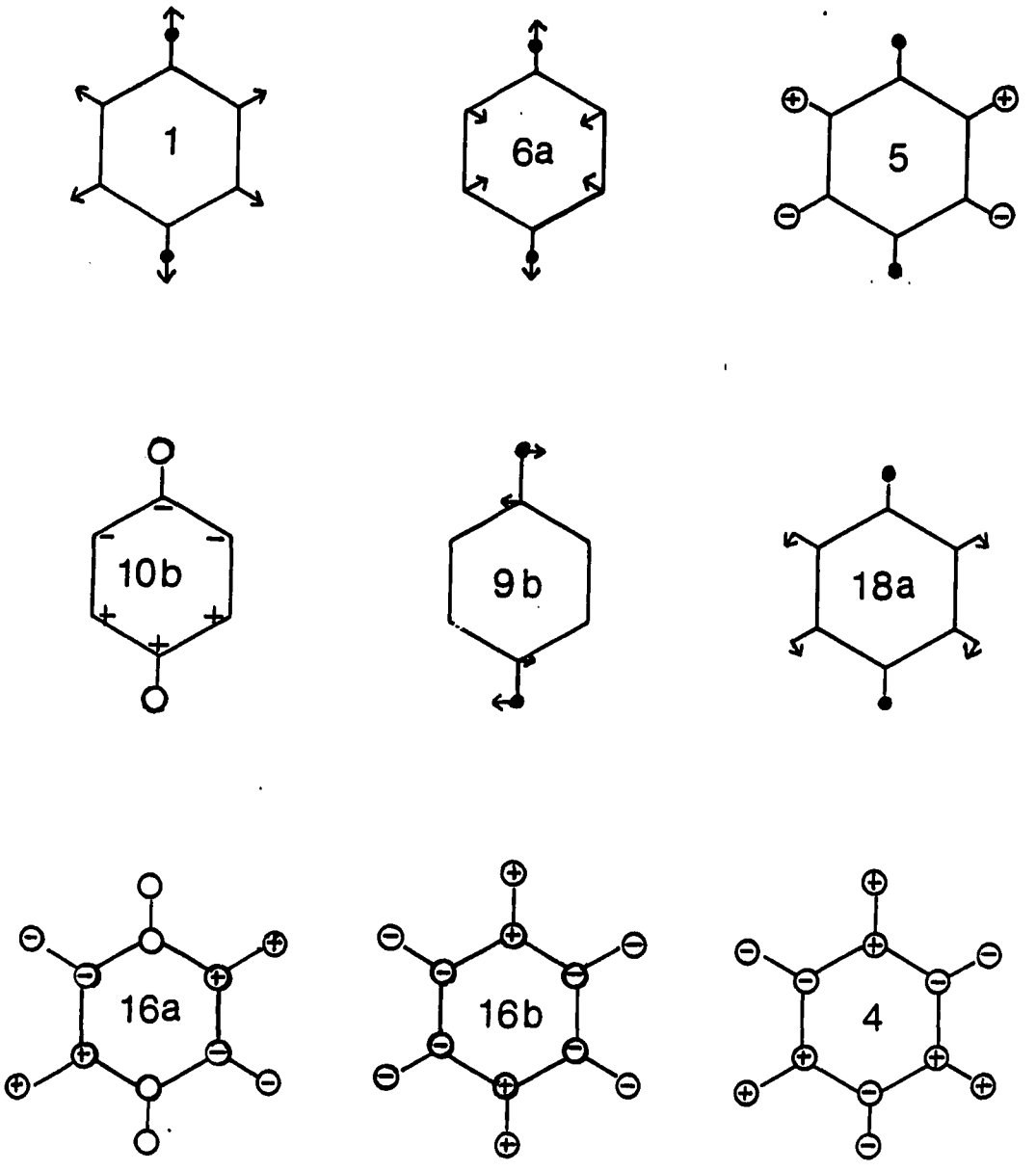

Figure 2. Normal vibrations of benzene

vibrational modes of benzene as shown in Fig. 2. The notation for these assignments is the same as used by Varsanyi (38).

Several intense bands are attributed to the totally symmetric modes (e.g., mode 1 and mode 6a). The most intense band at 35338 cm^{-1} is assigned to the (0-0) origin band and the 35760 cm^{-1} band is attributed to the $6a^1$. If the vibrational frequencies of p-cresol are compared to those of phenol, the 12^1 band and the 1^1 band are expected to be strong. This is true for the 1^1 band which shows very strong intensity at 806 cm^{-1} from the origin band, but it is not the case for the 12^1 band, since the band at 784 cm^{-1} to higher energy of origin, which is the most likely candidate for mode 12, is assigned as mode 4. This 784 cm^{-1} mode was previously assigned to the $16b^2$ overtone band by Tembreull and coworkers (23). We reject this assignment, because the overtone band of $16b^1$ is expected to occur at ~ 1000 cm^{-1} to higher energy of origin when comparing with the frequencies of the 16b modes of other molecules, such as p-ethylphenol and p-isopropylphenol. The assignment is also rejected because the dispersed fluorescence spectrum by origin excitation of p-cresol shows a band at 746 cm^{-1} from the origin, which is very close to the frequency of mode 4 according to Varsanyi (38). It should be noted that mode 4 has b_1 symmetry in the C_{2v} point group and the vibronic transition is not allowed by the electric dipole selection rule. Therefore, the point group of p-cresol in the first excited singlet state (S_1) is regarded as C_s instead of C_{2v}.

The band at 816 cm^{-1} to higher energy of origin has been assigned as the $6a^2$ overtone band by Tembreull and coworkers (23). We reject their assignment of this band also, because its band intensity is almost

as strong as the $6a^1$ band and because 843 cm^{-1} is very close to the overtone of the 424 cm^{-1} mode (6a) in energy, and not the 816 cm^{-1} mode. Furthermore, mode 5 can occur in this frequency region in view of its vibrational frequency in the ground state (38). Therefore, the 816 cm^{-1} vibration is assigned as mode 5 and the band at 843 cm^{-1} to higher energy of origin is assigned as overtone of the 6a mode. The 373 cm^{-1} mode observed in the excitation spectrum is assigned as the $16a^1$ band and not the $16a^2$ band as assigned by Tembreull and coworkers (23). This is because the $16a^1$ band usually occurs at lower energy than ~ 400 cm^{-1} from the origin in these types of molecules (38).

Several bands that appear in the low frequency region of the excitation spectrum at 16 cm^{-1}, 53 cm^{-1} and 97 cm^{-1} to higher energy of origin, which were not assigned by Tembreull et al. (23), are assigned to transitions between internal rotational energy levels of methyl torsional motions. The same type of torsional modes in substituted benzenes has been observed by Breen et al. (26-28) and Ito and his coworkers (29-30). The 407 cm^{-1} vibration is assigned as the $10b^2$ band by Tembreull et al. (23). However, the vibrational frequency of the 10b mode is observed at 338 cm^{-1} in the ground state (38), and therefore, the assignment of the Tembreull et al. for the 407 cm^{-1} mode observed in the excitation spectrum is not reasonable. The 407 cm^{-1} vibration is closer to the 9b mode in energy which is observed at 430 cm^{-1} in the ground state (38). Therefore, the 407 cm^{-1} vibration is assigned as $9b^1$. Since evidence of hydrogen bonding between p-cresol and water has been observed in the lower frequency region (red shifted ~ 350 cm^{-1} from the monomer bands), several bands including the 35406 cm^{-1} and

Figure 3. Fluorescence excitation spectrum of p-cresol in a supersonic free jet. Sample temperature is 50 °C. Helium backing pressure is 1 atm

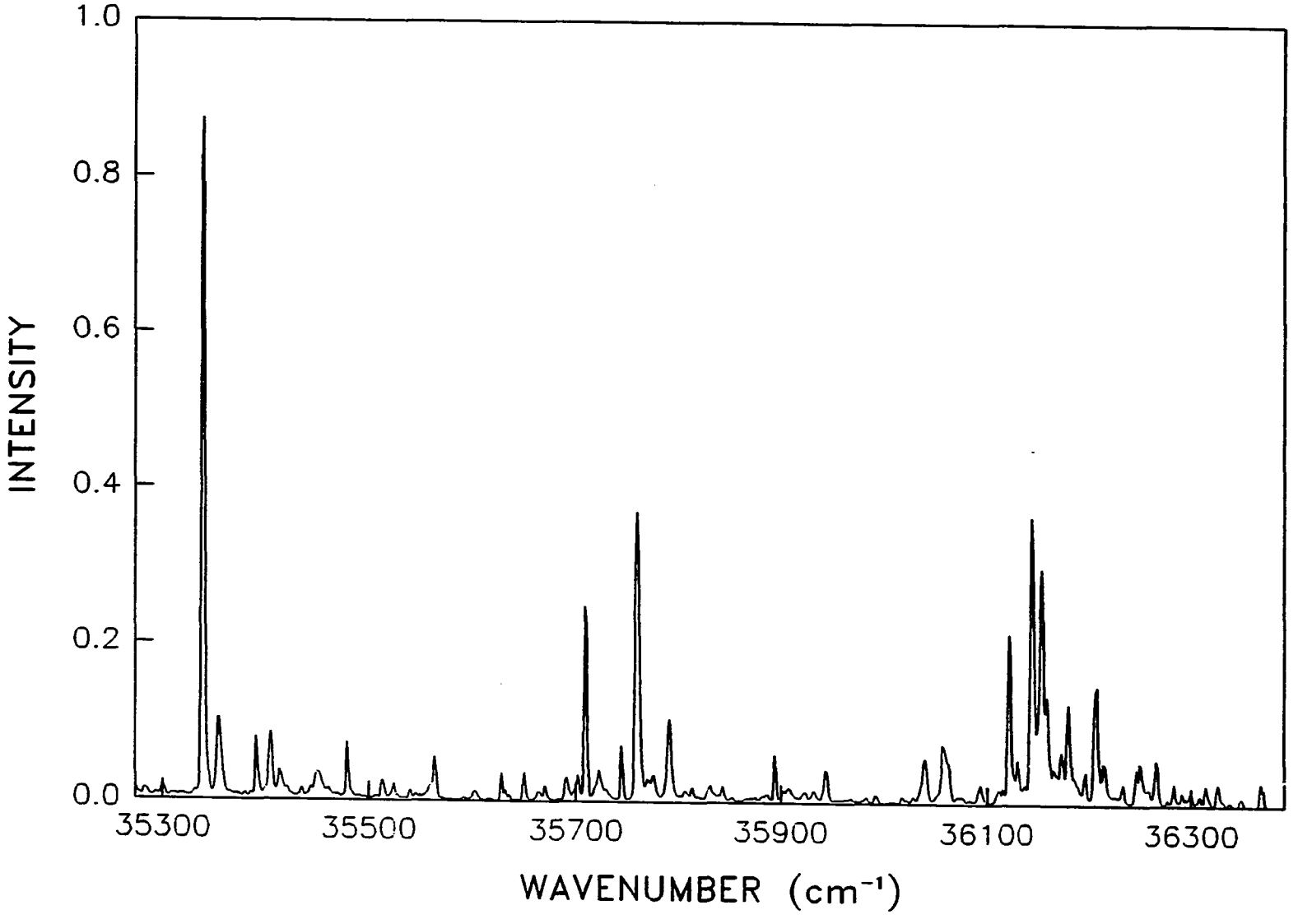
1.0
0.8
0.6
0.4
0.2
0.0
INTENSITY
35300
35500
35700
35900
36100
36300
WAVENUMBER (cm⁻¹)

Table 1. Assignment of vibronic bands observed in the fluorescence excitation spectrum of p-cresol in a supersonic jet in the region of the $S_1 \leftarrow S_0$ transition

observed freq. $\nu(cm^{-1})$	relative freq. $\Delta\nu(cm^{-1})$	assignment
35338	0	0-0
35354	16	methyl
35391	53	torsional
35435	97	motions.
35710	372	$16a^1$
35745	407	$9b^1$
35760	422	$6a^1$
36122	784	4^1
36144	806	1^1
36153	815	5^1
36159	821	$9b^2$
36181	843	$6a^2$
36209	871	$18a^1$

Figure 4. Dispersed fluorescence spectrum of p-cresol in supersonic free jet obtained by exciting the 35338 cm^{-1} band. Sample temperature is 66 °C. Helium backing pressure is 1 atm. Resolution is 14 cm^{-1}. Band positions are displayed relative to the 35338 cm^{-1} band

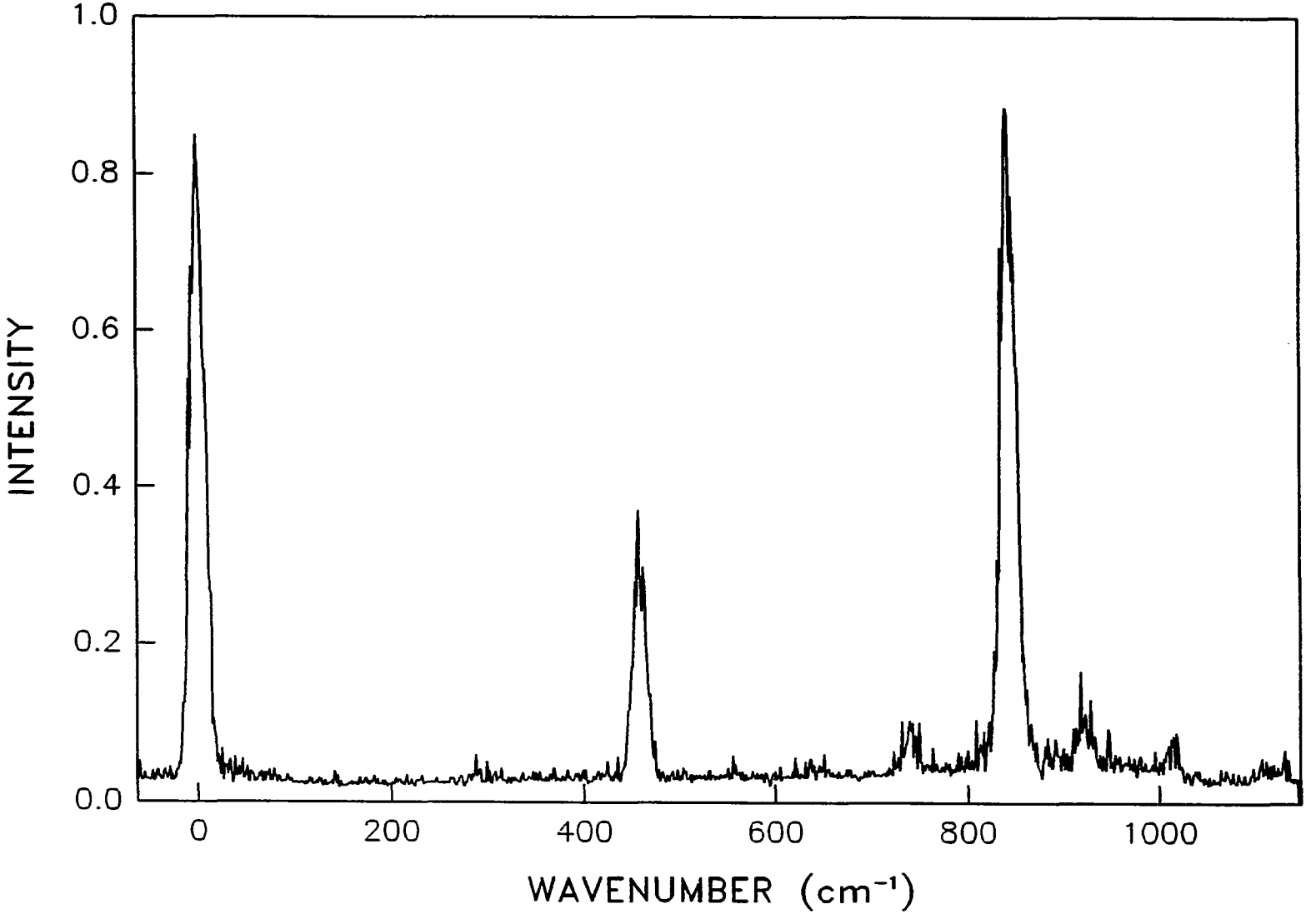
1.0
0.8
0.6
0.4
0.2
0.0
INTENSITY
0
200
400
600
800
1000
WAVENUMBER (cm⁻¹)

Table 2. Vibrational analysis of the dispersed fluorescence spectrum of p-cresol

Excitation : 35338 cm^{-1}			Excitation : 35760 cm^{-1}	
relative freq. $\Delta\nu(cm^{-1})$	solution i.r. data[a]	assignment	relative freq. $\Delta\nu(cm^{-1})$	assignment
460	460	$6a_1$	460	$6a_1$
	508		494	$6a^1 16b_1$
			544	
746	738	4^1	737	$6a^1 4_1$
845	842	1_1	847	$6a^1 1_1$
			873	$6a_1 15_1$(?)
926	920	$6a_2/5_1$	924	$6a_2/5_1$[b]
1024	1016	$18a_1$		

[a] From reference (38).

[b] $6a_2/5_1$ means the mixture of two bands.

35792 cm^{-1} bands are assigned as vibrational modes of hydrogen bonded species. More discussion of the hydrogen bonded species will follow in a later section of this manuscript.

The dispersed fluorescence spectrum of p-cresol with origin excitation is shown in Fig. 4 and vibrational assignments of observed bands are listed in Table 2. Among these bands, the band at 926 cm^{-1} from the origin is assigned as a mixture with contributions from the overtone of the $6a_1$ band and the 5_1 band. This is because the intensity of the 926 cm^{-1} band increases in the dispersed fluorescence spectrum when exciting $6a^1$ band compared to its intensity when using origin excitation and because the frequency of mode 5 in the ground state of p-cresol has been reported to be at ~ 926 cm^{-1} (38).

P-ethylphenol

The fluorescence excitation spectrum and the origin excited dispersed fluorescence spectrum of p-ethylphenol are shown in Fig. 5 and Fig. 6. The excitation spectrum of p-ethylphenol is similar to that of p-cresol with similar vibrational frequencies. However, the 4^1 band frequency is shifted considerably compared to that of p-cresol. The very intense band at 35511 cm^{-1} is assigned as the (0-0) origin band. Several bands in the low frequency region including the C^1 (35537 cm^{-1}) and D^1 (35593 cm^{-1}) bands can be assigned as torsional modes of the ethyl group. The same type of low frequency torsional modes have been observed previously for substituted benzenes (26,27). Both the C and D modes occur continuously, building on several modes as a progression

throughout the spectrum. Several weak bands including the 35970 cm^{-1} band are assigned as bands from the hydrogen bonded species with water. Bands observed at 35810 cm^{-1} and 35828 cm^{-1} are presumably hydroxyl torsional vibrations. The 846 cm^{-1} vibration can be assigned as a 5^1C^1 band or a $6a^2$ overtone band, but the 839 cm^{-1} mode is assigned as the 5^1C^1 band, and therefore, 846 cm^{-1} vibration is assigned as a $6a^2$ overtone band. While bands such as $16b^1C^1$, $6b^1C^1$ and 4^1C^1 are not observed, bands such as $16b^1D^1$, $6b^1D^1$ and 4^1D^1 are observed. This is due to the high intensity of the D^1 band compared to that of the C^1 band. The band at 409 cm^{-1} to higher energy of origin is assigned as the 9b mode by analogy to p-cresol. The band observed at 871 cm^{-1} to higher energy of origin is assigned as 18a mode, because the same mode is observed at ~ 870 cm^{-1} to higher energy of origin in the excitation spectrum of p-cresol and because the frequency of the $18a^1$ band may not be affected much by the different substituents in the para position of phenol as can be seen in Fig. 2.

In the origin excited dispersed fluorescence spectrum shown in Fig. 6, the 1074 cm^{-1} vibration can be assigned as the E_1 band (asymmetric - CH_3 rocking mode) because the observed frequency is very close to the frequency of the asymmetric CH_3 rocking mode (1065 cm^{-1}) (38). The assignment of bands observed in the origin excited dispersed fluorescence spectra is accomplished by analogy to the p-cresol case and by comparing the observed vibrational frequencies with the infrared data (38). The assignments of vibrational modes in the excited state and ground state are listed in Table 3 and Table 4.

Figure 5. Fluorescence excitation spectrum of p-ethylphenol in a supersonic free jet. Sample temperature is 83 °C. Helium backing pressure is 1 atm

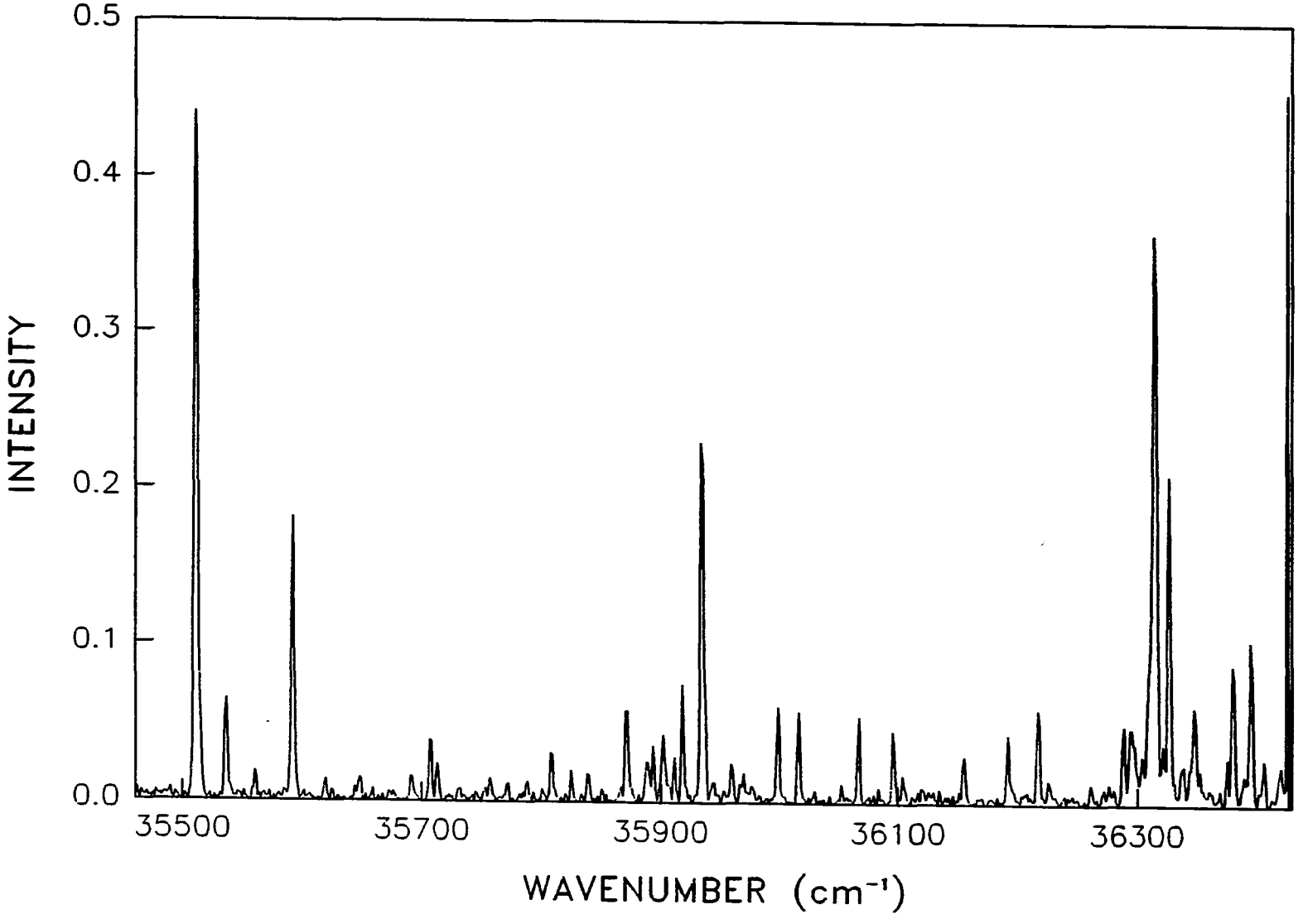
0.5
0.4
0.3
0.2
0.1
0.0
INTENSITY
35500
35700
35900
36100
36300
WAVENUMBER (cm⁻¹)

Table 3. Assignments of vibronic bands in the fluorescence excitation spectrum of p-ethylphenol in a supersonic jet in the region of the $S_1 \leftarrow S_0$ transition

observed frequency $\nu(cm^{-1})$	relative frequency $\Delta\nu(cm^{-1})$	assignment	observed frequency $\nu(cm^{-1})$	relative frequency $\Delta\nu(cm^{-1})$	assignment
35511	0	(0-0)	35961	450	$6a^1C^1$
35537	26	C^1	36001	490	$16b^1/9b^1D^1$
35563	52	C^2	36018	507	$6a^1D^1$
35593	82	D^1	36069	558	$6b^1$
35623	112	D^1C^1	36100	589	
35649	138	D^1C^2	36158	647	
35692	181		36195	684	
35709	198		36220	709	4^1
35715	204		36229	718	$16a^1$
35810	299		36290	779	
35828	317		36297	786	$16a^16a^1$
35842	331		36307	796	4^1D^1
35872	361	$16a^1$	36315	806	1^1
35890	379		36329	818	5^1
35896	385	$16a^1C^1$	36340	829	1^1C^1
35903	392		36350	839	5^1C^1
35914	403		36357	846	$6a^2$
35920	409	$9b^1$	36380	869	$18a^1$
35935	424	$6a^1$	36396	885	1^1D^1
35946	435		36408	897	5^1D^1
35953	442	$16a^1D^1$	36421	910	$1^1D^1C^1$

Figure 6. Dispersed fluorescence spectrum of p-ethylphenol in a supersonic free jet obtained by exciting the 35511 cm^{-1} band. Sample temperature is 83 °C. Helium backing pressure is 1 atm. Resolution is 14 cm^{-1}. Band positions are displayed relative to the 35511 cm^{-1} band

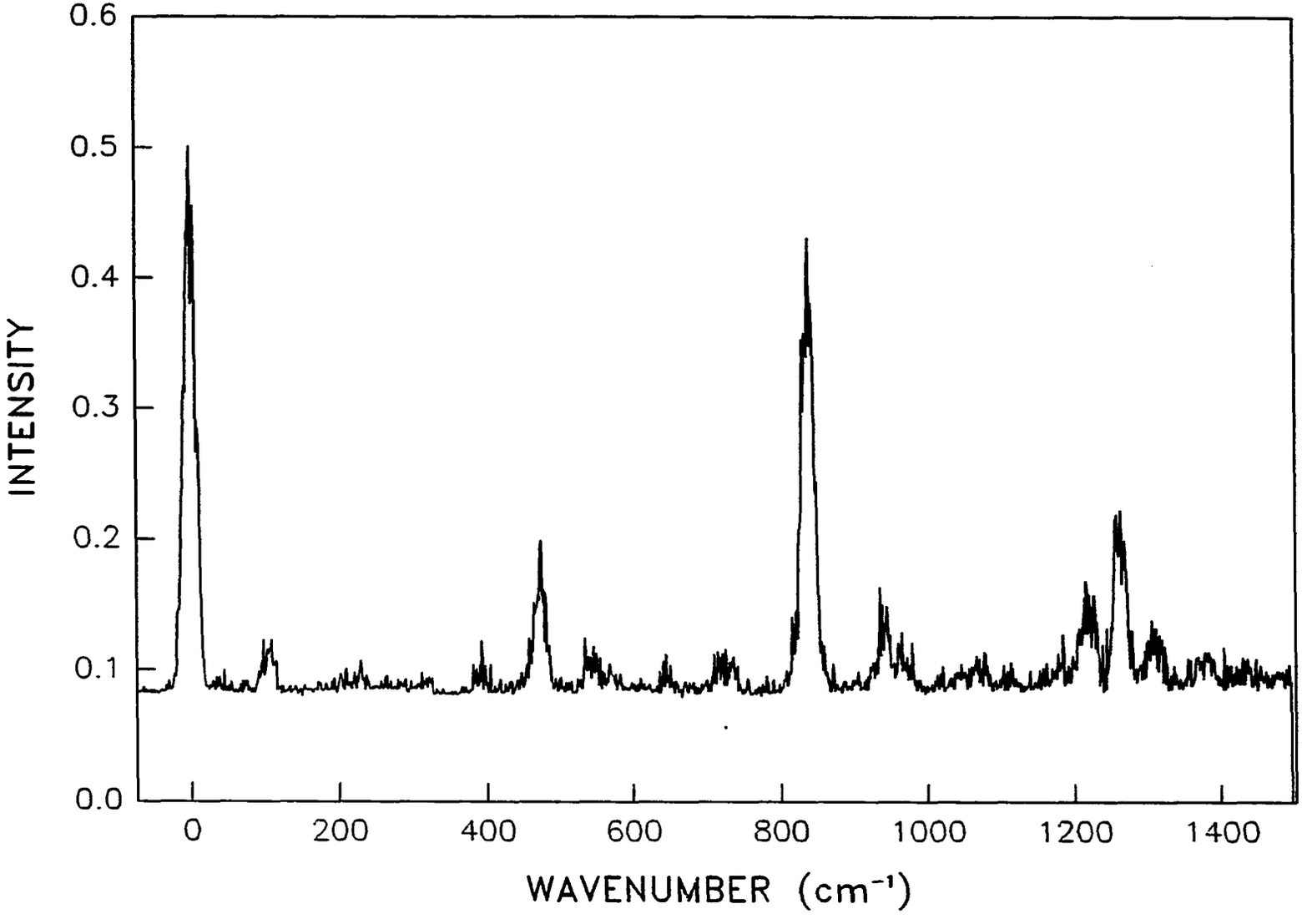
0.6
0.5
0.4
0.3
0.2
0.1
0.0
INTENSITY
0
200
400
600
800
1000
1200
1400
WAVENUMBER (cm⁻¹)

Table 4. Vibrational analysis of the dispersed fluorescence spectrum of p-ethylphenol using origin excitation (35511 cm^{-1})

relative freq. ν (cm^{-1})	solution i.r. data $\Delta\nu$(cm^{-1}) (ref. 38)	assignment
101		D_1[a]
392		$16a_1$
472	477	$6a_1$
539	543	$16b_1$
721	714	4_1
841		1_1
939		$6a_2/5_1$
1074	1065	E_1[b]
1224	1223	F_1[c]
1267	1247	$7a_1$
1308	1312	3_1

[a]Ethyl torsional motion.

[b]Asymmetric -CH_3 rocking vibrational mode (From ref. 38).

[c]O-H bending vibrational mode (From ref. 38).

P-isopropylphenol

The fluorescence excitation spectrum of p-isopropylphenol is shown in Fig. 7. The 35586 cm^{-1} band and the 35600 cm^{-1} band are assigned as origin bands of two isomers in the excited state because doubling of bands continues throughout the spectrum. The 35633 cm^{-1} band and 35644 cm^{-1} band are assigned as isopropyl torsional modes. All of the vibrational band assignments are based on these two isomer structures (cis- and trans- isomer). If only one origin band is considered, a vibrational structure similar to p-ethylphenol should be observed. This is due to the fact that both molecules have two carbon chains as para substituents. By comparing the band structures of these two molecules, very similar vibrational frequencies are observed as can be seen in Table 5. For example, the $6a^1$ band and the 1^1 band occur at 424 cm^{-1} and 804 cm^{-1} to higher energy of each conformer origin, respectively, in the p-isopropylphenol and at 423 cm^{-1} and 804 cm^{-1} to higher energy of origin, respectively, in the p-ethylphenol. Only for the 4^1 and $16b^1$ bands, slight deviation can be observed in the frequencies for the two molecules. Therefore, except for the doublet origin structures and some new bands in the p-isopropylphenol, e.g., 15^1, the vibrational structure of p-isopropylphenol in the excited state is very similar to that of p-ethylphenol.

For the dispersed fluorescence spectra, the sample temperature was usually higher than 80 °C. Two origin excited dispersed fluorescence spectra with 14 cm^{-1} resolution are shown in Fig. 8 and Fig. 9. These two spectra are identical except for a 14 cm^{-1} shift between the

Figure 7. Fluorescence excitation spectrum of p-isopropylphenol in a supersonic free jet. Sample temperature is 82 °C. Helium backing pressure is 1 atm

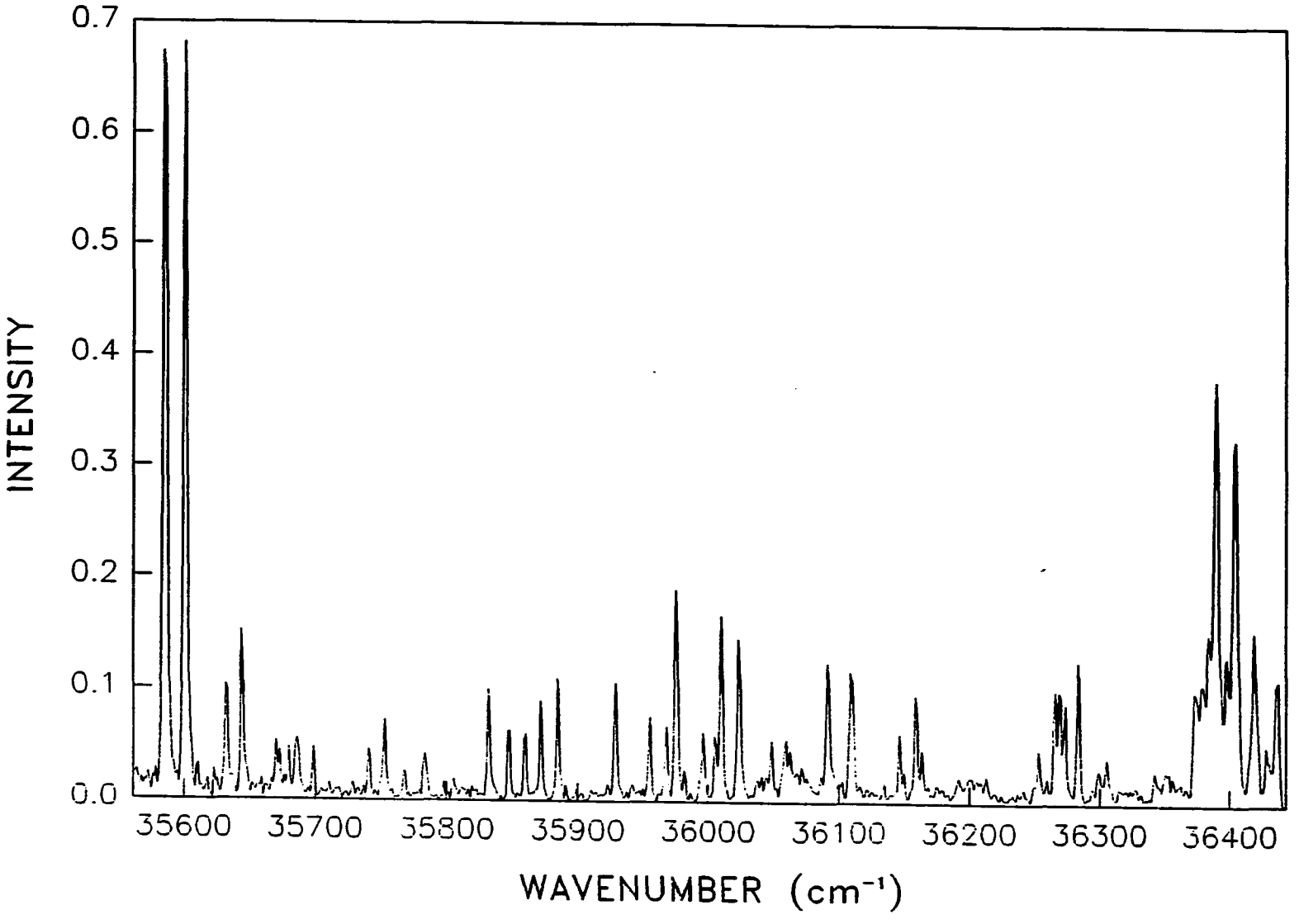
0.7
0.6
0.5
0.4
0.3
0.2
0.1
0.0
INTENSITY
35600
35700
35800
35900
36000
36100
36200
36300
36400
WAVENUMBER (cm⁻¹)

Table 5. Assignments of vibronic bands observed in the fluorescence excitation spectra of p-isopropylphenol in a supersonic jet in the region of the $S_1 \leftarrow S_0$ transition

observed freq. ν (cm^{-1})	$\Delta\nu$ (cm^{-1}) relative to 35586 cm^{-1}	$\Delta\nu'$ (cm^{-1}) relative to 35600 cm^{-1}	assignment
35586	0		(0-0)(c)[a]
35600	14	0	(0-0)(t)[b]
35633	47		
35644	58	44	
35832	246		15^1(c)
35847	261	247	15^1(t)
35859	273		
35871	285		Hydroxyl
35885	299	285	torsion.
35930	344		
35956	370		$16a^1$(c)
35968	382	368	$16a^1$(t)
35976	390		
36010	424		$6a^1$(c)
36024	438	424	$6a^1$(t)
36092	505		$16b^1$(c)
36110	524	510	$16b^1$(t)
36160	574		
36267	681		

[a]Cis-isomer

[b]Trans-isomer

Table 5. (continued)

observed freq. ν (cm^{-1})	$\Delta\nu$ (cm^{-1}) relative to 35586 cm^{-1}	$\Delta\nu'$ (cm^{-1}) relative to 35600 cm^{-1}	assignment
36271	685		4^1(c)
36275	689		
36385	699	685	4^1(t)
36375	789		
36379	793		
36384	798		
36389	804		1^1(c)
36398	812	798	
36404	818	804	1^1(t)

Figure 8. Dispersed fluorescence spectrum of p-isopropylphenol in a supersonic free jet obtained by exciting the 35586 cm^{-1} band. Sample temperature is 80 °C. Helium backing pressure is 1 atm. Resolution is 14 cm^{-1}. Band positions are displayed relative to the 35586 cm^{-1} band

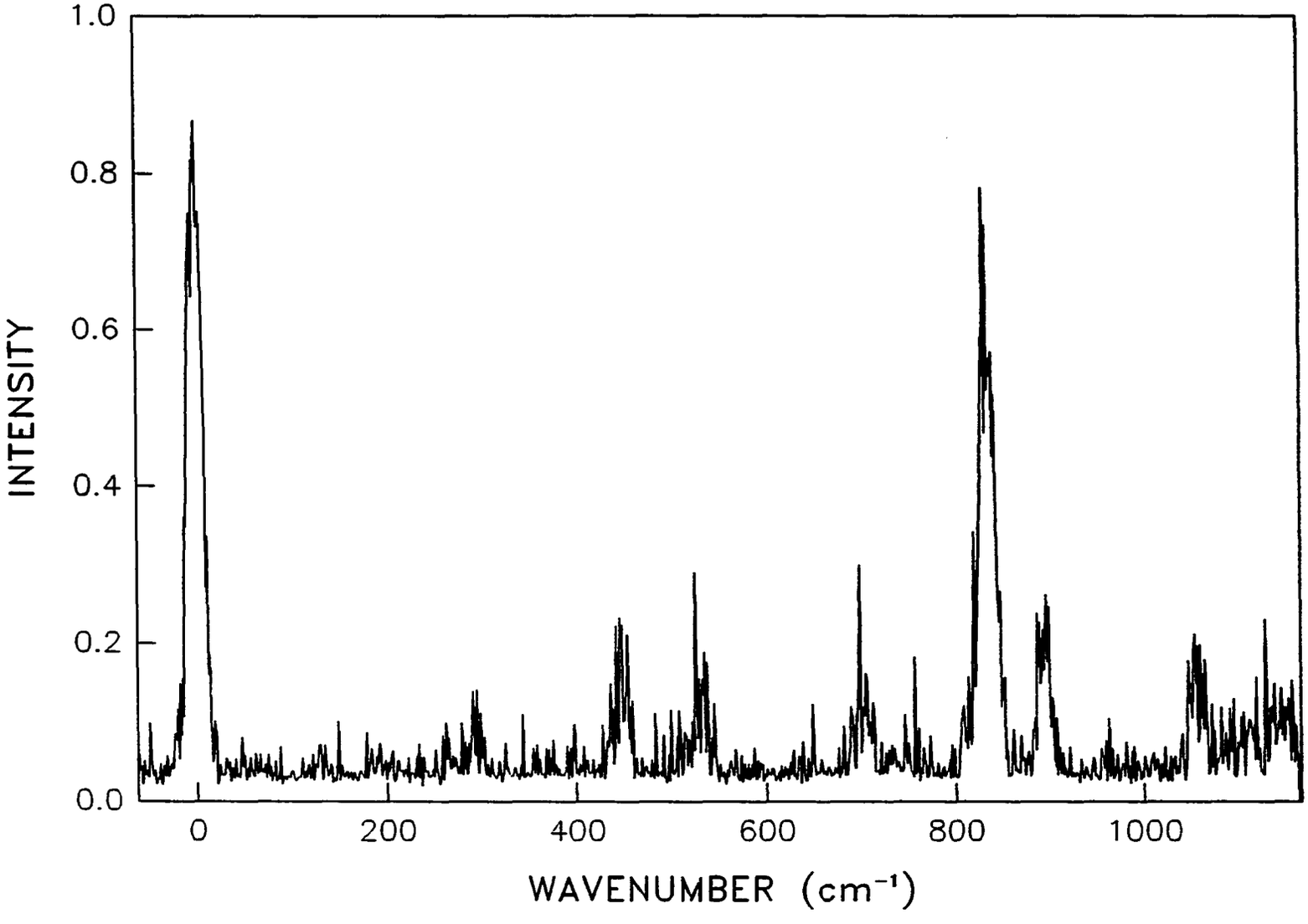
1.0
0.8
0.6
0.4
0.2
0.0
INTENSITY
0
200
400
600
800
1000
WAVENUMBER (cm⁻¹)

Figure 9. Dispersed fluorescence spectrum of p-isopropylphenol in a supersonic free jet obtained by exciting the 35600 cm^{-1} band. Sample temperature is 80 °C. Helium backing pressure is 1 atm. Resolution is 14 cm^{-1}. Band positions are displayed relative to the 35600 cm^{-1} band

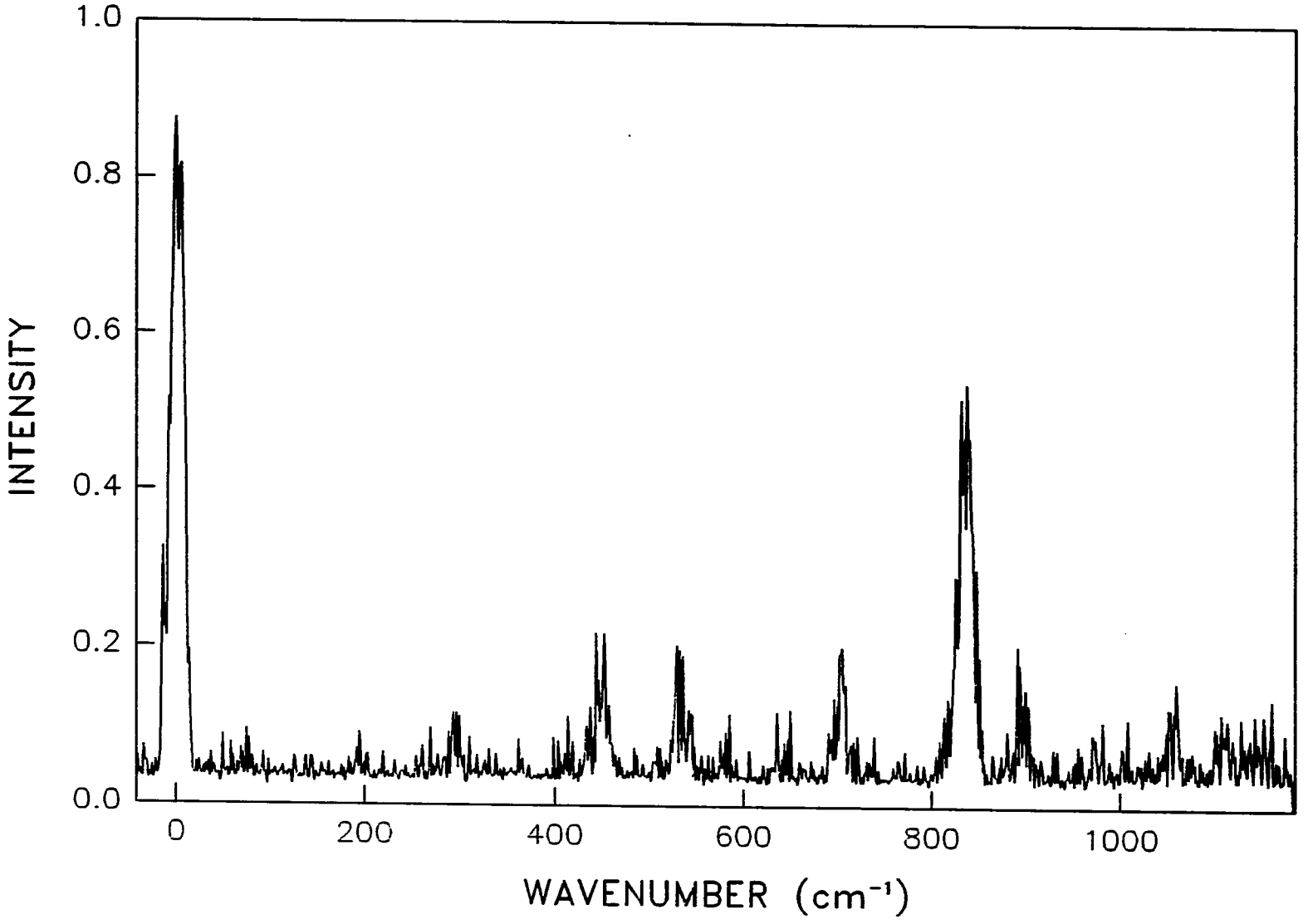
1.0
0.8
0.6
0.4
0.2
0.0
INTENSITY
0
200
400
600
800
1000
WAVENUMBER (cm⁻¹)

Table 6. Vibrational analysis of the dispersed fluorescence spectra of p-isopropylphenol

35586 cm^{-1} excit. relative freq. $\Delta\nu$ (cm^{-1})	35600 cm^{-1} excit. relative freq. $\Delta\nu$ (cm^{-1})	From ref. (38)	assignment
296	301		G_1[a]
448	446	445	$6a_1$
530	534	543	$16b_1$
706	709	705	4_1
834	839	800	1_1
905	903		$6a_2/5_1$
1061	1065	1052	E_1[b]

[a]Hydroxyl torsional mode.

[b]Asymmetric $-CH_3$ rocking mode (From ref. 38).

corresponding bands. Although the frequency of 10a mode is reported as 835 cm^{-1} and that of 1 mode is reported as 800 cm^{-1} in the ground state (38), the band at ~ 834 cm^{-1} from the origin in the dispersed fluorescence spectra is assigned as 1_1 band due to the high intensity of this band and by analogy to the p-cresol and p-ethylphenol cases. The assignments of the vibrational bands in the dispersed fluorescence spectra are listed in Table 6.

P-sec-butylphenol

The fluorescence excitation spectrum and the dispersed fluorescence spectra of p-sec-butylphenol obtained by exciting the 35537 cm^{-1} and 35550 cm^{-1} bands are shown in Fig. 10-12. The assignments of the bands in these spectra are listed in Table 7 and Table 8. Vibrational assignments of observed bands are made with the dispersed fluorescence data and by analogy with the band assignments of p-isopropylphenol. As was observed in the p-isopropylphenol case, the doublet origin bands are observed at 35537 cm^{-1} and 35550 cm^{-1} in the excitation spectrum of p-sec-butylphenol, and therefore, the characteristics of this doublet are regarded to be the same as that of the p-isopropylphenol case. The energy separation between the two origin bands is measured as 13 cm^{-1} which is almost the same separation as in the p-isopropylphenol case (14 cm^{-1}). Vibrational frequencies of the bands measured in the excited state are slightly lower than those observed in the p-isopropylphenol case. A comparison between the two spectra is shown in Table 16.

Although the vibrational structures of these two molecules (p-isopropylphenol and p-sec-butylphenol) in the excited state (S_1) are very similar, there is an obvious structural difference. The p-sec-butylphenol has a three carbon alkyl chain in the sec-butyl group, while the p-isopropylphenol has a two carbon alkyl chain in the isopropyl group. Therefore, for p-sec-butylphenol, isomer formation is possible in the same manner as was described by Hopkins et al. (25) in addition to the same types of isomers as p-isopropylphenol case. Bands located in the range from 35590 cm^{-1} to 35670 cm^{-1}, especially the bands observed at 35595 cm^{-1} and 35608 cm^{-1}, could be assigned as arising from the different isomers, or torsional motions, or hydrogen bonded species. Several bands in this energy region have been identified as vibronic modes of the hydrogen bonded species with water. Additionally, if these two bands (35595 cm^{-1} and 35608 cm^{-1}) are origin bands arising from isomers other than the two isomers which have origin bands at 35537 cm^{-1} and at 35550 cm^{-1}, the doublet (35595 cm^{-1} and 35608 cm^{-1}) should continue to occur in the high frequency region with the doublet assigned as (0-0)(trans) and (0-0)(cis). However, only peaks built on origins at 35537 cm^{-1} and at 35550 cm^{-1} occur repeatedly in the high frequency region. Therefore, only the bands at 35537 cm^{-1} and 35550 cm^{-1} are regarded as origin bands for the two isomers, while bands at 35595 cm^{-1} and 35608 cm^{-1} are assigned as bands representing torsional motions of sec-butyl group for each isomer.

Similar low frequency bands have been observed in the fluorescence excitation spectra of p-cresol (16 cm^{-1}), p-ethylphenol (26 cm^{-1} and 82 cm^{-1}), and p-isopropylphenol (45 cm^{-1}). These bands have been also tentatively assigned as bands which represent torsional motions of each

Figure 10. Fluorescence excitation spectrum of p-sec-butylphenol in a supersonic free jet. Sample temperature is 72 °C. Helium backing pressure is 1 atm

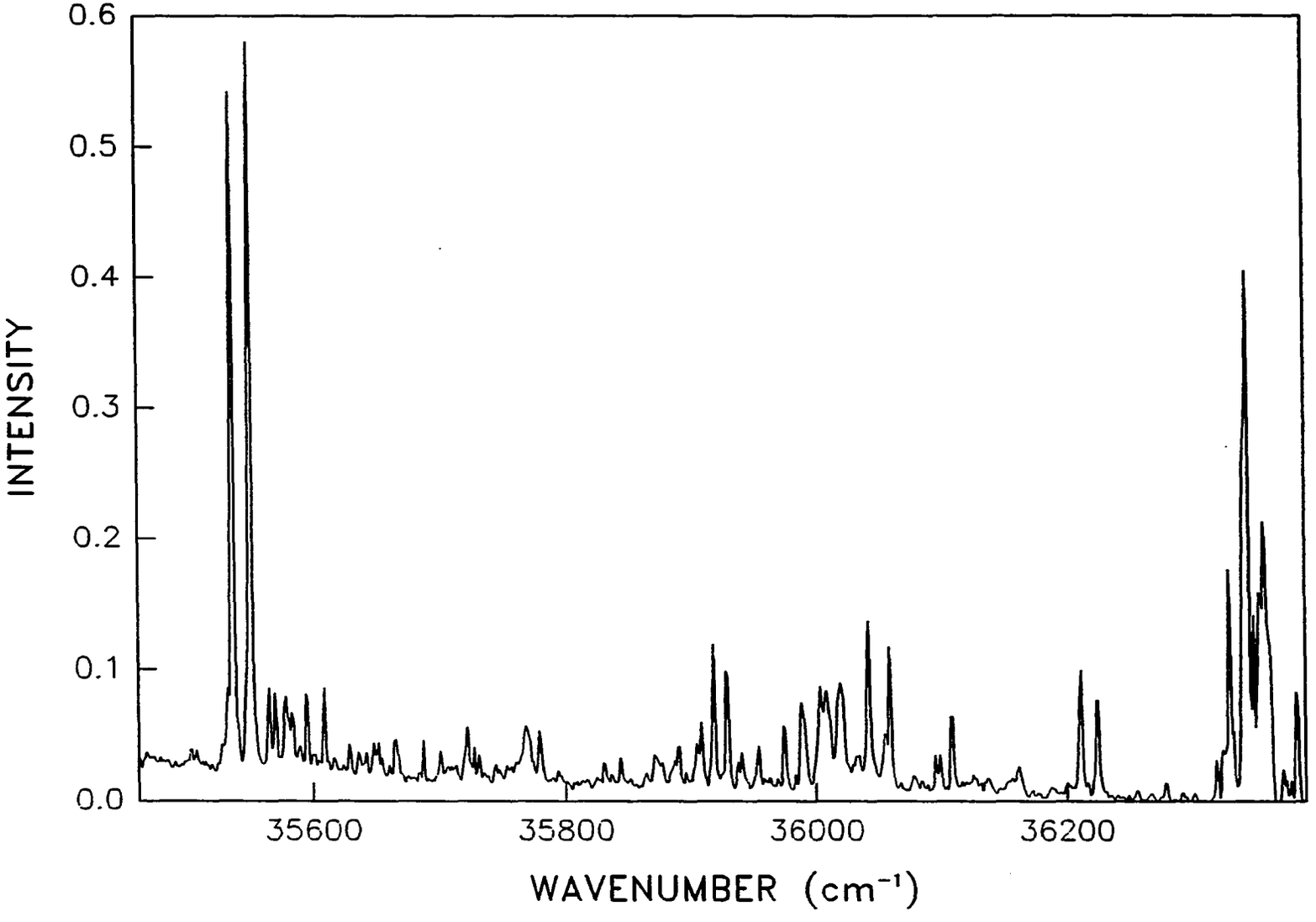
0.6
0.5
0.4
0.3
0.2
0.1
0.0
INTENSITY
35600
35800
36000
36200
WAVENUMBER (cm⁻¹)

Table 7. Assignment of vibronic bands in the fluorescence excitation spectrum of p-sec-butylphenol in a supersonic jet in the region of the $S_1 \leftarrow S_0$ transition

observed freq. (cm^{-1})	$\Delta\nu$ (cm^{-1}) relative to 35537 cm^{-1}	$\Delta\nu$ (cm^{-1}) relative to 35550 cm^{-1}	assignment
35537	0		(0-0)(c)[a]
35550	14	0	(0-0)(t)[b]
35595	58		D^1(c)[c]
35608	72	58	D^1(t)
35651	114		D^2(c)
35664	128	114	D^2(t)
35579	232		15^1(c)
35780	244	230	15^1(t)
35831	294		Hydroxyl
35845	309	295	torsion.
35918	381		$16a^1$(c)
35928	392	378	$16a^1$(t)
35941	404		$9b^1$(c)
35954	418	404	$9b^1$(t)
35975	438		$6a^1$(c)
35988	452	438	$6a^1$(t)

[a]Cis-isomer.

[b]Trans-isomer.

[c]Torsional motion of sec-butyl group.

Table 7. (continued)

observed freq. (cm^{-1})	$\Delta\nu$ (cm^{-1}) relative to 35537 cm^{-1}	$\Delta\nu$ (cm^{-1}) relative to 35550 cm^{-1}	assignment
36008	471		1^1(H,c)[d]
36021	485	471	1^1(H,t)
36042	505		$16b^1$(c)
36059	523	509	$16b^1$(t)
36109	573		
36212	675		4^1(c)
36225	689	675	4^1(t)
36329	792		
36343	806		1^1(c)
36349	812		5^1(c)
36357	821	807	1^1(t)
36362	826	812	5^1(t)

[d] 1^1(H,t) means 1^1(t) band for the hydrogen bonded species with water.

Figure 11. Dispersed fluorescence spectrum of p-sec-butylphenol in a supersonic free jet obtained by exciting the 35537 cm^{-1} band. Sample temperature is 86 °C. Helium backing pressure is 1 atm. Resolution is 14 cm^{-1}. Band positions are displayed relative to the 35537 cm^{-1} band

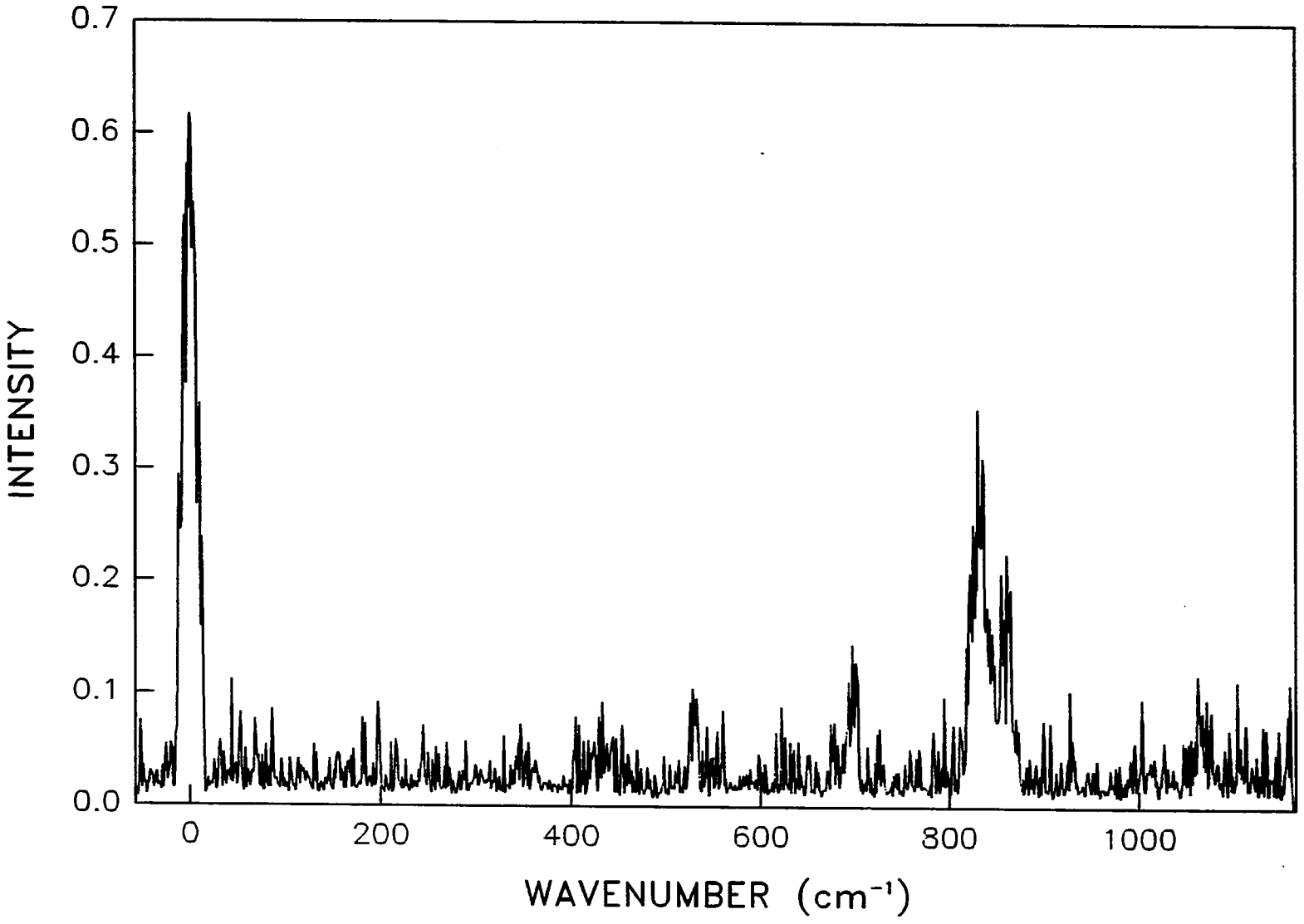
0.7
0.6
0.5
0.4
0.3
0.2
0.1
0.0
INTENSITY
0
200
400
600
800
1000
WAVENUMBER (cm⁻¹)

Figure 12. Dispersed fluorescence spectrum of p-sec-butylphenol in a supersonic free jet obtained by exciting the 35550 cm^{-1} band. Sample temperature is 86 °C. Helium backing pressure is 1 atm. Resolution is 14 cm^{-1}. Band positions are displayed relative to the 35550 cm^{-1} band

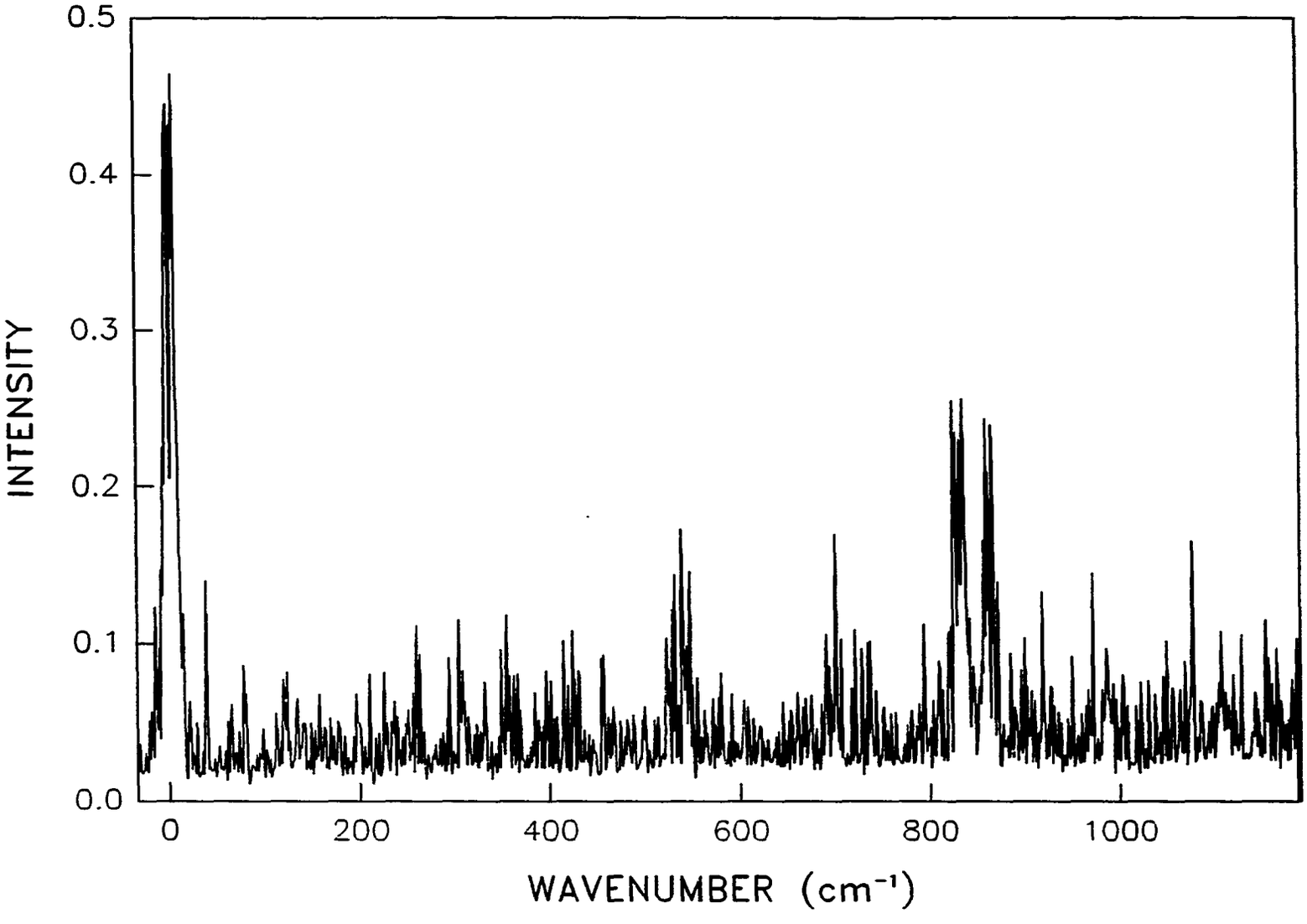
0.5
0.4
0.3
0.2
0.1
0.0
INTENSITY
0
200
400
600
800
1000
WAVENUMBER (cm⁻¹)

Table 8. Vibrational analysis of the dispersed fluorescence spectrum of p-sec-butylphenol

35537 cm^{-1} excit. relative freq. $\Delta\nu$ (cm^{-1})	35550 cm^{-1} excit. relative freq. $\Delta\nu'$ (cm^{-1})	assignment
356	356	$16a_1$
	424	$6a_1$
534	534	$16b_1$
702	706	4_1
835	834	1_1
861	869	5_1
	993	

corresponding alkyl substituents. The observation of only two origin bands means that there is no evidence of the type of isomers mentioned by Hopkins et al. (25) for the alkyl benzenes even though there is an alkyl chain with three carbon atoms in the sec-butyl group. Additional discussion of the geometry of the isomers will be presented later. The assignment of 404 cm^{-1} mode observed in the fluorescence excitation spectrum is analogous to the assignment of 407cm^{-1} mode in the p-cresol and of 409 cm^{-1} mode in the p-ethylphenol case. The band at ~ 860 cm^{-1} from each origin of isomer observed in the dispersed fluorescence spectrum is tentatively assigned as 5^1 band by analogy to the p-cresol, p-ethylphenol, and p-isopropylphenol cases. The vibrational assignment of the rest of the bands is made by analogy with the p-isopropylphenol case.

P-tert-butylphenol

The fluorescence excitation spectrum of p-tert-butylphenol is shown in Fig. 13 and the assignments of vibrational bands are listed in Table 9. The doublet origin bands have been also observed in this case as for the p-isopropylphenol and p-sec-butylphenol cases. The energy separation between the two origin bands has been measured as 36 cm^{-1}, which is a larger separation than those of the previous two molecular cases (14 cm^{-1} for the p-isopropylphenol and 13 cm^{-1} for the p-sec-butyl phenol). This energy separation between isomers may represent the difference in the energy barrier among isomers.

Bands at 35711 cm^{-1} and 35747 cm^{-1} are assigned as origin bands of the two isomers, and bands at 36073 cm^{-1} and at 36109 cm^{-1} are assigned as the 16a mode for both isomers. Mode 1 cannot be observed in the fluorescence spectrum, because the laser dye coverage did not extend to the mode 1 frequency range (R-590 frequency doubling). The frequency of the mode 4 is reduced to 642 cm^{-1} compared to 685 cm^{-1} for p-isopropylphenol and 675 cm^{-1} for p-sec-butylphenol. This frequency shift might be interpreted as a size effect of the alkyl substituents, but cannot be confirmed.

The dispersed fluorescence spectra obtained by exciting the two origin bands are shown in Fig. 14 and Fig. 15, and the vibrational band assignments are listed in Table 10. The spectrum shown in Fig. 14 shows more bands than Fig. 15. This is not because the vibrational structure of the ground state between the two isomers is different, but because the intensities of bands are stronger in the former case than in the latter case. This means that one of isomers is more strongly fluorescent. The intensity ratio between the two origin bands is approximately 1:1.5. Although it is not clear which isomer is the more strongly fluoresce, the more intense band at 35747 cm^{-1} is tentatively assigned as the origin band of the trans-isomer because the trans-isomer is regarded as the more stable isomer. Therefore, the origin band of the trans-isomer may occur to higher energy than that of the cis-isomer. The 1120 cm^{-1} mode observed in the origin excited dispersed fluorescence spectra is tentatively assigned as either an asymmetric $-CH_3$ rocking mode or $18a^1$ by analogy to the other molecules studied.

Figure 13. Fluorescence excitation spectrum of p-tert-butylphenol in a supersonic free jet. Sample temperature is 72 °C. Helium backing pressure is 1 atm

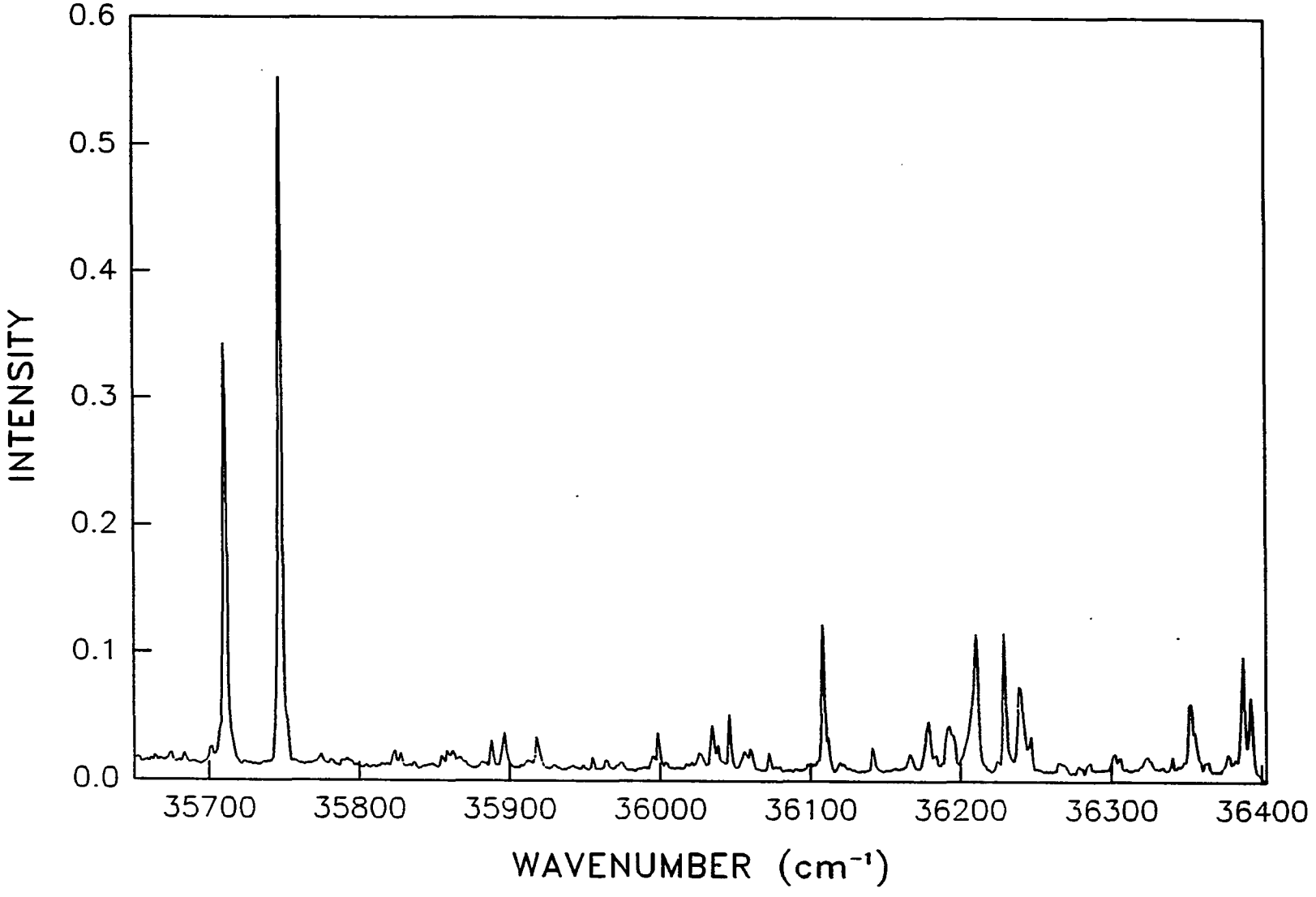
0.6
0.5
0.4
0.3
0.2
0.1
0.0
INTENSITY
35700
35800
35900
36000
36100
36200
36300
36400
WAVENUMBER (cm⁻¹)

Table 9. Assignments of vibronic bands observed in the fluorescence excitation spectrum of p-tert-butylphenol in a supersonic jet in the region of the $S_1 \leftarrow S_0$ transition

observed freq. ν (cm^{-1})	$\Delta\nu$ (cm^{-1}) relative to 35711 cm^{-1}	$\Delta\nu'$ (cm^{-1}) relative to 35747 cm^{-1}	assignment
35711	0		(0-0)(c)[a]
35747	36	0	(0-0)(t)[b]
36000	289		Hydroxyl
36036	325	289	torsion.
36073	362		$16a^1$(c)
36109	398	362	$16a^1$(t)
36142	431		$6a^1$(c)
36180	469	433	$6a^1$(t)
36193	482		$16b^1$(c)
36230	519	483	$16b^1$(t)
36354	643		4^1(c)
36389	678	642	4^1(t)

[a]Cis-isomer.

[b]Trans-isomer.

Figure 14. Dispersed fluorescence spectrum of p-tert-butylphenol in a supersonic free jet obtained by exciting the 35711 cm^{-1} band. Sample temperature is 84 °C. Helium backing pressure is 1 atm. Resolution is 14 cm^{-1}. Band positions are displayed relative to the 35711 cm^{-1} band

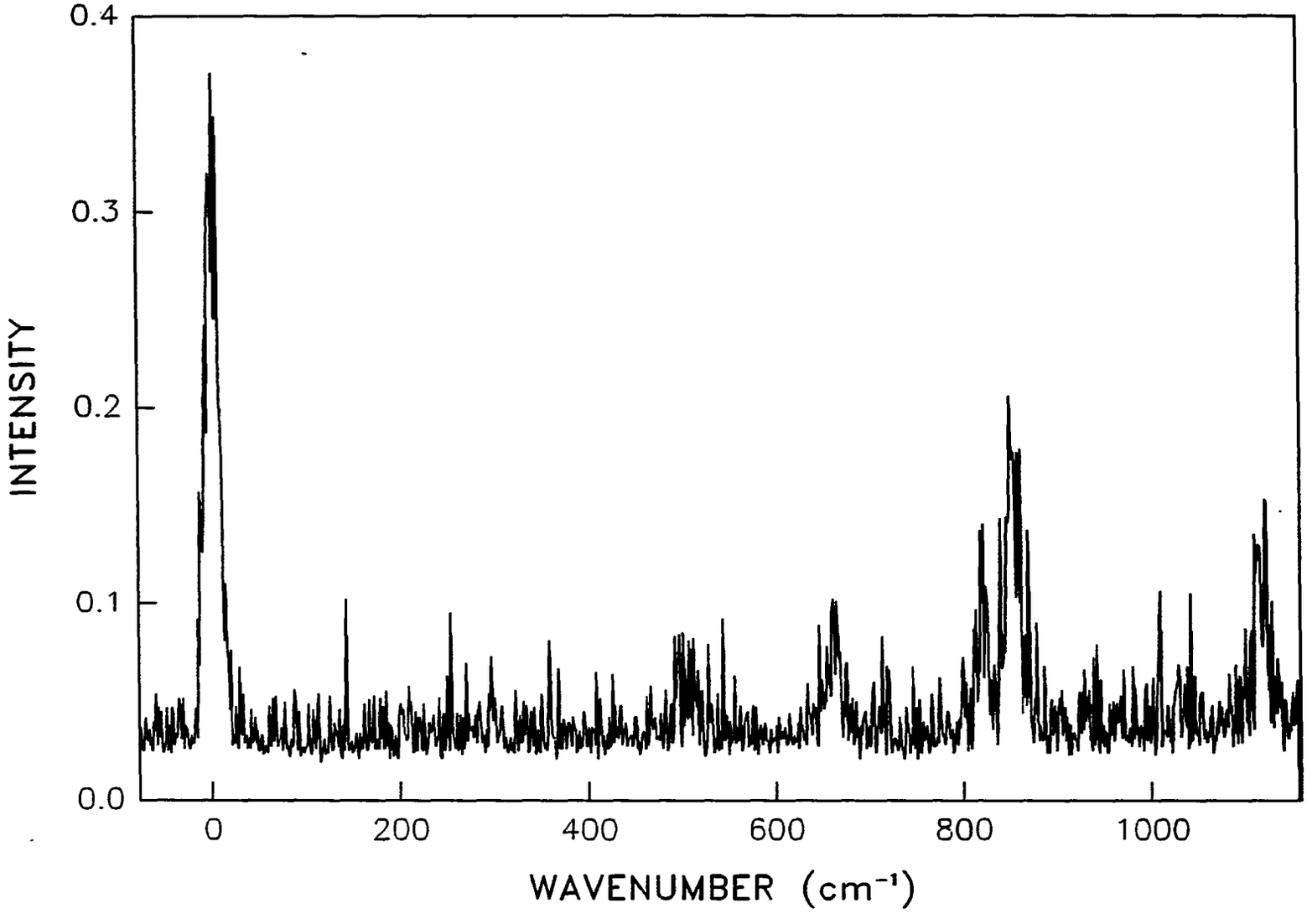
0.4
0.3
0.2
0.1
0.0
INTENSITY
0
200
400
600
800
1000
WAVENUMBER (cm⁻¹)

Figure 15. Dispersed fluorescence spectrum of p-tert-butylphenol in a supersonic free jet obtained by exciting the 35747 cm^{-1} band. Sample temperature is 84 °C. Helium backing pressure is 1 atm. Resolution is 14 cm^{-1}. Band positions are displayed relative to the 35747 cm^{-1} band

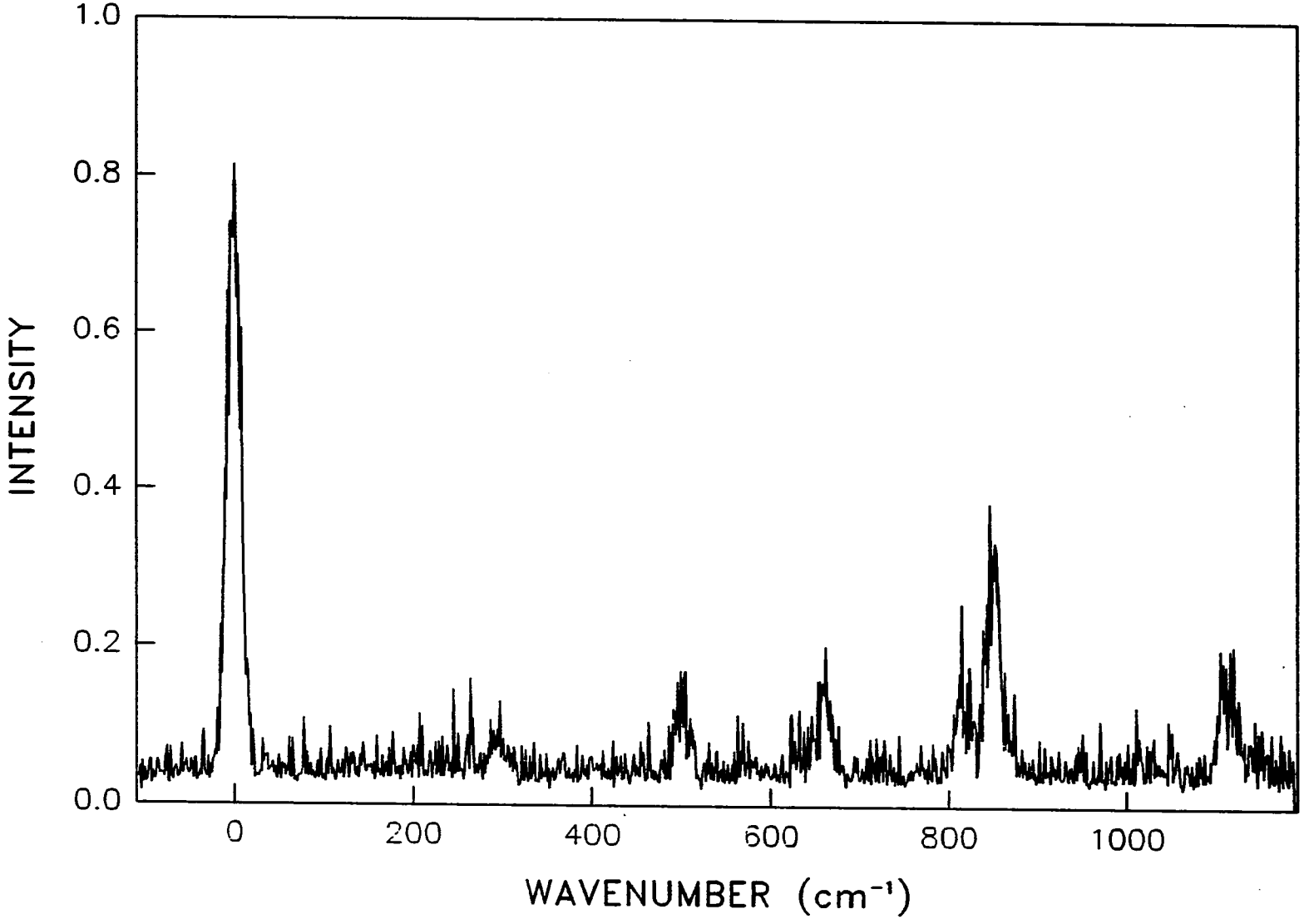
1.0
0.8
0.6
0.4
0.2
0.0
INTENSITY
0
200
400
600
800
1000
WAVENUMBER (cm⁻¹)

Table 10. Vibrational analysis of the dispersed fluorescence spectra of p-tert-butylphenol

35711 cm^{-1} excit. $\Delta\nu$ (cm^{-1})	35747 cm^{-1} excit. $\Delta\nu'$ (cm^{-1})	From Ref. (44)	assignment
	269		
	297		Hydroxyl torsion.
508	505	507	$16b_1$
664	663	660	4_1
823	828	827	1_1
855	858	851	5_1
1119	1120	1112	$18a_1$ or E_1[a]

[a]Asymmetric $-CH_3$ rocking vibrational mode.

P-propylphenol

The fluorescence excitation spectrum of p-propylphenol is presented in Fig. 16 and the vibrational band assignments are listed in Table 11. The excitation spectrum of p-propylphenol shows multiple origin bands (more than two), which is different from the previously discussed molecules. As mentioned earlier, doublet origin bands have been observed for the n-propylbenzene (49 cm^{-1} energy separation between the two origin bands) by Hopkins et al. and for the p-propylaniline (55 cm^{-1} energy separation between the two origin bands) by Powers et al., respectively (25,39). Recently, Breen et al. (26) have studied p-propyltoluene in a supersonic jet and they observed two origin bands with an energy separation of 49 cm^{-1}. These two origin bands have been assigned as origin bands for the anti- and gauche- isomers.

In the p-propylphenol case, five to ten possible origin bands are observed. However, only five bands in the lower energy region will be regarded as origin bands. The other bands which occur between 35517 cm^{-1} and 35554 cm^{-1} are assigned as bands representing propyl torsional motions for each isomer because only those five bands in the lower frequency region occur continuously throughout the excitation spectrum. The five origin bands are regarded as bands representing five different isomers. Although mode C repeatedly builds on each obvious vibrational mode of benzene, it is difficult to assign several bands in the 36250 cm^{-1} to 36400 cm^{-1} region due to spectral congestion. Therefore, a C^1 mode built on the 1^1 band or 5^1 band could not be assigned.

The dispersed fluorescence spectrum obtained by exciting the band

Figure 16. Fluorescence excitation spectrum of p-propylphenol in a supersonic free jet. Sample temperature is 77 °C. Helium backing pressure is 1 atm

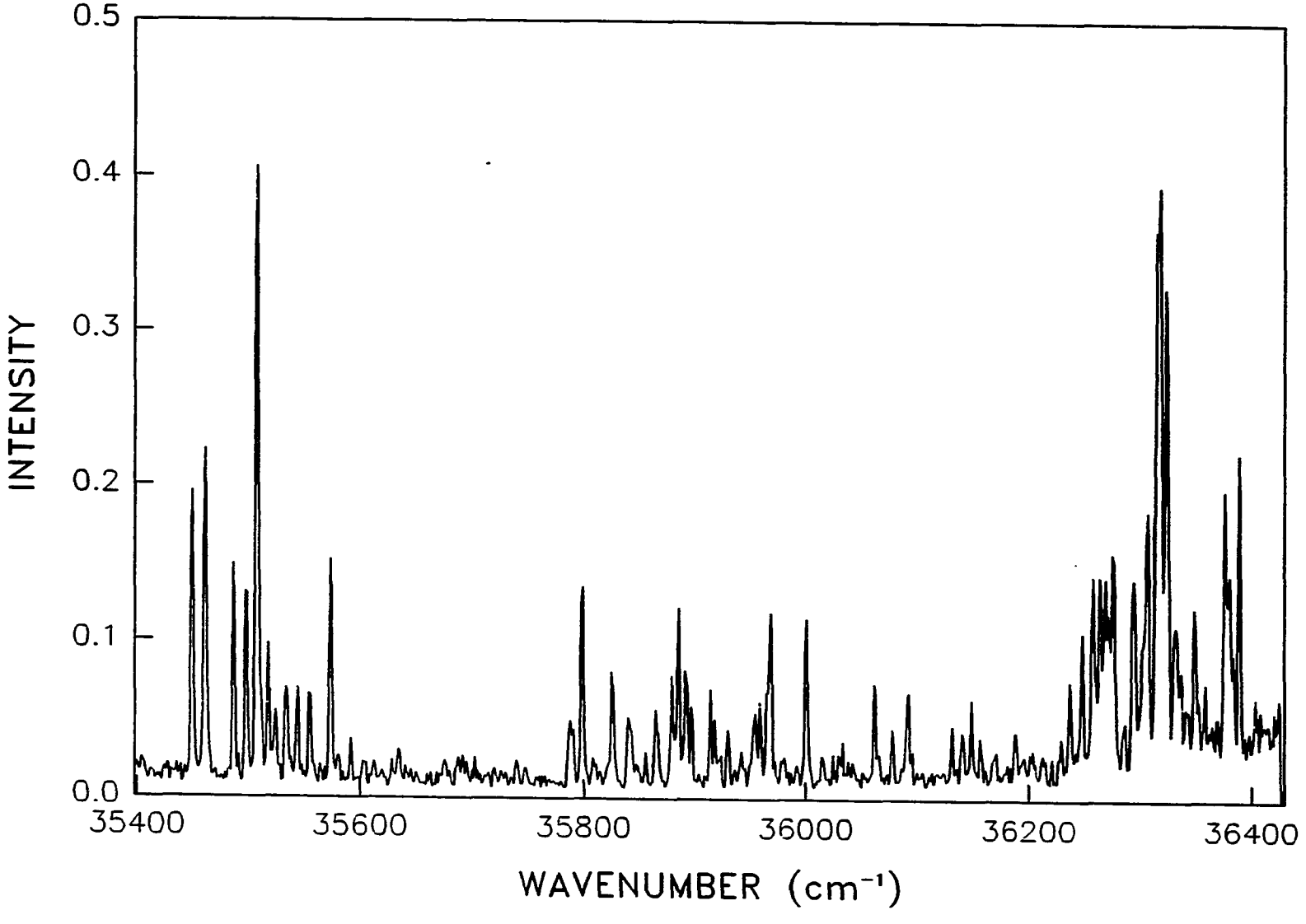
0.5
0.4
0.3
0.2
0.1
0.0
INTENSITY
35400
35600
35800
36000
36200
36400
WAVENUMBER (cm⁻¹)

Table 11. Assignments of vibronic bands observed in the fluorescence excitation spectrum of p-propylphenol in a supersonic jet in the region of the $S_1 \leftarrow S_0$ transition

observed freq. ν (cm^{-1})	$\Delta\nu$ (cm^{-1}) relative to 35507 cm^{-1}	$\Delta\nu'$ (cm^{-1}) relative to each origin	assignment
35449	-58	0	(0-0)(t-s)[a]
35461	-46	0	(0-0)(t-a)[b]
35486	-21	0	(0-0)(s-g)[c]
35498	-90	0	(0-0)(a-g)[d]
35507	0	0	(0-0)(t)[e]
35517	10	68	C^1(t-s)
35532	25	71	C^1(t-a)
35543	36	57	C^1(s-g)
35554	47	56	C^1(a-g)
35573	66	66	C^1(t)
35633	127		C^2(t)
35798	291		
35825	318	376	$16a^1$(t-s)
35839	332	378	$16a^1$(t-a)
35864	357	378	$16a^1$(s-g)
35879	372	381	$16a^1$(a-g)

[a]Trans-syn isomer.

[b]Trans-anti isomer.

[c]Syn-gauche isomer.

[d]Anti-gauche isomer.

[e]Trans isomer.

Table 11. (continued)

observed freq. ν (cm^{-1})	$\Delta\nu$ (cm^{-1}) relative to 35507 cm^{-1}	$\Delta\nu'$ (cm^{-1}) relative to each origin	assignment
35884	377	377	$16a^1(t)$
35892	385	443	$16a^1c^1(t\text{-}s)$
35903	396	442	$16a^1c^1(t\text{-}a)$
35929	422	443	$16a^1c^1(s\text{-}g)$
35954	447	447	$16a^1c^1(t)$
35968	461		$6a^1(t)$
36000	493		$16b^1(t)$
36091	584		
36188	681	739	$4^1(t\text{-}s)$
36203	696	742	$4^1(t\text{-}a)$
36229	722	743	
36236	729	750	$4^1(s\text{-}g)$
36247	740	749	$4^1(a\text{-}g)$
36256	749	749	$4^1(t)$
36263	756	814	$1^1(t\text{-}s)$
36267	760		
36274	767	813	$1^1(t\text{-}a)$
36285	778		
36296	789	810	$1^1(s\text{-}g)$
36313	807	816	$1^1(a\text{-}g)$
36323	818	818	$1^1(t)$

Table 11. (continued)

observed freq. ν (cm^{-1})	$\Delta\nu$ (cm^{-1}) relative to 35507 cm^{-1}	$\Delta\nu'$ (cm^{-1}) relative to each origin	assignment
36332	825	825	$5^1(t)$
36336	829		
36342	835		
36350	843	843	$18a^1(t)$
36360	852		

Figure 17. Dispersed fluorescence spectrum of p-propylphenol in a supersonic free jet obtained by the exciting 35424 cm^{-1} band. Sample temperature is 82 °C Helium backing pressure is 1 atm. Resolution is 14 cm^{-1}. Band positions are displayed relative to the 35424 cm^{-1} band

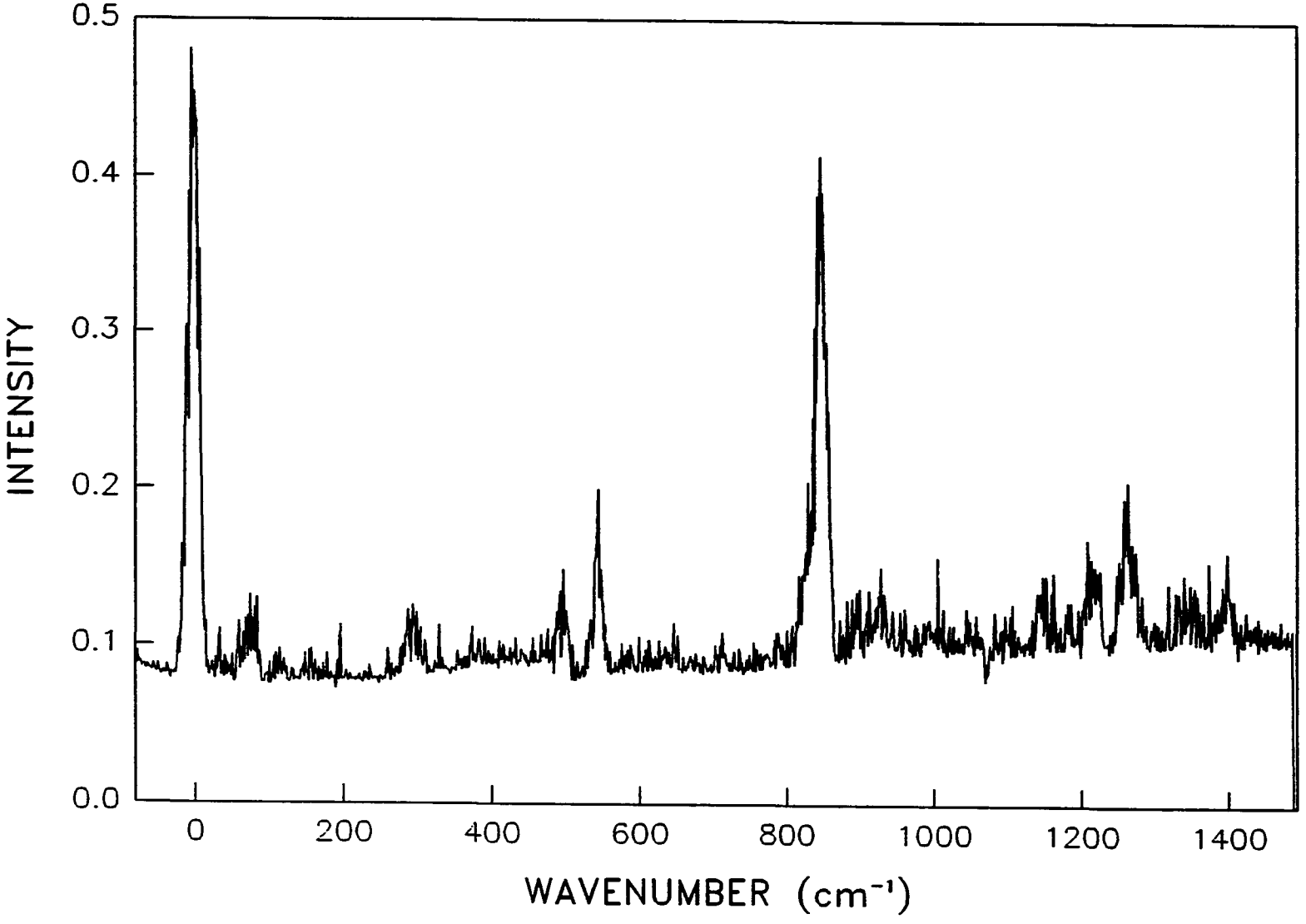
0.5
0.4
0.3
0.2
0.1
0.0
INTENSITY
0
200
400
600
800
1000
1200
1400
WAVENUMBER (cm⁻¹)

Table 12. Vibrational analysis of the dispersed fluorescence spectrum of p-propylphenol

35507 cm^{-1} excit. relative freq. $\Delta\nu$ (cm^{-1})	36324 cm^{-1} excit. relative freq. $\Delta\nu$ (cm^{-1})	assignment
80		C_1[a]
296		Hydroxyl torsion
	342	$1^1 16a_1$
504	500	$6a_1$
549		$16b_1$
854	848	1_1, 1^1
907		
939	939	5_1
1156		$18a_1$ or E_1[b]
1227		F_1[c]
1273		$7a_1$
1364		3_1

[a]Propyl torsional motion.

[b]Asymmetric $-CH_3$ rocking vibrational motion.

[c]O-H bending vibration.

at 35507 cm^{-1} [(0-0)(trans)] is shown in Fig. 17 and the assignments of the observed bands are listed in Table 12. The 80 cm^{-1} vibration is assigned as a mode C and the 296 cm^{-1} vibration is tentatively assigned to the ground state hydroxyl torsional mode. The dispersed fluorescence spectrum obtained by 1^1 band excitation shows a very broad feature at ~840 cm^{-1} lower in frequency ($1\frac{1}{1}$) from the excitation energy, and this may be an indication of intramolecular vibrational relaxation at ~ 800 cm^{-1}.

P-pentylphenol

The fluorescence excitation spectrum of p-pentylphenol is shown in Fig. 18 and the assignments of observed bands are listed in Table 13. The excitation spectrum shows very complicated structures in the (0-0) origin band region as well as 1^1 band region. Therefore, it is very difficult to confidently assign all the features. However, at least twelve different isomers could be identified based on bands in the origin band region. By applying the same interpretations as discussed for the p-propylphenol case, the 35489 cm^{-1} band is assigned as an origin band of the trans-isomer. Four bands between 35443 cm^{-1} and 35458 cm^{-1} are assigned as origin bands of anti-isomers (e.g., anti-gauche and anti-eclipsed), and other bands in the lower frequency region are assigned as the origin bands of the syn-isomers (e.g., syn-gauche and syn-eclipsed). To get a better understanding of the molecular vibrational structures, more data, such as dispersed fluorescence data via excitation of several bands in origin band region or infrared and Raman data, would be required.

Fig. 19 and Fig. 20 show dispersed fluorescence spectra of p-pentyl phenol obtained by exciting at 35489 cm^{-1} and 35424 cm^{-1}. The vibrational assignments of these spectra are listed in Table 14. From the analysis of these spectra, some additional vibrational modes of benzene ring are identified. Although experiments to excite several more bands for the dispersed fluorescence spectra were performed, no useful data were obtained due to the very low fluorescence quantum yield of p-pentylphenol.

Figure 18. Fluorescence excitation spectrum of p-pentylphenol in a supersonic free jet. Sample temperature is 85 °C. Helium backing pressure is 1 atm

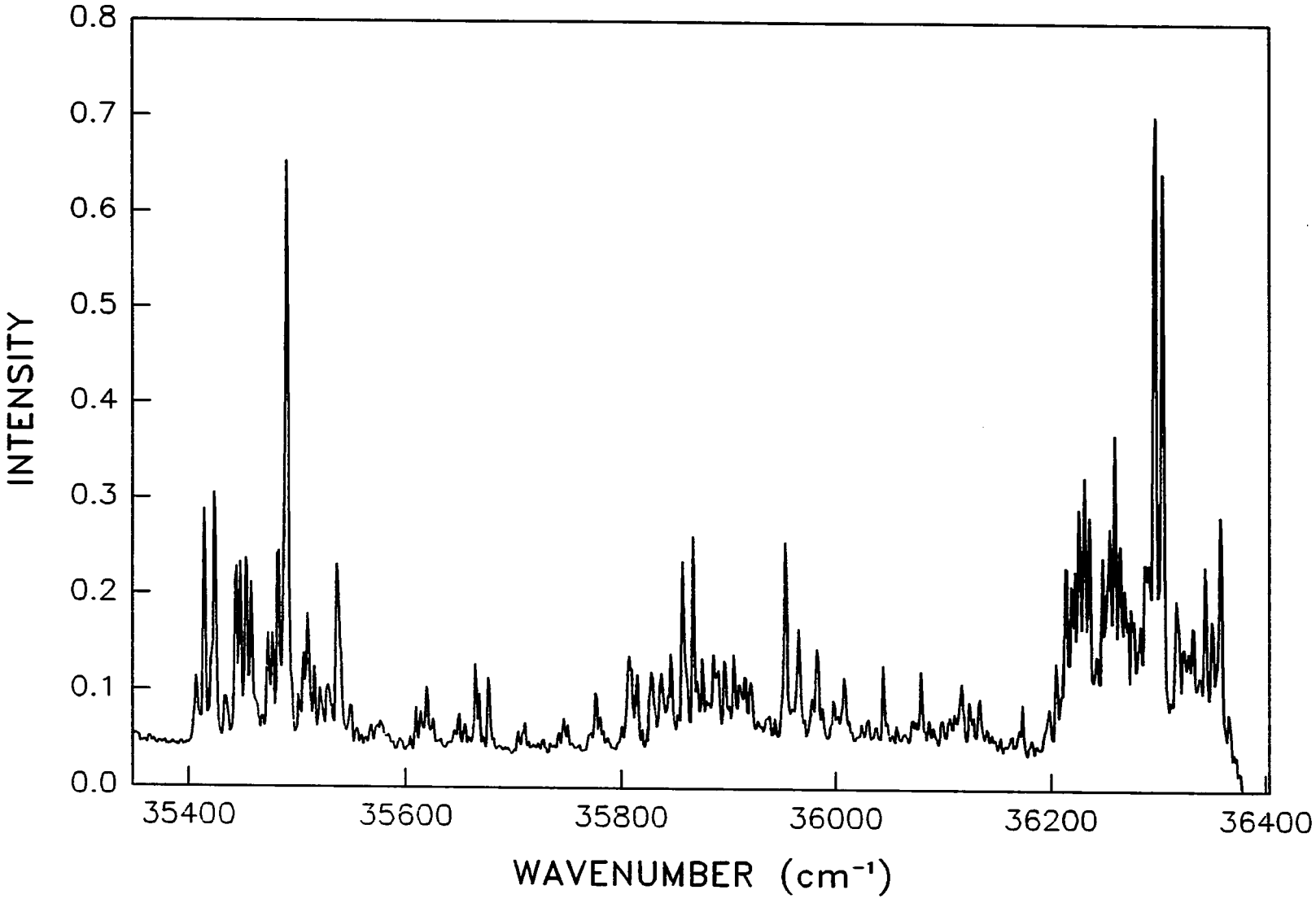
0.8
0.7
0.6
0.5
0.4
0.3
0.2
0.1
0.0
INTENSITY
35400
35600
35800
36000
36200
36400
WAVENUMBER (cm⁻¹)

Table 13. Assignment of vibronic bands observed in the fluorescence excitation spectrum of p-pentylphenol in a supersonic jet in the range of the $S_1 \leftarrow S_0$ transition

observed freq. ν (cm^{-1})	$\Delta\nu$ (cm^{-1}) relative to 35489 cm^{-1}	assignment
35407	-82	(0-0)(s)[a]
35414	-75	
35420	-69	
35424	-65	
35443	-46	
35448	-41	(0-0)(a)[b]
35453	-36	
35458	-31	
35472	-17	
35477	-12	
35482	-7	
35489	0	(0-0)(t)[c]
35501	12	
35505	16	
35509	20	
35515	26	
35520	31	
35527	38	

[a]Syn-isomers (syn-gauche and syn-eclipsed).

[b]Anti-isomers (anti-gauche and anti-eclipsed).

[c]Trans-isomers.

Table 13. (continued)

observed freq. ν (cm^{-1})	$\Delta\nu$ (cm^{-1}) relative to 35489 cm^{-1}	assignment
35536	47	
35539	50	
35665	176	
35668	179	
35678	189	$16a^1(s)$
35801	312	
35809	320	
35815	326	
35828	339	$16a^1(a)$
35838	349	
35844	355	
35858	369	
35867	378	$16a^1(t)$
35876	387	$6a^1(s)$
35886	397	
35891	402	
35896	407	
35910	421	$6a^1(a)$
35915	426	
35921	432	
35953	464	$6a^1(t)$
35965	476	
35999	510	

Table 13. (continued)

observed freq. ν (cm^{-1})	$\Delta\nu$ (cm^{-1}) relative to 35489 cm^{-1}	assignment
36009	520	
36045	556	
36080	591	
36205	716	
36214	725	
36220	731	
36223	734	
36226	737	
36231	742	$1^1(s)$
36236	747	
36243	754	
36249	760	
36256	767	$1^1(a)$
36260	771	
36265	776	
36270	781	
36273	784	
36276	787	
36279	790	
36285	796	
36289	800	
36293	804	

Table 13. (continued)

observed freq. ν (cm^{-1})	$\Delta\nu$ (cm^{-1}) relative to 35489 cm^{-1}	assignment
36299	810	$1^1(t)$
36395	816	$5^1(t)$
36319	830	
36326	837	
36334	846	
36346	857	

Figure 19. Dispersed fluorescence spectrum of p-pentylphenol in a supersonic free jet obtained by the exciting 35424 cm^{-1} band. Sample temperature is 90 °C. Helium backing pressure is 1 atm. Resolution is 14 cm^{-1}. Band position are displayed relative to the 35424 cm^{-1} band

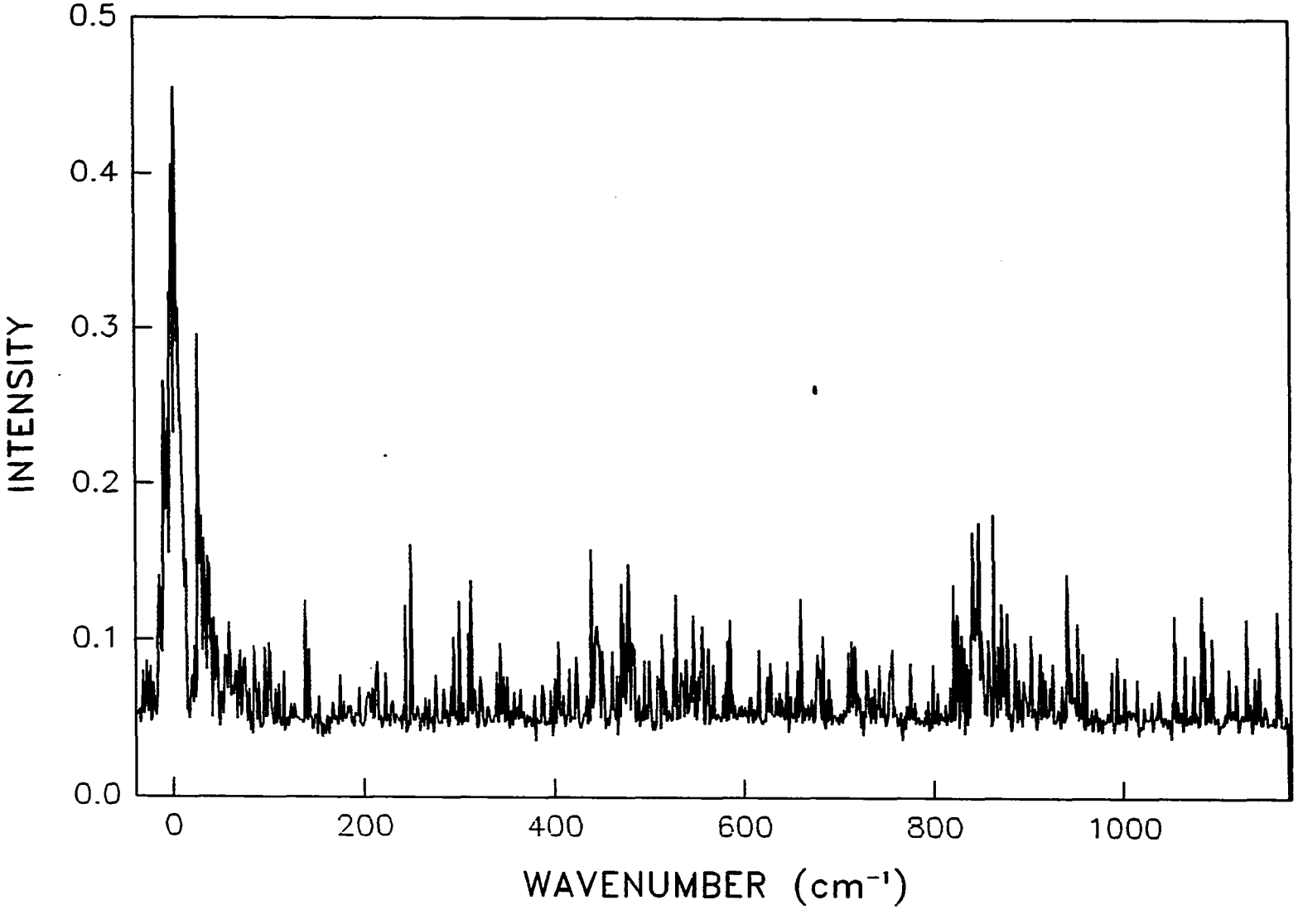
0.5
0.4
0.3
0.2
0.1
0.0
INTENSITY
0
200
400
600
800
1000
WAVENUMBER (cm⁻¹)

Figure 20. Dispersed fluorescence spectrum of p-pentylphenol in a supersonic free jet obtained by the exciting 35489 cm^{-1} band. Sample temperature is 90 °C. Helium backing pressure is 1 atm. Resolution is 14 cm^{-1}. Band positions are displayed relative to the 35489 cm^{-1} band

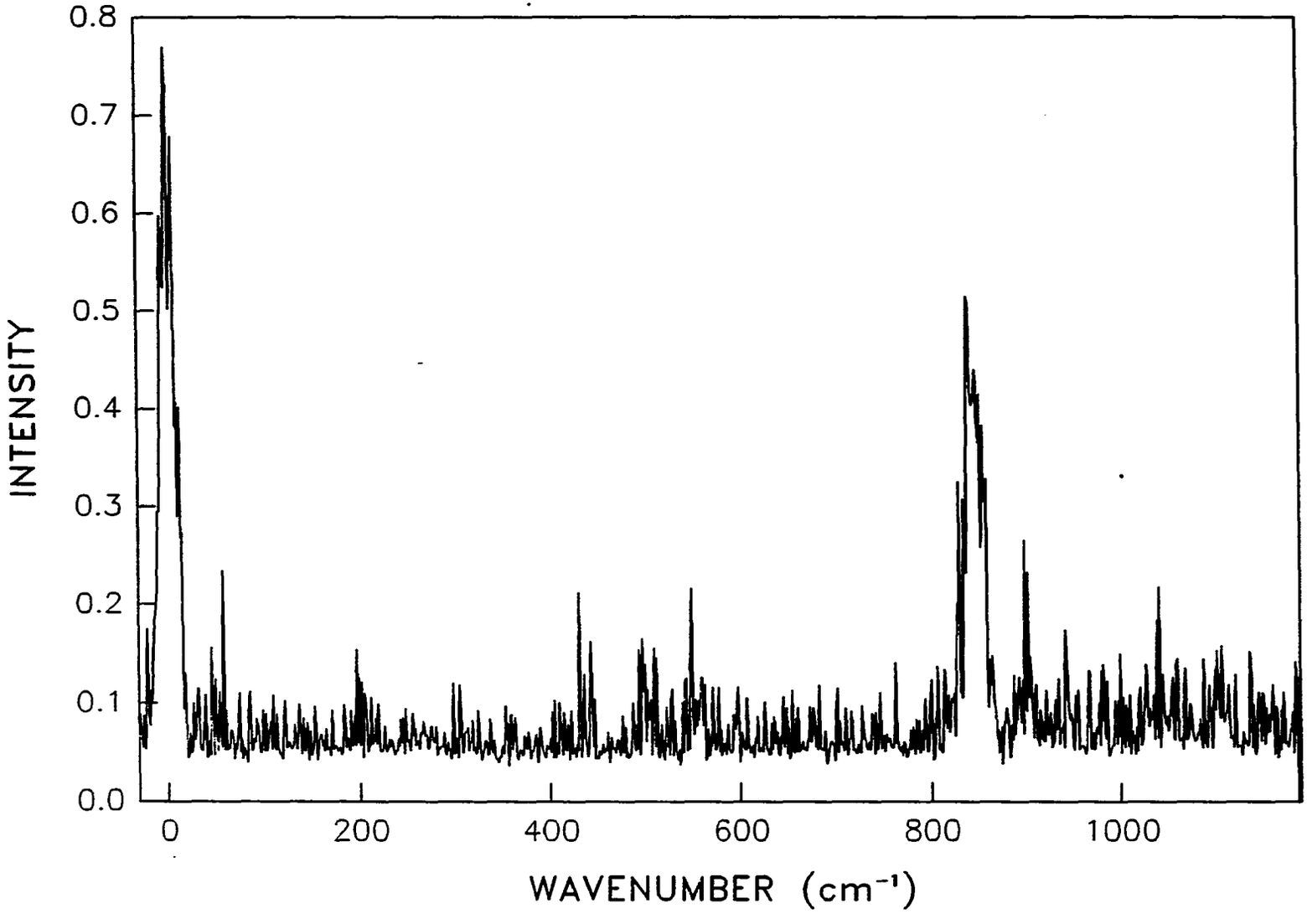
0.8
0.7
0.6
0.5
0.4
0.3
0.2
0.1
0.0
INTENSITY
0
200
400
600
800
1000
WAVENUMBER (cm⁻¹)

Table 14. Vibrational analysis of the dispersed fluorescence spectra of p-pentylphenol

35489 cm^{-1} excit. relative freq. $\Delta\nu$ (cm^{-1})	35424 cm^{-1} excit. relative freq. $\Delta\nu'$ (cm^{-1})	assignment
	440	
	475	
549		$6a_1$
555		
	825	
848	849	1_1
904		5_1

DISCUSSIONS

P-cresol and P-ethylphenol

The features of the fluorescence excitation spectra of p-cresol and p-ethylphenol are very similar except for extra bands in the excitation spectrum of p-ethylphenol due to the ethyl torsional motions. One common feature between the two spectra is the single origin band, i.e., there is only one isomer. Studies on toluene, ethylbenzene, and p-ethyltoluene by Breen et al. (26-28) have also shown only one origin band in the multiphoton ionization spectra. In their study of ethylbenzene and diethylbenzenes, they suggested that the terminal carbon atom of the ethyl group projected up out of the plane of the benzene ring (26). The microwave study of ethylbenzene by True et al. also showed that the terminal carbon atom in the ethyl group projected up out of the plane of benzene ring (40).

If their suggestion concerning the spatial position of the terminal carbon atom in the ethyl group is applied to the present study, one isomer or two isomers can be identified depending on the position of the hydrogen in the hydroxyl group for the p-ethylphenol case. If the hydrogen of the hydroxyl group projects up out of the plane, two isomers can be obtained. In one isomer, the hydrogen of the hydroxyl group and the terminal carbon atom of the ethyl group project up out of the plane in the same direction, while in the other isomer, these project up out of the plane in the opposite directions. As a matter of a fact, another possible origin band is observed at 82 cm^{-1} to higher energy of the

35511 cm^{-1} origin band. This band occurs repeatedly throughout the spectrum with ~ 80-85 cm^{-1} energy separation from the vibrational modes belonging to the isomer which has the origin band at 35511 cm^{-1}.

However, the study on o-, m-, and p-dihydroxy benzene performed by Dunn et al. (41) has shown that the hydroxyl groups in dihydroxy benzenes lie in the plane of the benzene ring. Additionally, Kojima (42) showed that the hydroxyl group lies in the plane of benzene ring in his microwave study on phenol. Furthermore, the repulsion between the non-bonding electron pairs on the oxygen and the π electron cloud of the benzene ring makes the hydroxyl group lie in the plane of the benzene ring. Therefore, it is concluded that the hydroxyl group must lie in the plane of the benzene ring. Meanwhile, the terminal carbon atom of the ethyl group in the p-ethylphenol is thought to project up out of the plane of the benzene ring. In this conformation, only one stable isomer can exist. As a result, the band at 82 cm^{-1} to higher energy of origin band is assigned to the ethyl torsion. The conclusion that the hydroxyl group lies in the plane of the benzene ring will be applied to all of the molecules considered in this manuscript.

Doublet Origin Bands of P-isopropylphenol, P-sec-butylphenol, and P-tert-butylphenol

The fluorescence excitation spectra of p-isopropylphenol, p-sec-butylphenol and p-tert-butylphenol show different features when compared to those of p-cresol and p-ethylphenol with regard to the doublet origin bands. The doublet origin bands have been assigned in the results

section to two isomers. The energy separation between the two origin bands of p-isopropylphenol, p-sec-butylphenol and p-tert-butylphenol have been measured as 14 cm^{-1}, 13 cm^{-1} and 36 cm^{-1}, respectively.

What, then, is the cause of the doublet origin bands in the fluorescence spectra of p-isopropylphenol, p-sec-butylphenol, and p-tert-butylphenol? Two rotational isomers have been observed with a energy separation of 221 cm^{-1} by Oikawa et al. for p-dimethoxy benzene (32). They have assigned one of the isomers as a cis-isomer with C_{2v} symmetry and the other isomer as a trans-isomer with C_{2h} symmetry depending on the position of one methoxy group relative to the other methoxy group. Hopkins et al. have also observed isomers for the alkyl benzenes when the length of the carbon chain extends more than three (e.g., n-propylbenzene, n-butylbenzene etc.). They have explained that the two isomers (gauche, trans) are formed through the van der Waals interaction between the terminal hydrogen of the alkyl substituents and π electrons of the benzene ring (25). However, there was no evidence of isomers for the n-isopropylbenzene in their study. If the assignment for the rotational isomers by Hopkins et al. (25) is correct, any band from isomers should not be observed in the fluorescence excitation spectrum of p-isopropylphenol. Since evidence for isomers has been observed for the p-isopropylphenol in the present study, the hydroxyl group is expected to play some role in forming isomers.

If the p-isopropylphenol case is considered, the conformations of isomers are different depending on the whether the hydroxyl group and the terminal carbon atom of the isopropyl group lie in the plane of the benzene ring or on the plane perpendicular to the plane of the benzene

ring. Among these possible conformations of isomers, the position of hydroxyl group is regarded to lie in the plane of the benzene ring as was discussed in the p-ethylphenol case. Therefore, there are two possible situations for the conformations of these isomers. One situation is that the hydrogen atom (H_1) in the isopropyl group of p-isopropylphenol lies in the same plane as the benzene ring plane, and therefore the two methyl groups lie on the top and bottom of the benzene ring with certain angle (not 90° from the benzene ring plane). Then, there can be two isomers depending on whether the hydrogen of the hydroxyl group is on the trans position relative to the position of the hydrogen (H_1) in the alkyl substituents (a) or the hydrogen of the hydroxyl group is on the cis position (b) shown in Fig. 21. The isomer (a) is called as a cis-isomer and the isomer (b) is called a trans-isomer. These isomers are considered to form before the vaporization of the sample. The number ratio of the two isomers is fixed by the expansion through the nozzle. However, the number ratio of the two isomers is considered to change in the gas phase, because a variation in the intensity ratio between the origin bands of two isomers (~ 3 %) from one scan to another scan has been observed. This change of the intensity ratio between the two origin bands among the scans might be explained as being due to the equilibrium change between the carrier gas (helium) and the sample molecules inside the sample chamber. If there is a stable equilibrium between the carrier gas and the sample molecules in the gas phase, the intensity ratio should not be changed.

The other situation in forming isomers of p-isopropylphenol is that the terminal carbon atom in the isopropyl group lies in the plane

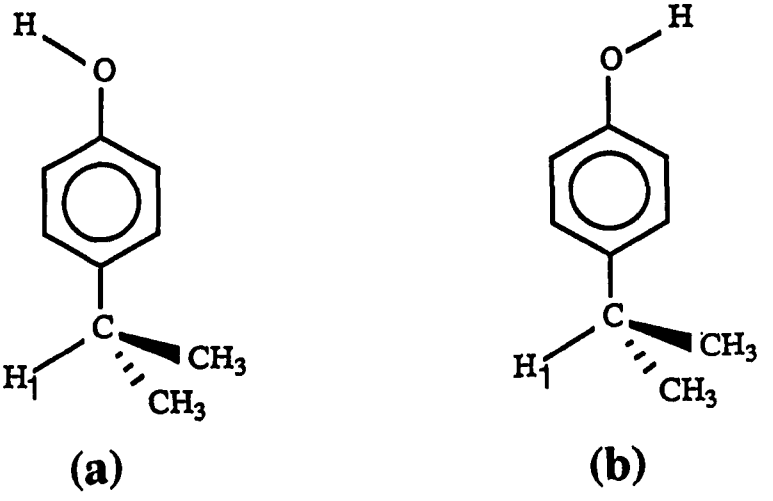

Figure 21. Conformational isomers of p-isopropylphenol assuming that the hydrogen (H_1) of the isopropyl group lies on the same plane as the plane of the benzene ring

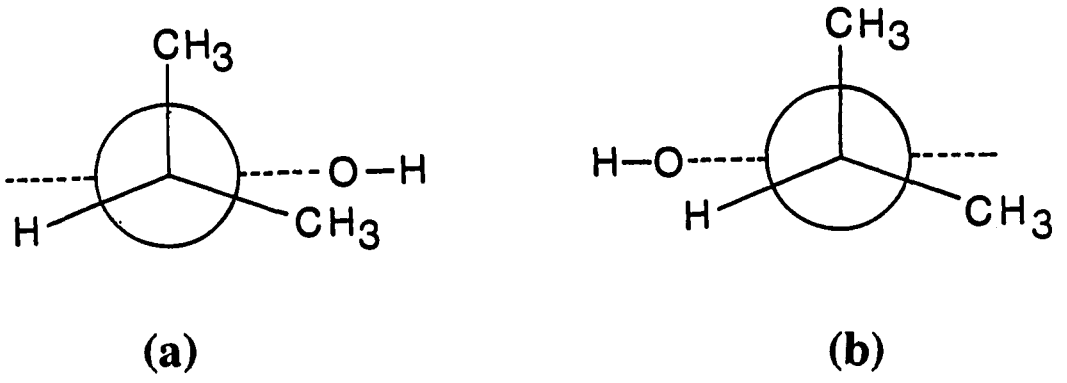

Figure 22. Conformational isomers of p-isopropylphenol assuming that one of the two methyl group in the isopropyl substituent lies on the plane perpendicular to the plane of the benzene ring

perpendicular to the benzene ring plane as Breen et al. (26) have suggested for ethyltoluene and as has been explained for the p-ethylphenol, then there are two possible isomers for the p-isopropyl phenol as shown in Fig. 22. In this case, one methyl group and a hydrogen in the isopropyl group lie out of the plane of the benzene ring, while the other methyl group lies on the plane perpendicular to the plane of the benzene ring. If this is the case, these conformations for the two isomers can be applied to the p-sec-butylphenol and p-tert-butylphenol cases, because all of these molecules show two origin bands with similar energy separations between them. However, in the p-tert-butylphenol case, no differences in the two possible conformers can be seen by assuming similar arrangements for the atoms in the p-tert-butyl group as in the p-isopropylphenol case.

There have been several studies concerning the conformations of isomers for the molecules which have isopropyl group as a para substituent (40,43). True et al. (40) have reported observing isomers of p-isopropyl benzaldehyde using microwave spectroscopy. They have explained that the two isomers of p-isopropyl benzaldehyde originated from the rotation of the isopropyl group with respect to the benzene ring plane. Additionally, their result shows that the hydrogen (H_1 in Fig. 21) in the isopropyl group is in the plane of benzene ring. Carrabba et al. (43) have also reported that isomer bands appear in the fluorescence excitation spectra of guaiazulene (1,4 - dimethyl-7-isopropyl azulene) in a supersonic jet with an energy separation of 105 cm^{-1}. They also pointed out that these isomers were formed by the rotation of the isopropyl group by 0° or 180° with respect to the

benzene ring plane. These results on the conformations of isomers are in agreement with our explanation on isomers of p-isopropylphenol. Therefore, the explanation by Breen et al. (26) about the position of the terminal carbon atom in the ethyl group cannot be applied to the cases of p-isopropylphenol, p-sec-butylphenol, and p-tert-butylphenol. Further discussion of these arguments for the formation of isomers will be done in the section on p-propyl phenol. High resolution (better than 0.05 cm^{-1}) scans of the origin bands did not reveal any additional spectral feature which might be due to other isomeric structures.

The fluorescence excitation spectrum of p-tert-butylphenol shows two origin bands at 35711 cm^{-1} and 35747 cm^{-1} corresponding to two isomers. These two isomers can be explained by assuming that the carbon atom in the one of the methyl groups lies in the plane of the benzene ring as shown in Fig. 23. The isomer (a) is called a cis-isomer and the isomer (b) is called as a trans-isomer. The larger energy separation (36 cm^{-1}) between the two isomer compared to that of p-isopropylphenol (14 cm^{-1}) might be explained as size effect of alkyl substituents. The bulky size of the tert-butyl group may cause the higher energy barrier between the two isomers compared to those of p-isopropylphenol's two isomers.

P-sec-butylphenol is structurally different from p-isopropylphenol and the p-tert-butylphenol because the sec-butyl group has a three carbon chain which could form isomers in the manner described by Hopkins et al. (25). A further consideration is that, structurally, p-sec-butylphenol has ability to have both isomers similar to those of p-isopropylphenol and those of n-propylbenzene as possible isomers.

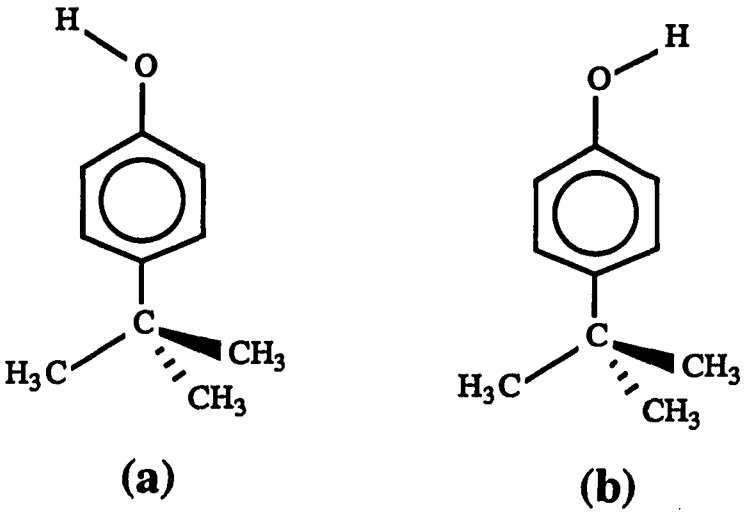

Figure 23. Conformational isomers of p-tert-butylphenol. A carbon atom of the one methyl group is assumed to lie in plane of the benzene ring

Thus, the number of isomers are expected to be the product of the number of isomers for the p-isopropylphenol and the p-propylphenol cases. As was discussed previously, the p-isopropylphenol has two isomers. P-propylphenol, which will be discussed later, has at least five isomers. Therefore, the number of stable isomers of p-sec-butylphenol is expected to be at least ten.

However, the fluorescence excitation spectrum of p-sec-butylphenol shows only two very intense bands in the origin region. Several weak intensity bands near the two intense bands are identified as bands due to hydrogen bonding between p-sec-butylphenol and water. Only the two very intense bands at 35537 cm^{-1} and 35550 cm^{-1} are clearly assignable as origins of the two isomers. Therefore, there is no indication of ten origin bands. We conclude that there are only two stable isomers in p-sec-butylphenol. Since the energy separation between the two origin bands is similar to that of p-isopropylphenol, the conformations of isomers are regarded as similar to those of the p-isopropylphenol case as shown in Fig. 24. The isomer (a) in Fig. 24 is called a cis-isomer and the isomer (b) is called a trans-isomer.

Why, then, there are only two isomers instead of ten in the p-sec-butylphenol? One possible explanation is steric hindrance between the alkyl groups in the sec-butyl substituent. The structural difference between the sec-butyl group and the propyl group is the existence of a extra methyl group instead of a hydrogen in the sec-butyl group. The presence of the methyl group in the p-sec-butylphenol sterically hinders rotation of the terminal ethyl group along the C_α-C_β bond. This steric hindrance prevents the rotation of the terminal ethyl group, and

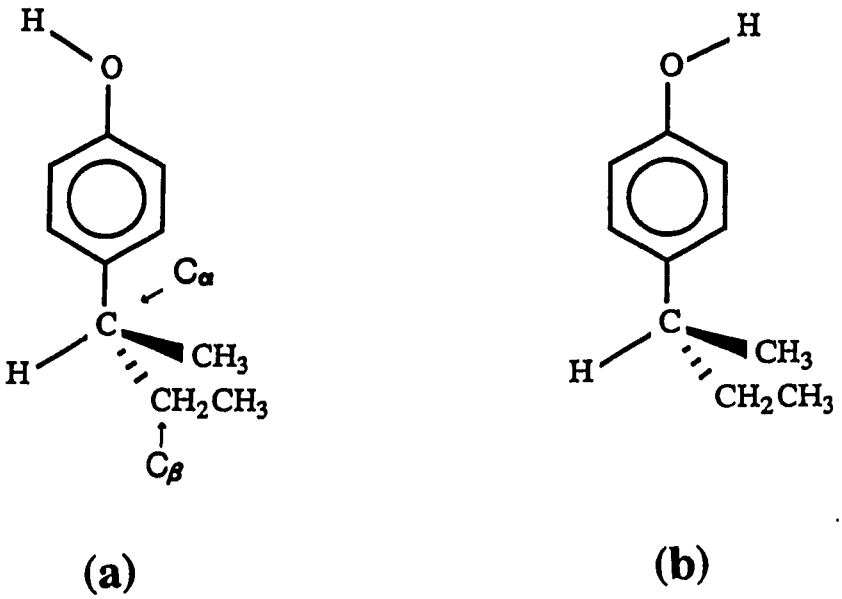

Figure 24. Conformational isomers of p-sec-butylphenol. The conformations of the two isomers are analogous to those of the p-isopropylphenol and p-tert-butylphenol case. The rotation of the ethyl chain in the sec-butyl group is regarded to be difficult due to the steric hindrance between the ethyl chain and the methyl group

therefore limits the conformations. Only the rotation along the single bond between the carbon atom of the benzene ring and C_α can occur. The two isomers come from this rotation. Additional calculations on the potential energy surface for the possible isomers would be necessary for a more accurate understanding of this situation.

Multiple Origin in P-propylphenol and P-pentylphenol

The previous studies by Breen et al. (27) and Hopkins et al. (25) have shown that there are only two stable conformational isomers in the p-propyltoluene and n-propylbenzene. However, the present fluorescence excitation spectrum of the p-propylphenol shows at least five origin bands. The conformations of the five isomers (conformers) can be understood if two rotational angles (τ_1, τ_2) are considered as shown in Fig. 25. If only τ_2 is considered, three rotational isomers can be suggested as shown in Fig. 26. The isomers (a), (b) and (c) are called trans, anti-gauche, and syn-gauche isomers, respectively, following the same notation used in the references (26-28). The terminal methyl group is regarded as freely rotating, and therefore, no isomers are produced by the rotation of this terminal methyl group.

Now, consider the possibility of the same type of isomers as Hopkins et al. assigned for the alkyl benzene (25). If their argument is applied to explain the conformations of the other two isomers, the isomers have the eclipsed conformations. The eclipsed conformation is regarded as the least stable isomer. Nevertheless, if this eclipsed conformer is a stable conformer, then two more eclipsed conformers can

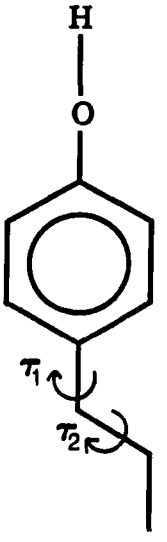

Figure 25. Rotational angles of propyl group in the p-propylphenol

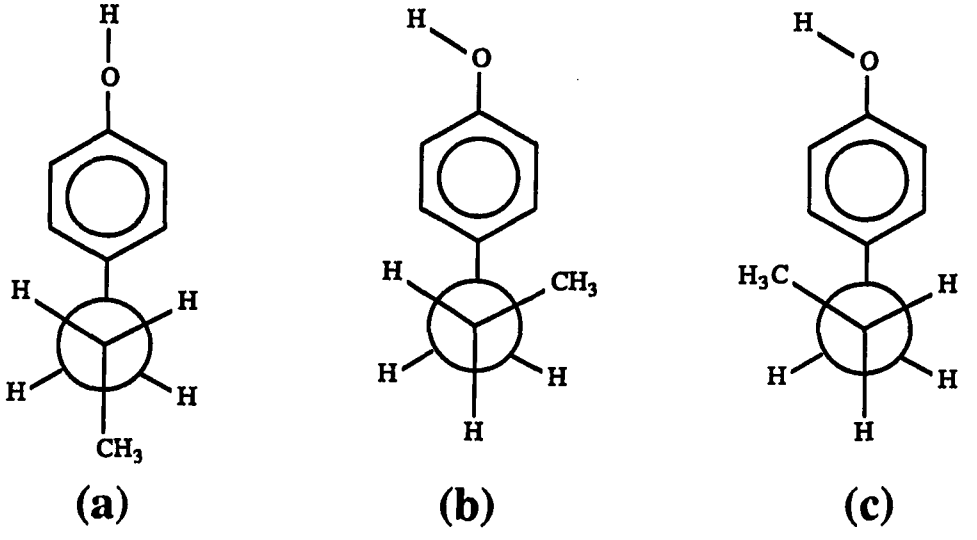

Figure 26. Conformational isomers of the p-propylphenol considering the rotation of τ_2 in Fig. 25

be generated by rotating the terminal ethyl group by 120° and 240°. Next, the rotation of the τ_1 should be considered. The rotation of τ_1 by 90° or 270° from the cis-eclipsed conformation, i.e., the terminal methyl group is right on the top of the benzene ring, yields two isomers depending on the site of the propyl group relative to the position of the hydroxyl hydrogen atom. If the τ_1 is rotated by 90° or 270° from the trans-conformation (isomer (a) in Fig. 26), two more isomers can be obtained depending on the site of the propyl group relative to the position of the hydroxyl hydrogen atom. Therefore, there are as many as eighteen possible isomers in the p-propylphenol even though the fluorescence excitation spectrum of p-propylphenol (Fig. 16) indicates that only five are seen. At this stage, however, the steric hindrance between alkyl substituents and π electrons of the benzene ring as well as among the hydrogens in the propyl substituents should be considered. If steric hindrance is considered, all of the eclipsed isomers are not as stable as other isomers which have been discussed. Steric hindrance also prevents the rotation of the propyl group in some conformations. Therefore, only five isomers are regarded as stable isomers.

The five origin bands observed in the fluorescence excitation spectra correspond to the above explained five isomers. The two isomers yielded by the τ_1 rotation from the trans-isomer are shown in Fig. 27. Isomer (a) is called a trans-syn isomer and the isomer (b) is called a trans-anti isomer. Among five isomers shown in Fig. 26 and Fig. 27, the trans- isomer is regarded as the most stable isomer if steric hindrance is considered. Additionally, the interaction between alkyl substituents and the π electrons of the benzene ring as well as between alkyl

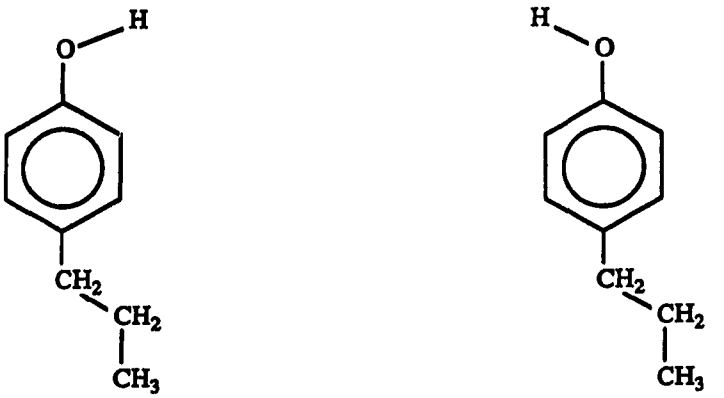

Figure 27. Conformational isomer of the p-propylphenol considering the rotation of the τ_1 in Fig. 25

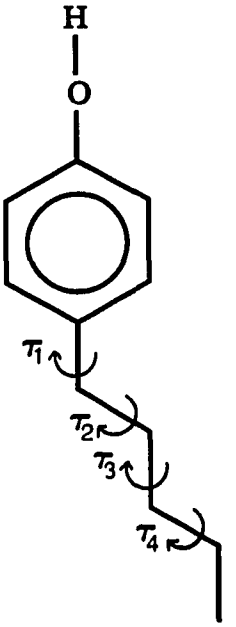

Figure 28. Rotational angles of the alkyl groups in the p-pentylphenol along the C-C single bonds

substituents and the non-bonding electron pairs in the oxygen tend to shift the position of the (0-0) band to lower energy through complex formation (27). Therefore, the most intense band at 35507 cm^{-1} is assigned as the origin band of the trans-isomer. Bands at 35449 cm^{-1} and 35461 cm^{-1} are assigned as origin bands of the syn-gauche isomer and the anti-gauche isomer, respectively. The other two origin bands at 35486 cm^{-1} and 35498 cm^{-1} are assigned as origin bands of the syn-trans isomer and the anti-trans isomer respectively. The observation of the five isomers in the p-propylphenol, which is different from the case of the p-sec-butylphenol, is understood by considering steric hindrance.

The fluorescence excitation spectrum of p-pentylphenol has a very complicated structure, especially in the (0-0) band region and in the 1^1 band region as shown in Fig. 18. Although it is difficult to assign isomers from this spectrum, at least six different isomers have been identified by analogy to the p-propylphenol case as shown in Fig. 29. Among the six isomers, isomers (a) and (d) are assigned as trans-isomers, and isomers (b) and (e) are assigned as anti-isomers. Isomers (c) and (f) are assigned as syn-isomers. Then, how many isomers does p-pentylphenol possess? In the excitation spectrum, at least twelve isomer can be distinguished. However, if all the rotational angles (τ_1, τ_2, τ_3, τ_4) in the pentyl group are considered, there will be more than twelve isomers in p-pentylphenol. Next, steric hindrance should be considered as was considered in the p-sec-butylphenol case and p-propylphenol case. We conclude tentatively that there are only twelve stable isomers in p-pentylphenol. However, the conformations of all the isomers cannot be understood easily because of the very complicated

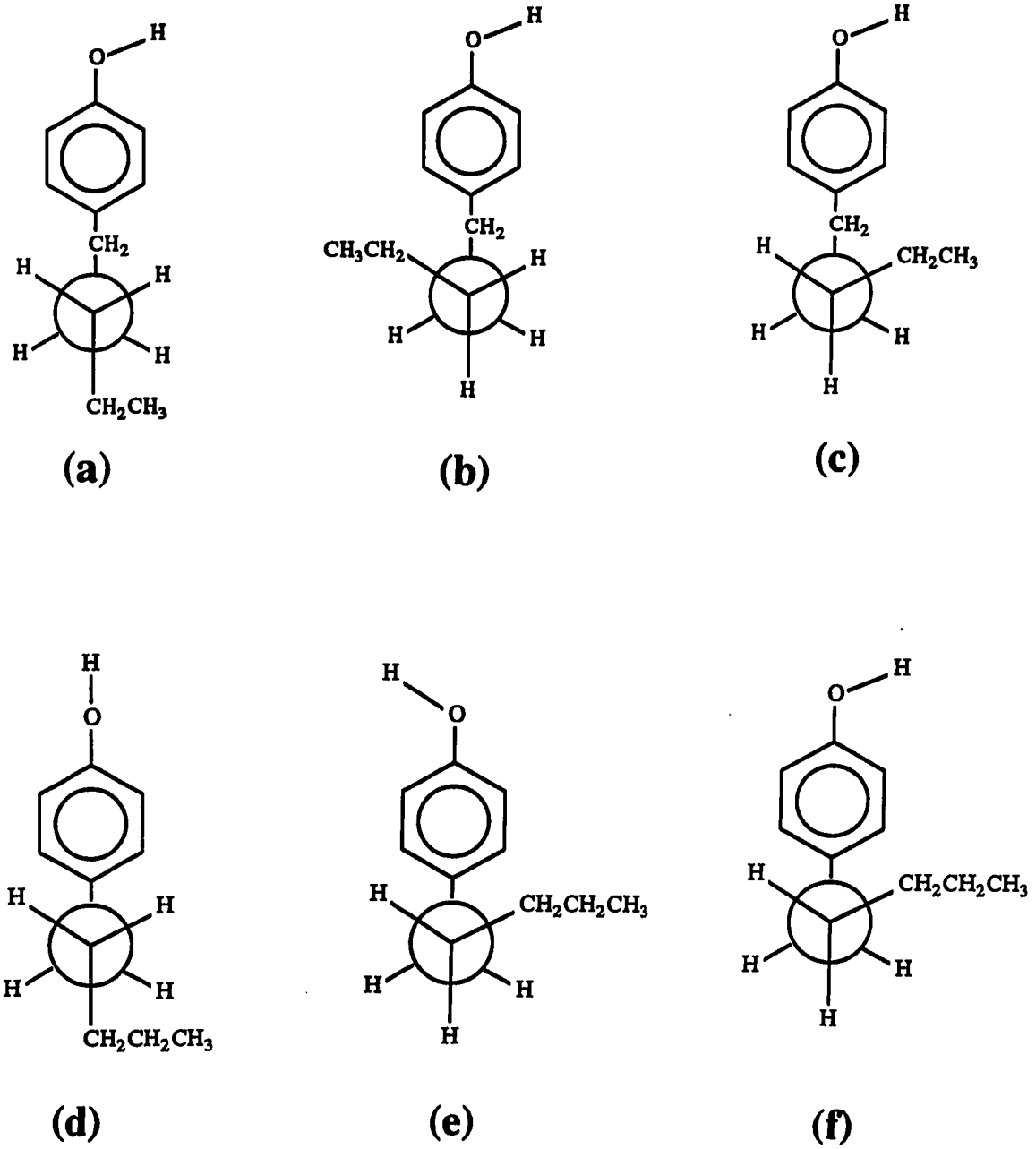

Figure 29. Conformational isomers of p-pentylphenol. Only six isomers are considered

excitation spectrum and the lack of confirming information. Nevertheless, the 35489 cm^{-1} band is tentatively assigned as an origin band for the trans-isomer. Four bands between 35443 cm^{-1} and 35458 cm^{-1} are assigned as origin bands of anti-isomers (anti-gauche and anti-eclipsed), and other bands in the lower frequency region are assigned as origin bands of syn-isomers (syn-gauche, syn-eclipsed). To get a better understanding of the electronic energy structures and the isomers, more data, such as dispersed fluorescence obtained by exciting several bands in origin band region or infrared and Raman data, are needed.

Hydrogen Bonded Structures of The P-alkyl Substituted Phenols with H_2O

Figures 30-34 show extended scans to lower energy in the fluorescence excitation spectra of several molecules described in this manuscript. These spectra contain another group of bands at ~350 cm^{-1} lower in energy from the (0-0)(trans) band of each molecule. To understand these possible hydrogen bonded structures, excess amounts of water vapor was seeded into the expansion with helium carrier gas. For p-cresol and phenol, several bands in this energy region showed decreased intensities with added water while several other bands showed increased intensities. Bands which showed increased intensities were assigned as bands from the transitions among energy levels of hydrogen bonded species with water. Bands which showed decreased intensities were assigned as bands from the p-cresol dimer and phenol dimer. Homodimers of phenol (phenol + phenol) have been studied by Fuke and

Figure 30. Extended scan of fluorescence excitation spectrum for p-cresol in a supersonic jet. Sample temperature is 50 °C. Helium backing pressure is 1 atm

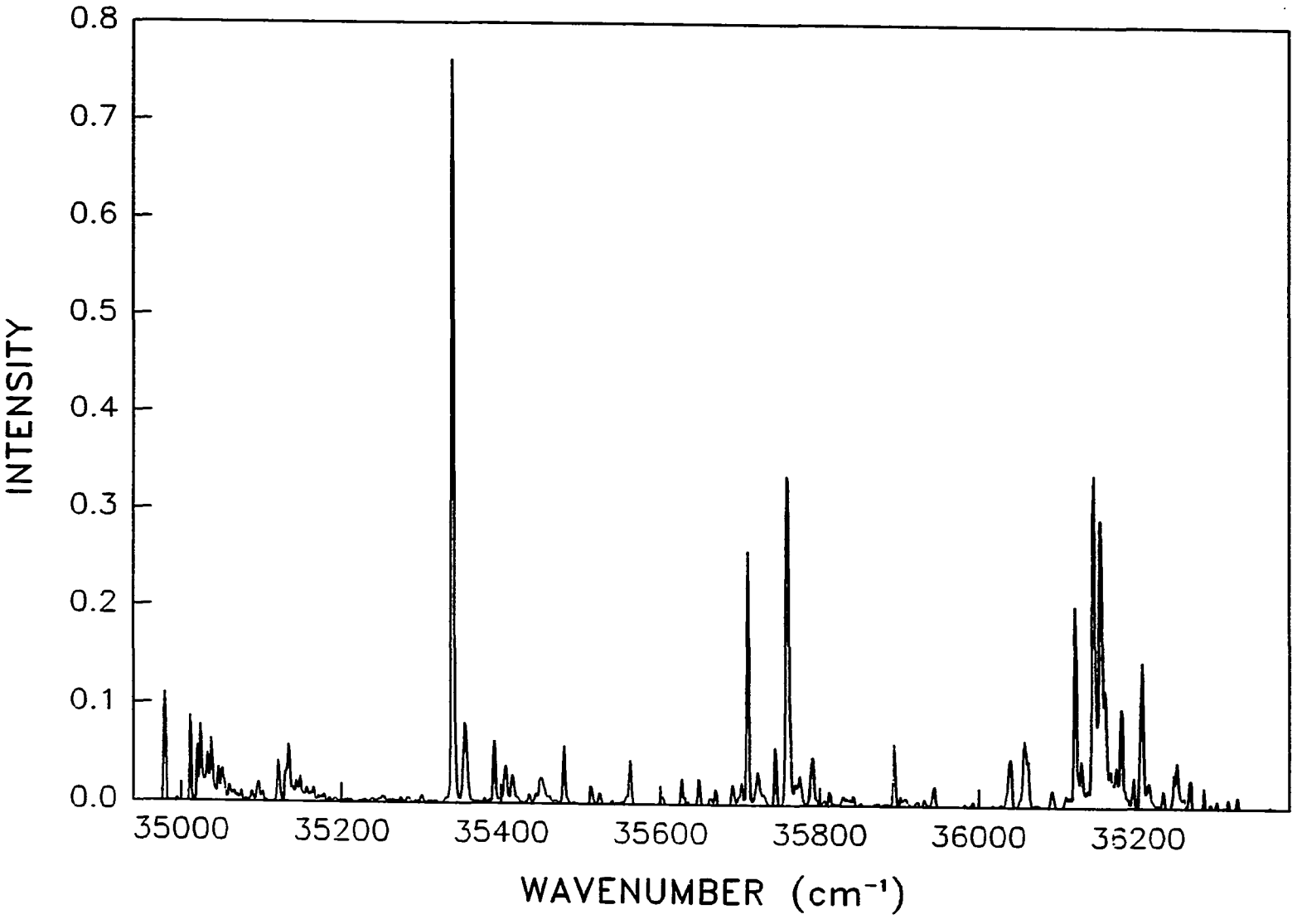
0.8
0.7
0.6
0.5
0.4
0.3
0.2
0.1
0.0
INTENSITY
35000
35200
35400
35600
35800
36000
36200
WAVENUMBER (cm⁻¹)

Figure 31. Extended scan of fluorescence excitation spectrum for p-isopropylphenol in a supersonic jet. Sample temperature is 82 °C. Helium backing pressure is 1 atm

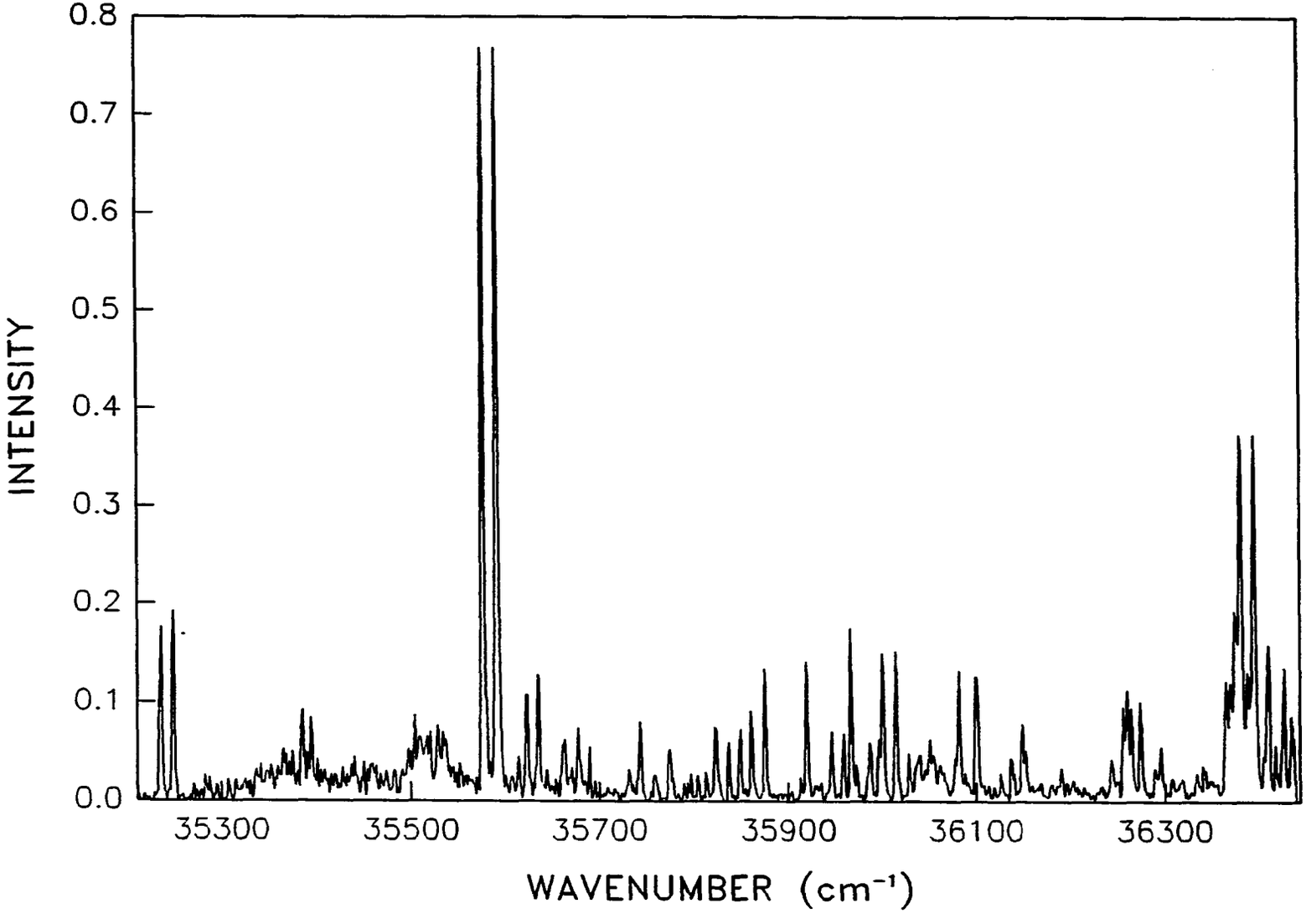
0.8
0.7
0.6
0.5
0.4
0.3
0.2
0.1
0.0
INTENSITY
35300
35500
35700
35900
36100
36300
WAVENUMBER (cm⁻¹)

Figure 32. Extended scan of fluorescence excitation spectrum for p-sec-butylphenol in a supersonic jet. Sample temperature is 72 °C. Helium backing pressure is 1 atm

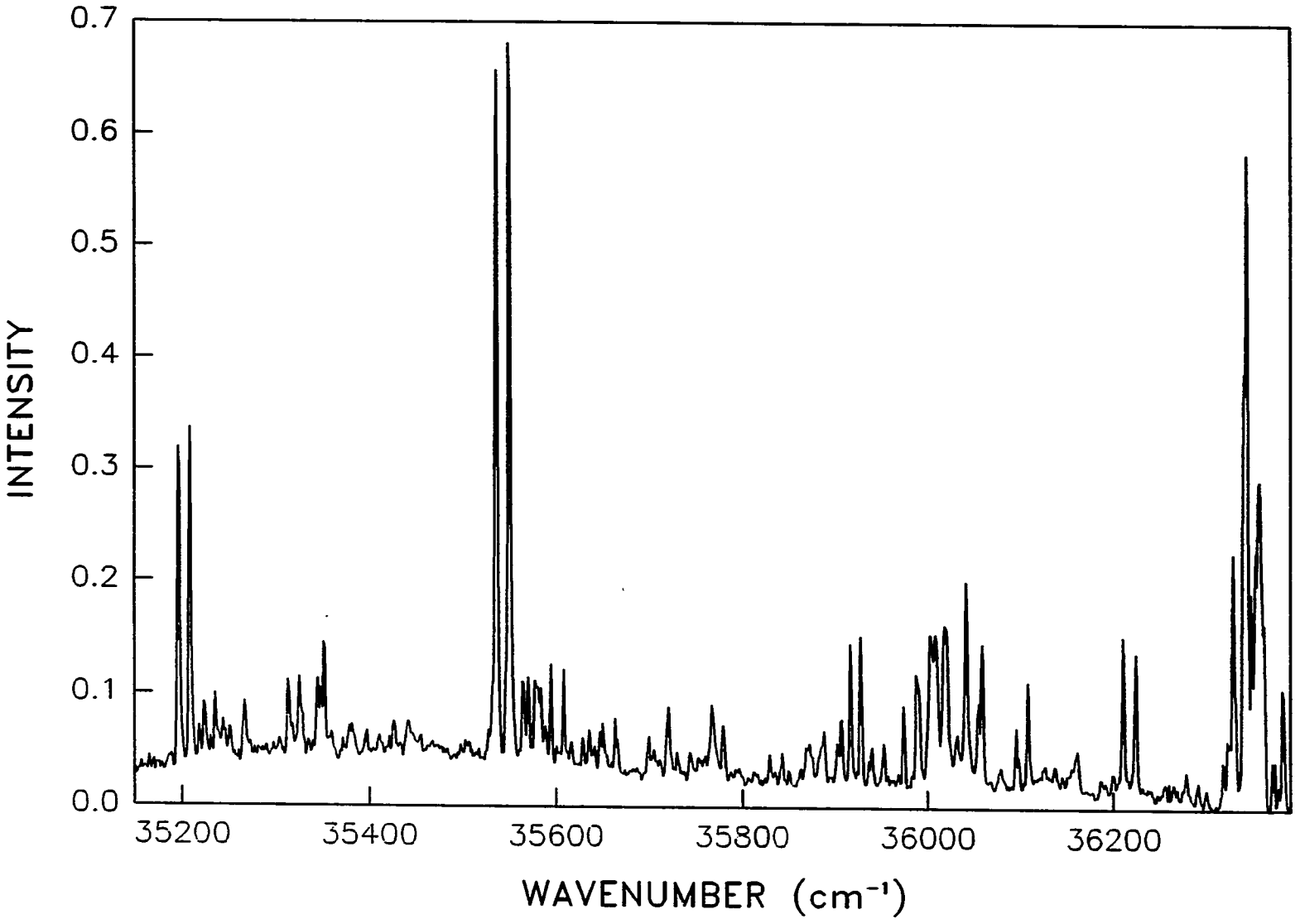
0.7
0.6
0.5
0.4
0.3
0.2
0.1
0.0
INTENSITY
35200
35400
35600
35800
36000
36200
WAVENUMBER (cm⁻¹)

Figure 33. Extended scan of fluorescence excitation spectrum for p-tert-butylphenol in a supersonic jet. Sample temperature is 72 °C. Helium backing pressure is 1 atm

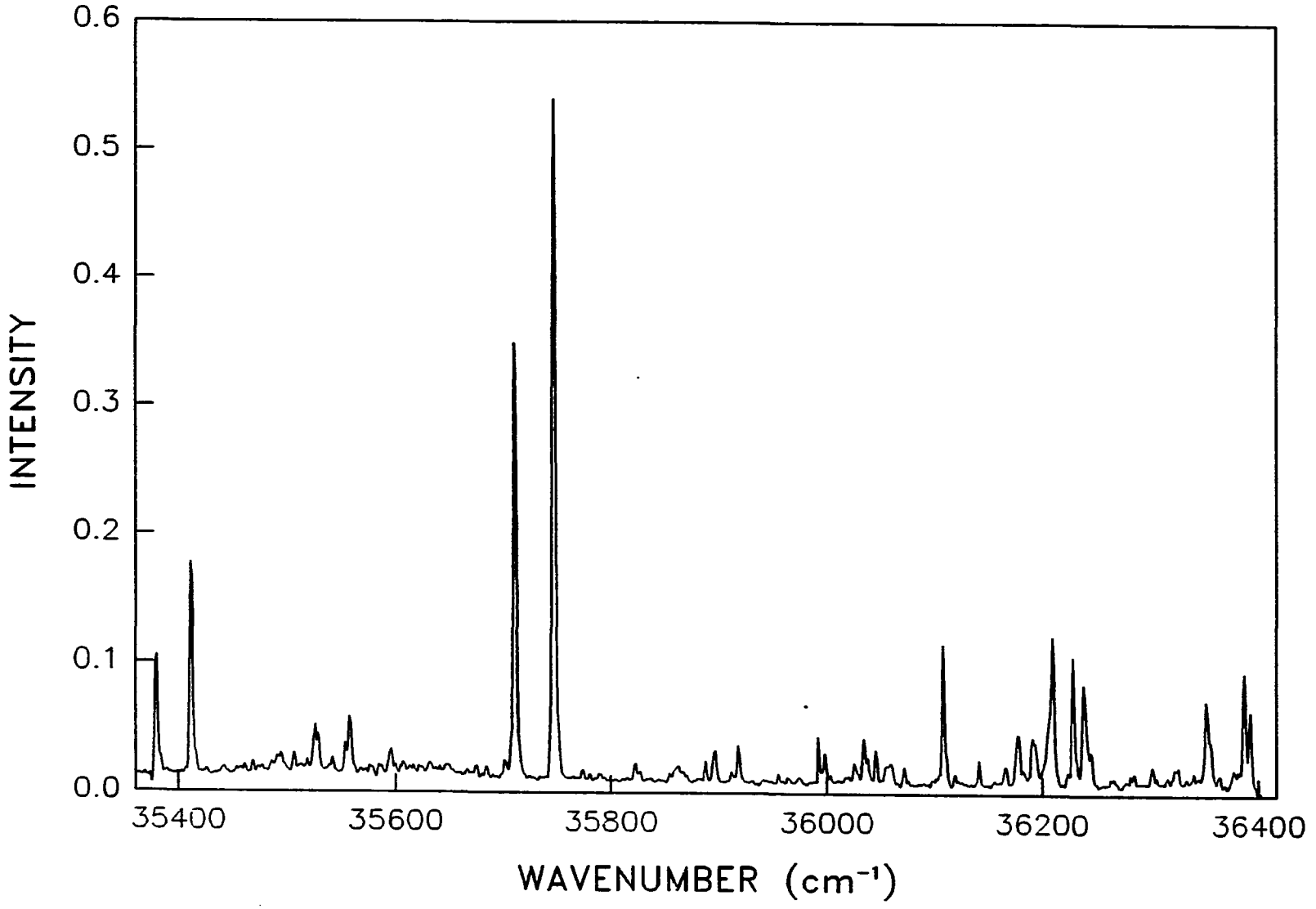
0.6
0.5
0.4
0.3
0.2
0.1
0.0
INTENSITY
35400
35600
35800
36000
36200
36400
WAVENUMBER (cm⁻¹)

Figure 34. Extended scan of fluorescence excitation spectrum for p-pentylphenol in a supersonic jet. Sample temperature is 85 °C. Helium backing pressure is 1 atm

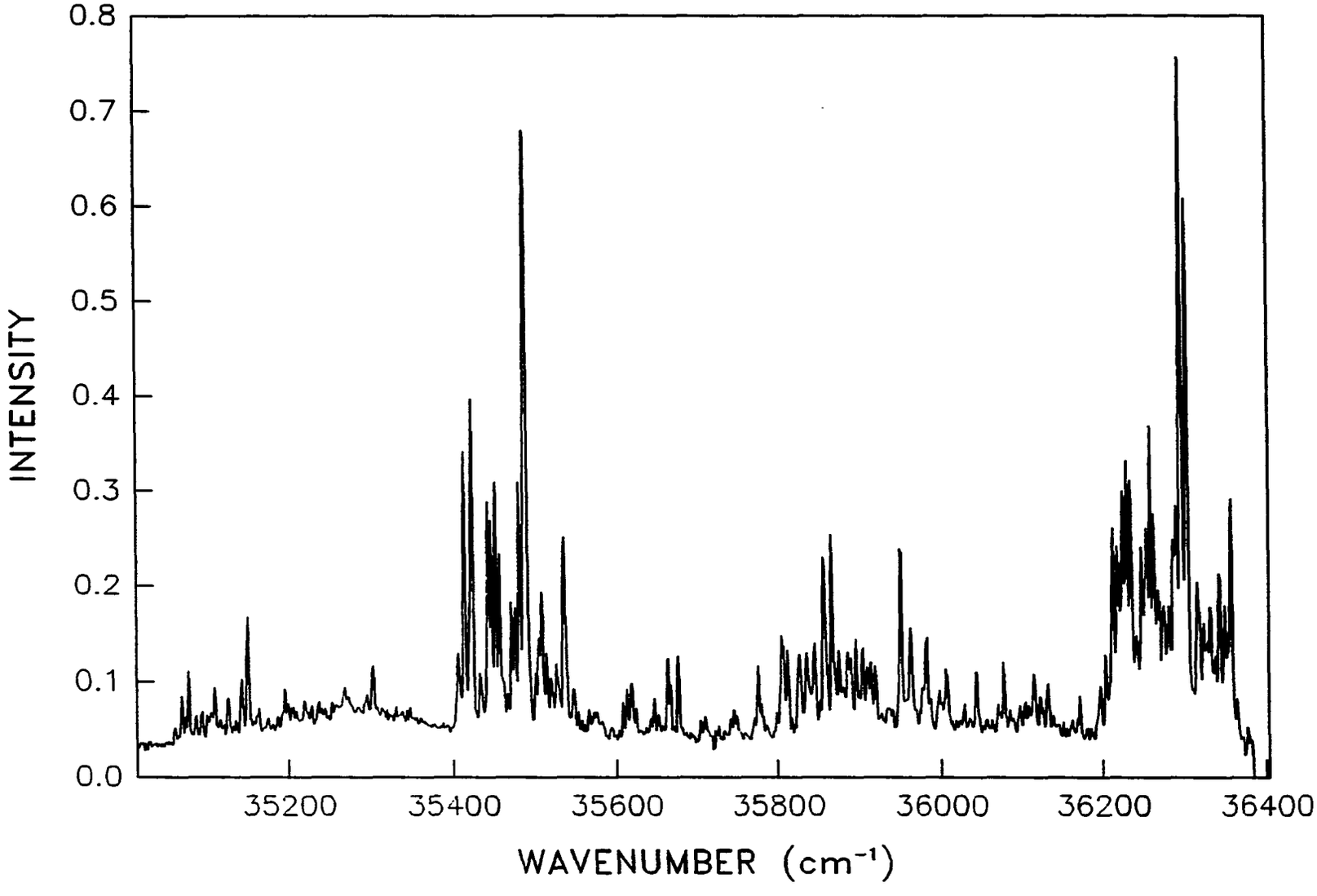
0.8
0.7
0.6
0.5
0.4
0.3
0.2
0.1
0.0
INTENSITY
35200
35400
35600
35800
36000
36200
36400
WAVENUMBER (cm⁻¹)

Kaya (45) and the spectroscopic studies of the heterodimer (phenol + water) have been reported by Abe et al. (16). After comparing our results with theirs, it is concluded that bands at ~ 350 cm^{-1} lower frequency region in the excitation spectra of p-cresol and phenol are bands from transitions among energy levels of homodimers and heterodimers. This result is the combined results of the studies by Abe et al. (16) and by Kaya and Fuke (45).

Then, where does the water come from? It is assumed that the water comes from the air via sample introduction, because the molecules studied here are very hygroscopic. Therefore, monomers and the homodimers (phenol + phenol, p-cresol + p-cresol) which have been formed in the original liquid or solid samples tend to form heterodimers by the introduction of water in the air.

$$C_7H_8O + H_2O \rightarrow C_7H_8O \cdot H_2O$$

or

$$2C_7H_8O + H_2O \rightarrow C_7H_8O \cdot H_2O + C_7H_8O$$

However, the concentration of water inside the sample chamber will be decreased as time increase. This is because the amount of water in the sample chamber is initially fixed and water will be pumped out as time increases by the pulsed valve operation. This is the reason why the intensities of several bands of the hydrogen bonded species with water decrease as time increases. Since there is no mass selectivity in the present experimental system, the exact assignment of bands cannot be made in the dimer bands region. For the other molecules, except for

phenol and p-cresol, which were studied here, only bands from the heterodimer (p-substituted phenols + water) are identified. The structure of the bands of the dimers resembles that of monomer with only the frequency shifted. The frequency shift of these dimer bands from the origin band [(0-0)(trans)] for all molecules which are studied here are listed in table 15.

Table 15. Comparison of the origin bands of the p-alkyl substituted phenols

	observed origin cm^{-1}(t)	Δν from p-cresol		t-c (cm^{-1})	H-bonded origin from(0-0)(t)
		trans	cis		
phenol	36356	1018			-352
p-cresol	35338	0			-358
p-ethylphenol	35511	173			-346
p-isopropylphenol	35600	262	248	14	-344
p-propylphenol	35507	169	111[a],148	58,21	-341
p-sec-butylphenol	35550	212	199	13	-342
p-tert-butylphenol	35747	409	373	36	-335
p-pentylphenol	35489	151			-339

[a]In p-propylphenol, two isomers are anti-gauche and syn-gauche.

Table 16. Vibrational frequencies of p-alkyl substituted phenols

modes / molecules	$16a^1$	$16a_1$	$6a^1$	$6a_1$	$16b^1$	$16b_1$	4^1	4_1	1^1	1_1	5^1	5_1
phenol[a]			476	521					934	997		
p-cresol	372		422	460			784	746	806	845	815	926
p-ethylphenol	361	392	424	472	490	539	709	721	806	841	818	
p-isopropylphenol	370		424	446	505	534	685	706	804	834		902
p-propylphenol	378	342	461	504	493	549	749		817	854	825	939
p-sec-butylphenol	378	356	438	424	505	534	675	706	807	834	815	869
p-tert-butylphenol	362		433		483	508	643	663		828		858
p-pentylphenol	378		465	549			760		810	834	816	904

[a]From ref. (16).

CONCLUSION

It has been demonstrated that electronic spectroscopy in supersonic jet is a useful tool for studying the stable isomers of p-alkyl substituted phenols. In this study, all of the molecules discussed, except for the p-cresol and p-ethylphenol, show doublet or multiplet origin bands. The observation of these bands is explained as evidence for several stable isomers for the corresponding molecules. The difference between the excitation energies among isomers for any molecule may represent the change in the potential for the rotation of the alkyl substituents. However, a complete discussion of the change in potential cannot be made due to the lack of information on the ground state potential. Through this study, it is concluded that the long range interaction between the p-substituted alkyl groups and the non-bonding electron pairs in the oxygen as well as the interaction between the p-substituted alkyl groups and the π electrons of the benzene ring is important in conformer formation. This study also showed that studies of the origin band region by electronic spectroscopy in a supersonic jet could yield information on the number of isomers and the possible conformations of those isomers.

Bands in the ~ 350 cm^{-1} lower frequency region from the (0-0)(trans) band are assigned as bands representing transitions among energy levels of heterodimers (phenol derivatives + H_2O) and homodimers (phenol derivatives + phenol derivatives). In particular, the fluorescence excitation spectrum of p-cresol shows the existence of both heterodimers and homodimers. The frequency shift by hydrogen bonding

and the comparison of energy separation among isomers of each molecules are listed in Table 15.

Frequencies of some vibrational modes of the benzene ring in the ground state as well as the excited state for all molecules discussed here are listed and compared in Table 16. The assignment of the vibrational modes are made with the assumption that these molecules belong to the C_s symmetry point group in the S_1 state. Each mode shows approximately the same frequency for all molecules studied here except for mode 4 and mode 6a. However, the substitution of the alkyl group on the para position of the phenol causes a big shift in frequencies of the vibrational modes as shown in Table 16.

Although several bands in the low frequency region are assigned as bands representing torsional motions of alkyl substituents, complete assignments of torsional modes are not made. There are many studies on methyl torsional modes for the methyl indoles (46) and for the substituted benzenes (26,27,29) using electronic spectroscopy in a supersonic jet, but few studies on other alkyl torsional modes, e.g. ethyl torsional mode and propyl torsional mode, are reported. Therefore, additional studies on alkyl torsional modes and hydroxyl torsional modes will reveal more information on the energy structure of the excited state as well as the ground state.

REFERENCES

1. J. R. Lakowitz, Principles of Fluorescence Spectroscopy (Plenum, New York, 1983).
2. I. Weinryb and R. F. Steiner, in Excited States of Protein and Nucleic Acids, edited by I. Weinryb and R. F. Steiner (Plenum, New York, 1971).
3. D. Creed, Photochem. Photobiol. 39, 563 (1984).
4. D. Creed, Photochem. Photobiol. 39, 537 (1984).
5. J. M. Beechem and L. Brand, Ann. Rev. Biochem. 54, 43 (1985).
6. T. R. Rizzo, Y. D. Park, and D. H. Levy, J. Chem. Phys. 85, 6945 (1986).
7. T. R. Rizzo, Y. D. Park, L. A. Peteanu, and D. H. Levy, J. Chem. Phys. 84, 6539 (1986).
8. J. A. Warren, J. M. Hayes, and G. J. Small, Chem. Phys. 102, 313 (1986).
9. R. E. Smalley, L. Wharton, and D. H. Levy, Account Chem. Res. 10, 139 (1977).
10. N. L. Allinger, J. J. Maul, and M. J. Hicky, J. Org. Chem. 36, 2747 (1971).
11. J. H. S. Green, D. J. Harrison, and W. Kynaston, Spectrochim. Acta 27A, 2199 (1971).
12. G. L. Carlson and W. G. Fateley, J. Phys. Chem. 77, 1157 (1973).
13. K. U. Ingold and D. R. Taylor, Can. J. Chem. 39, 481 (1961).

14. V. Bartok, R. B. Hartman, and D. J. Lucchsei, Photochem. Photobiol. 4, 499 (1965).

15. S. S. Lehrer and G. D. Fasman, J. Am. Chem. Soc. 87, 4687 (1965).

16. H. Abe, N. Mikami, and M. Ito, J. Phys. Chem. 86, 1768 (1982).

17. H. Abe, N. Mikami, M. Ito, and Y. Udagawa, Chem. Phys. Lett. 93, 217 (1982).

18. H. Abe, N. Mikami, M. Ito, and Y. Udagawa, J. Phys. Chem. 86, 2567 (1982).

19. A. Oikawa, H. Abe, N. Mikami, and M. Ito, J. Phys. Chem. 87, 5083 (1983).

20. N. Gonoe, H. Abe, N. Mikami, and M. Ito, J. Phys. Chem. 89, 3642 (1985).

21. V. K. Methrotra, Indian J. Pure Appl. Phys. 6, 206 (1968).

22. M. A. Shashidhar and K. S. Rao, Proc. Int. Conf. Spectrosc. 1st. Bombay, 1, 242 (1967).

23. R. Tembreull, T. M. Dunn, and D. M. Lubman, Spectrochim. Acta 42A, 899 (1986).

24. H. D. Bist, J. C. D. Brand, and D. R. Willams, J. Mol. Spectrosc. 24, 413 (1967).

25. J. B. Hopkins, D. E. Powers, and R. E. Smalley, J. Chem. Phys. 72, 5039 (1979).

26. P. J. Breen, E. R. Bernstein, and J. I. Seeman, J. Chem. Phys. 87, 3269 (1987).

27. P. J. Breen, J. A. Warren, E. R. Bernstein, and J. I. Seeman, J. Chem. Phys. 87, 1927 (1987).

28. P. J. Breen, J. A. Warren, E. R. Bernstein, and J. I. Seeman, J. Chem. Phys. 87, 1917 (1987).

29. K. Okuyama, N. Mikami, and M. Ito, Laser Chem. 7, 197 (1987).

30. M. Ito, J. Phys. Chem. 91, 517 (1987).

31. M. Ito and A. Oikawa, J. Mol. Struct. 126, 133 (1985).

32. A. Oikawa, H. Abe, N. Mikami, and M. Ito, Chem. Phys. Lett. 116, 50 (1985).

33. A. Oikawa, H. Abe, N. Mikami, and M. Ito, J. Phys. Chem. 88, 5180 (1984).

34. D. H. Levy, L. Wharton, and R. E. Smalley, in Chemical and Biochemical Applications of Lasers, edited by R. Moore (Academic Press, New York, 1977) Vol. 2, Chap. 1.

35. R. Campargue, J. Phys. Chem. 88, 4466 (1984).

36. J. M. Hayes, Chem. Rev. 87, 745 (1987).

37. J. B. Anderson, in Molecular Beams and Low Density Gas Dynamics (Marcel Dekker inc. New York, 1974) Chapter 1.

38. G. Varsanyi, Assignments for Vibrational Spectra of Benzene Derivatives (John Wiley & Sons, New York, 1974).

39. D. E. Powers, J. B. Hopkins, and R. E. Smalley, J. Chem. Phys. 72, 5721 (1980).

40. N. S. True, M. S. Farag, R. K. Born, M. A. MacGregor, and J. Radhakrishnan, J. Phys. Chem. 87, 4622 (1983).

41. T. M. Dunn, R. Tembreull, and D. M. Lubman, Chem. Phys. Lett. 121, 453 (1985).

42. T. Kojima, J. Phys. Soc. Japan, 15, 284 (1960).

43. M. M. Carrabba, T. M. Wodenberg, and J. E. Kenney, J. Phys. Chem. 89, 4226 (1985).

44. R. Soda, Bull. Chem. Soc. Japan, 34, 1482 (1961).

45. K. Fuke and K. Kaya, Chem. Phys. 94, 97 (1983).

46. G. A. Bickel, G. W. Leach, D. R. Demmer, J. W. Hager, and S. C. Wallace, J. Chem. Phys. 88, 1 (1988).

SECTION II. SINGLE CRYSTAL FLUORESCENCE AND POLARIZED ABSORPTION STUDIES OF THE $S_1(^1A_u) \leftrightarrow S_0(^1A_g)$ TRANSITIONS OF 2,2,4,4-TETRAMETHYL CYCLOBUTANE-1,3-DIONE AT 4.2 K

ABSTRACT

The polarized low temperature single crystal absorption spectra and the low temperature fluorescence spectrum of 2,2,4,4-tetramethyl cyclobutane-1,3-dione (TMCBD) for the $S_1(^1A_u) \leftarrow S_0(^1A_g)$ transitions are measured in the range 320 nm - 370 nm and 365 nm - 440 nm, respectively. This forbidden pure electronic transition is allowed by the site group effect under the reduced C_{2v} symmetry of the S_1 state which has a boat form geometry. Most vibronic bands derive their intensity through vibronic coupling. Assignments of vibrational bands in the excited and ground electronic state are made based on twenty Herzberg-Teller vibronic origins in the excited state and three vibronic origins in the ground state. The vibronic couplings are very active and long progressions formed mainly by the 523 cm^{-1} totally symmetric mode and the 306 cm^{-1} non-totally symmetric b_{1u} mode are observed. The observation of C-H stretching vibrations in the single crystal fluorescence emission spectra confirms that bands occurring in the vicinity 3000 cm^{-1} higher in energy from the S_1 $(^1A_u) \leftarrow S_0$ (^1A_g) origin band in the polarized absorption spectra are C-H stretching vibrational modes of S_1 state, not vibrations from another excited electronic state (S_2). The difference in the vibronic activity between the excited and ground states is qualitatively explained in terms of the Duschinsky effect.

INTRODUCTION

Electronic spectroscopy and the photophysics of mono-carbonyl and di-carbonyl molecules have received considerable study for many years (1-12). Compounds belonging to the latter case can provide the opportunity to study radiationless decay and vibronic coupling between closely spaced carbonyl $n\pi^*$ states (13-16). A case in point is 2,2,4,4-tetramethyl cyclobutane-1,3-dione (TMCBD) (Fig. 1). There have been many studies on TMCBD (17-20). While the gas phase absorption spectra reported previously were diffuse (17-18), the absorption spectra of neat crystals at low temperature observed by Spafford, Baiardo, Wrobel, and Vala (Henceforth, SBWV will refer to these workers and their paper) (19) and Gordon, Caris, and Newman (GCN will refer to these workers and their paper) (20) showed sharp and complex vibronic structures.

TMCBD has D_{2h} symmetry in the ground state if the hydrogen atoms are assumed to have suitably symmetric conformations as shown in Fig. 1. Two carbonyl groups in TMCBD have two nonbonding orbitals (n_1 and n_2) and two antibonding π^* orbitals (π^*_1 and π^*_2). However, extended Hückel theory and CNDO/2 calculations on di-carbonyl compounds by Swenson and Hoffman (21) indicated that the nonbonded-pair molecular orbital's (MO) n_1 and n_2 of two carbonyl groups generally interact via 'through bond' coupling resulting in a splitting of the in-plane ($n_1 + n_2$) and out-of-plane ($n_1 - n_2$) combination MO's. The experimental verification of this splitting was provided by Cowan et al. (22) by photoelectron spectroscopic study. They indicated in their study of TMCBD that there was a large separation between the n orbitals (0.7 eV). In this case,

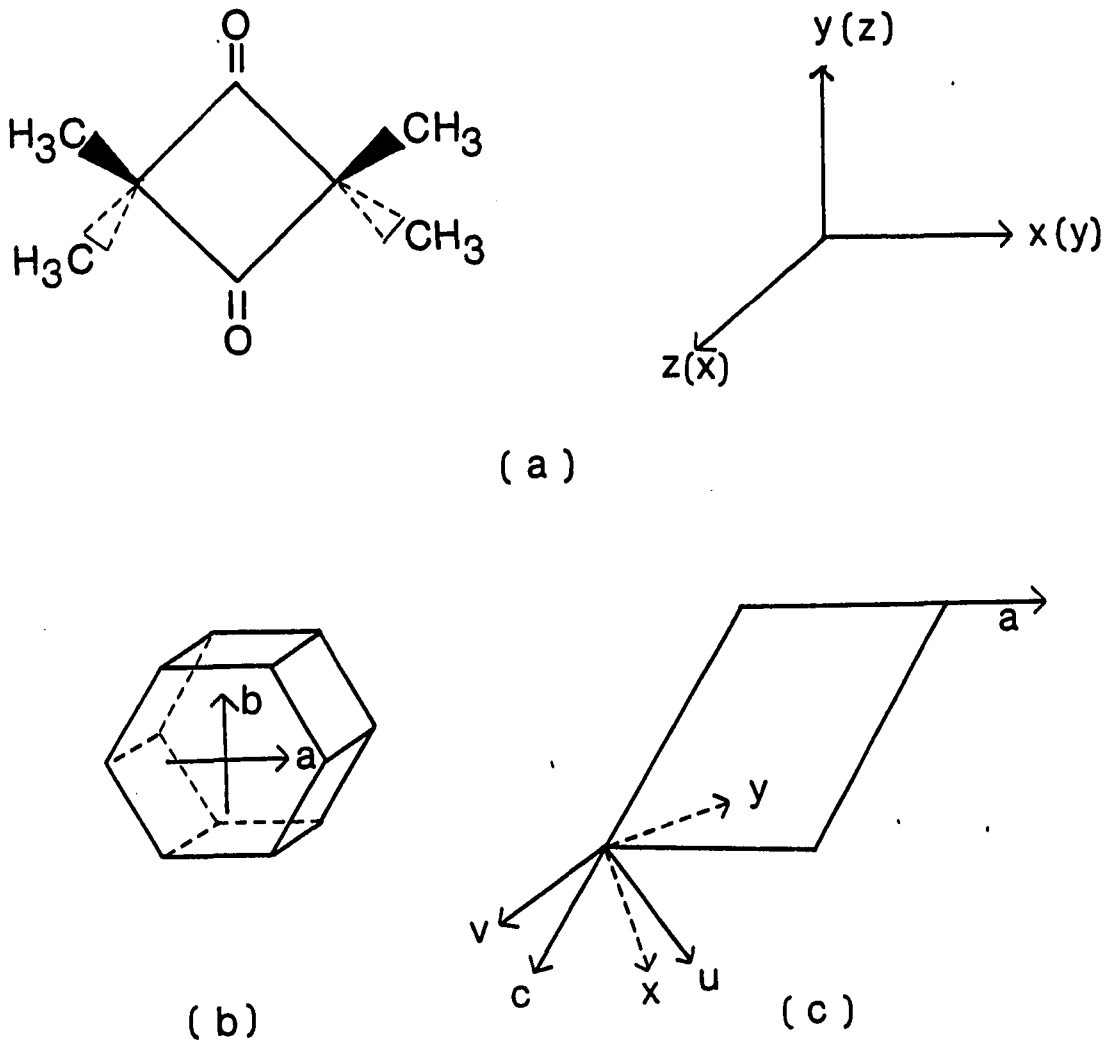

Figure 1. Axes definition and extinction directions of TMCBD crystals.
a) Axes definition of TMCBD. Axes definition of TMCBD by GCN is shown inside the parentheses.
b) Extinction direction in the ab face of TMCBD crystal (Taken from ref. 20).
c) Extinction directions (u and v) and molecular axes (x and y) in the ac face crystal of TMCBD (Taken from ref. 20)

the molecular orbital combination of the carbonyl n orbitals (n_1 and n_2) are :

$$n_+(b_{3u}) = (n_1 + n_2)/\sqrt{2}$$

$$n_-(b_{1g}) = (n_1 - n_2)/\sqrt{2}$$

with the indicated D_{2h} group symmetries (23,24). Similar molecular orbital combinations are regarded to be formed with the π^* orbitals (π_1^* and π_2^*) :

$$\pi_+^*(b_{1u}) = (\pi_1^* + \pi_2^*)/\sqrt{2}$$

$$\pi_-^*(b_{3g}) = (\pi_1^* - \pi_2^*)/\sqrt{2}$$

Therefore, in D_{2h} symmetry, TMCBD has four $n\pi^*$ states in the near ultraviolet region arising from the transitions between two nonbonding orbitals (nb_{3g} and nb_{2u} according to GCN (20) and nb_{1g} and nb_{3u} according to SBWV) (19) and two antibonding π^* orbitals (π^*b_{2g} and π^*b_{3u} according to GCN and π^*b_{3g} and π^*b_{1u} according to SBWV) as shown in Fig. 2. The difference in the notation of the orbitals between the two studies by GCN (20) and SBWV (19) resulted from the different definitions of molecular axes as shown in Fig. 1. Since the definition of molecular axes adopted in the present study is the same as that of the SBWV's, two nonbonding orbitals are thought to be nb_{3g} and nb_{1u} and the two antibonding π orbitals are regarded as π^*b_{3g} and π^*b_{1u}. Among

the studies of TMCBD in order to verify these possible four $n\pi^*$ transitions, the polarized optical crystal study by SBWV (19) led to the assignment of four $n\pi^*$ states in the range 250 nm - 370 nm, while a similar study by GCN (20) led to the assignment of only three $n\pi^*$ states in the same range as shown in Fig. 2. GCN indicated that the fourth $n\pi^*$ state would be to higher energy than 250 nm. GCN also studied TMCBD-d_{12} (deuterated TMCBD) using low temperature polarized single crystal absorption spectroscopy in the same frequency range as TMCBD-h_{12} (undeuterated TMCBD) (20).

Although the studies by SBWV (19) and GCN (20) on TMCBD led to an improved understanding of the excited state of TMCBD, there exist several conflicting interpretations between the two studies. The former workers concluded that the point symmetry group changed from D_{2h} to C_{2v} upon excitation to the S_1 state. These workers (SBWV) also assigned the 308 cm^{-1} (306 cm^{-1} in the present study, the 308 cm^{-1} mode observed by SBWV and GCN will be referred to as a 306 cm^{-1} mode) prominent progression forming mode as a b_{1u} mode which correlates with a 402 cm^{-1} fundamental in the ground state. However, GCN assigned the 306 cm^{-1} mode observed in the absorption spectra as a totally symmetric C-CH_3 bending mode which correlates with a 298 cm^{-1} fundamental in the ground state. In addition, GCN assigned the intense absorption bands which occur in the vicinity 3000 cm^{-1} higher in energy from the $S_1(^1A_u) \leftarrow S_0(^1A_g)$ origin to vibronically induced C-H stretching vibrations based on the results of the absorption studies on TMCBD-d_{12} (deuterated TMCBD). SBWV, however, assigned this structure to a second excited electronic state (S_2) and they concluded that the point symmetry group

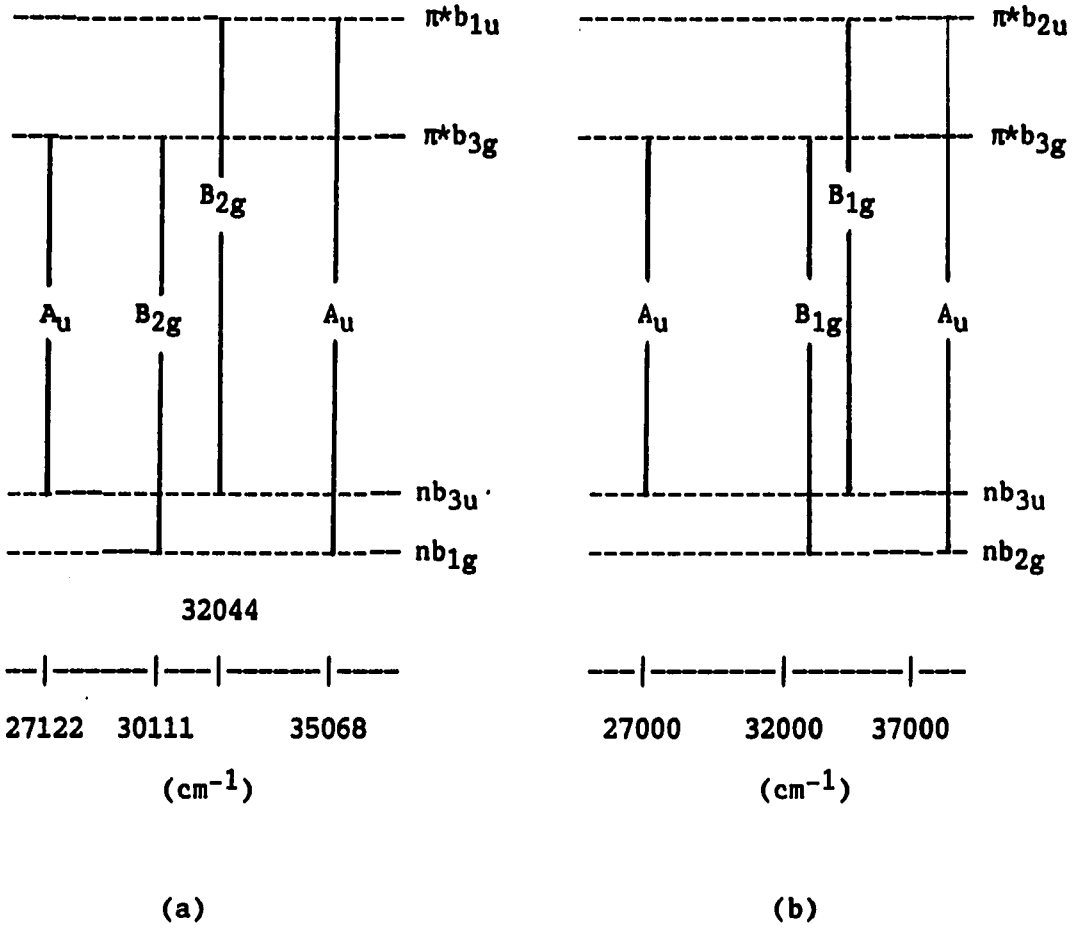

Figure 2. Four nπ* transitions of TMCBD.

(a) Four nπ* transitions of TMCBD observed by SBWV (19). The point symmetry group of S_1 state (A_u) is assumed as C_{2v}.

(b) Four nπ* transitions of TMCBD observed (Second A_u transition is not observed but assumed to occur at 40000 cm^{-1} region) by GCN (20). The point symmetry group of S_1 (A_u) state is assumed as D_{2h}

of the S_2 state changed from D_{2h} to C_{2h} upon excitation to the S_2 state. Since the assignment of the intense absorption bands which occur in the vicinity 3000 cm^{-1} higher in energy from the $S_1 \leftarrow S_0$ origin is different between the two studies (19,20), the number of observed vibronic origins is also different between the two studies.

Given these discrepancies in the understanding of the S_1 state of TMCBD, we undertook this work to understand better the $S_1 \leftarrow S_0$ absorption system of TMCBD and to resolve these arguments. Here, we present the results obtained from the low temperature high resolution polarized optical crystal absorption and fluorescence studies. It has been reported that TMCBD does not fluoresce or phosphoresce in an ethanol-ether-isopentane glass at 77 K (24). SBWV also reported that the single crystal of TMCBD does not show luminescence at 10 K (19). However, we observed, for the first time, the fluorescence emission spectra of the single crystals of TMCBD at 4.2 K by XeCl excimer laser (308 nm) excitation. The experimental conditions of high resolution (1.1 cm^{-1} resolution in the absorption studies and better than 10 cm^{-1} resolution in the fluorescence emission studies) and low temperature (4.2 K) have yielded more vibronic origins than the results of the previous two absorption studies (19,20), and therefore, gave more details on the vibronic structures for the $S_1 \leftarrow S_0$ of TMCBD. Meanwhile, the absorption study performed by GCN (20) showed that the bandwidths of observed bands in the S_1 state were ~ 40 cm^{-1} (FWHM) and their experiment was performed at 77 K. The absorption study performed by SBWV (19) was performed in the temperature range 1.8 - 20 K, but their paper did not give any details about the instrument resolution of or the bandwidths of the observed bands.

In the present study, the $S_1 \nleftarrow S_0$ is exclusively investigated by using several spectroscopic methods. The $S_1 \leftarrow S_0$ is forbidden by the electric dipole and magnetic dipole selection rules, but can appear in the free molecule by various vibronic coupling mechanism as shown in Table 1. Although (0-0) transition is forbidden, a weak (0-0) band has been observed by GCN (20) and SBWV (19). In the present study, this forbidden (0-0) band also showed moderate intensity in the z-polarized absorption spectrum of (001) crystal face as shown in Fig. 5. Since the forbidden (0-0) transition in the free molecule is allowed in the crystal, the reduced symmetry in crystals of TMCBD is regarded as an important factor for the appearance of the (0-0) band for the $S_1 \leftarrow S_0$. SBWV concluded that transition to an A_u state (S_1) was allowed solely along the z-direction due to the crystal site group effect of the distorted symmetry (C_{2v}) in the S_1 state as shown in Table 2. They also concluded that the inversion of molecule via a carbonyl wagging vibration should be assumed to understand the z-polarization of the (0-0) band (19). GCN, however, indicated that the A_u transition might be allowed by the reduced symmetry in a molecular crystal (20).

Our explanation concerning the observation of the (0-0) band, which is regarded as forbidden in the D_{2h} symmetry, is the same as that of SBWV because the vibrational assignment of the observed bands in the absorption spectra can be understood only by assuming the change of the point symmetry group from D_{2h} to C_{2v} upon excitation to the S_1 state. Furthermore, the presence of a long progression form by the non-totally symmetric mode, e.g., 306 cm^{-1} (b_{1u}) mode, is also regarded as an

Table 1. Mechanism for the appearance of $n\pi^*$ singlet transition in TMCBD

Free molecule (D_{2h})					
Symmetry species					polarization
electronic	x	vibrational	=	vibronic	
A_u	x	a_g	=	A_u	forbidden
	x	b_{3g}	=	B_{3u}	x
	x	b_{2g}	=	B_{2u}	y
	x	b_{1g}	=	B_{1u}	z

Table 2. Correlation diagram for TMCBD planer and distorted molecular (boat form) point group and site group[a]

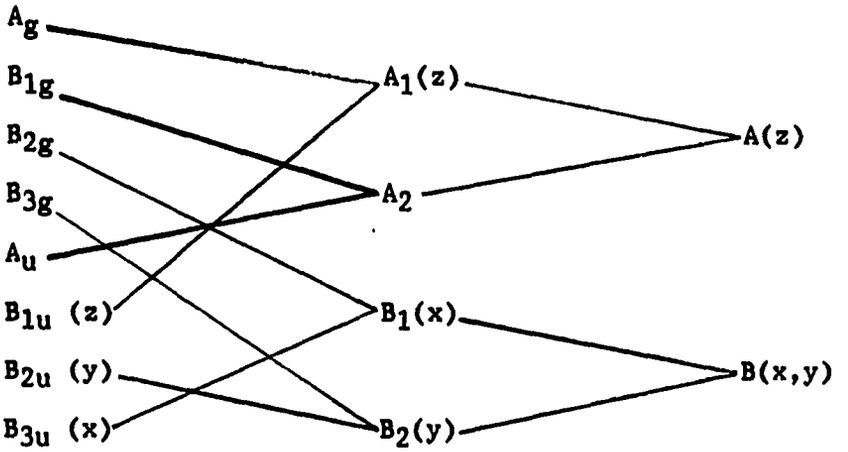

[a]Taken from Ref. (19). The site group is here taken to contain only those elements common to the new distorted molecular point symmetry and the unchanged crystal factor group.

indication of the change in the point symmetry group upon excitation to the S_1 state. The site group of the C_{2v} symmetry point group in crystals is C_s and the A transition in the C_s symmetry, which corresponds to the A_u transition in the D_{2h} symmetry, is allowed by electric dipole selection rules. Point symmetry group change to C_{2h} upon excitation to the S_1 state is not likely because the observed polarization of each band cannot be understood in relation to the assignments of vibrational modes in the S_1 state. In addition, the A_u transition is not allowed along the z-axis in the C_{2h} symmetry as can be seen in Table 3. Therefore, we conclude that the forbidden (0-0) transition for the $S_1 \leftarrow S_0$ gained intensity in the crystal by the crystal site group effect under the distorted symmetry (C_{2v}, boat form).

Nicolaisen and coworkers (25) reported the infrared and Raman spectra of TMCBD and they made a symmetry assignment for the fundamentals in the ground state. Shurvell and coworkers (26) also studied the vibrational structure of TMCBD as well as TMCBD-d_{12} in the ground state. Through the two infrared and Raman studies on TMCBD and TMCBD-d_{12} (25,26), symmetry assignments of forty-five observed fundamentals out of sixty possible vibrational modes ($10a_g + 5a_u + 7b_{1g} + 9b_{1u} + 7b_{2g} + 7b_{2u} + 6b_{3g} + 9b_{3u}$) (26) were determined. Although there is some disagreement on the vibrational assignment between the two infrared and Raman studies (25,26), assignment of the totally symmetric modes and the gerade (g) or ungerade (u) symmetry are firmly made. The assignment of vibrational modes observed in the present polarized absorption study are made based on the results of the two infrared and Raman studies (25,26) and the observed band polarization.

Table 3. Correlation diagram for TMCBD planer and distorted molecular (chair form) point group and site group[a]

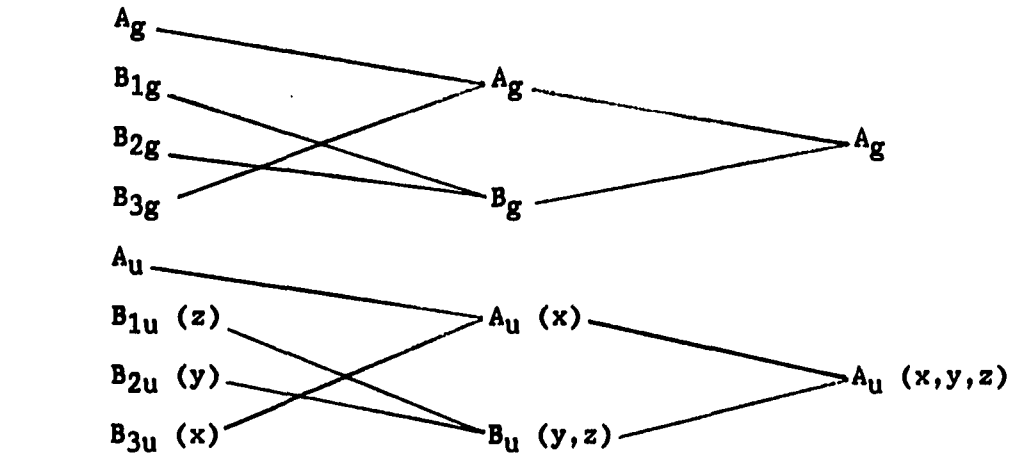

[a]Taken from Ref. (19). See footnote, Table 2.

In this study, the characteristics of the progression forming modes are thoroughly investigated and discussed with several new experimental results from a polarized infrared study and the fluorescence emission study. In addition, the characteristics of the intense bands which occur in the vicinity 3000 cm^{-1} higher in energy from the $S_1(^1A_u) \leftarrow S_0(^1A_g)$ origin are well understood since the C-H stretching vibrations are observed in the fluorescence emission spectra of TMCBD. The observation of C-H stretching modes in the fluorescence emission spectra as well as the polarized absorption spectra of TMCBD confirms that there is only one excited singlet state (S_1) in the frequency region studied here (320 nm-370 nm). That means the assignments of SBWV (19) about the bands occurring at ~330 nm as a second excited singlet state (S_2) is not reasonable. Finally, the difference of the vibronic activities between the ground and excited state (S_1) is qualitatively explained in terms of Duschinsky effect.

CRYSTAL STRUCTURE OF TMCBD

The crystal structure of TMCBD has been studied by several groups (27-29). These data have shown that the TMCBD crystal is monoclinic and has a space group of C2/m with two molecules per unit cell. The point group of the free molecule in the ground state has been reported as D_{2h} (19,20), and therefore, its site group in the crystal is C_{2h}. If the conformation of TMCBD is distorted in the excited state to C_{2v}, then the site group of the distorted molecule is C_2.

TMCBD crystals have been obtained in the three different faces, i.e., (001), (110), (010) faces. Description of the three different crystal faces has been made in detail previously by GCN (20). Therefore only a brief description will be provided here. The (001) crystal face is hexagonal and shows an extinction direction parallel and perpendicular to the edge of the crystal. The axis parallel to the edge is defined as the a-axis, and the axis perpendicular to the edge is defined as the b-axis as shown in Fig. 1. Therefore, the polarized absorption spectra of TMCBD with polarization parallel to the a-axis or parallel to the b-axis shows in-plane (xy-polarized) or out-of-plane polarized (z-polarized) spectra in the (001) crystal face. The (010) face crystal is a parallelogram and it shows oblique extinction along direction u and v. The (110) face crystal shows parallel extinction. The oriented gas polarization ratio (direction cosine squared) for light incident on (110) crystal face are x : y : z = 0.61 : 0.39 : 0. for direction parallel to c (see Fig. 1) and x : y : z = 0.13 : 0.20 : 0.67 for direction perpendicular to c.

EXPERIMENTAL SECTION

TMCBD was purchased from Aldrich Chemical Co. and single crystals were grown by vacuum sublimation. The crystal shape and characteristics of extinction have been described in the previous section. Crystals were mounted on a copper plate with a low temperature glue (G.E. adhesive vanish No. 7031) with the use of a polarizing microscope.

The experimental setup for the low temperature polarized absorption studies was a homebuilt double beam arrangement and its schematic diagram is shown in Fig. 3. The light from a 500 watt Xe arc lamp (Canrad Hanovia 959-C98, Oriel 6102 housing powered by an Oriel C-72-20 power supply) was dispersed by a 1.5 m high resolution monochromator (Jovin-Yvon HR-1500) equipped with stepping motors and controller. The monochromator with grating for visible (2400 grooves/mm) has a rated linear dispersion of 0.26 nm/mm and has a measured bandpass of 0.011 nm (1.1 cm^{-1}) with 20 μ slit width. The dispersed light in the monochromator passed through a Glan-Thompson polarizer for the polarized absorption studies and then split into two beams by a 50 % beamsplitter (Melles Griot). Each beam was modulated by a mechanical chopper (Laser Precision CTX-534). The light in the sample leg of the double beam spectrometer was focused by a convex lens into the sample crystal which was immersed in the liquid helium in a Janis Vari-Temp. 8DT convection cooled cryostat. The light on the reference leg was focused by a convex lens into a variable attenuator (Newport Co. model 925B). Both beams are then recombined by another beamsplitter (Melles Griot) and focused into the photomultiplier tube (PMT) (RCA C31034 in a PFR RR-1400RF

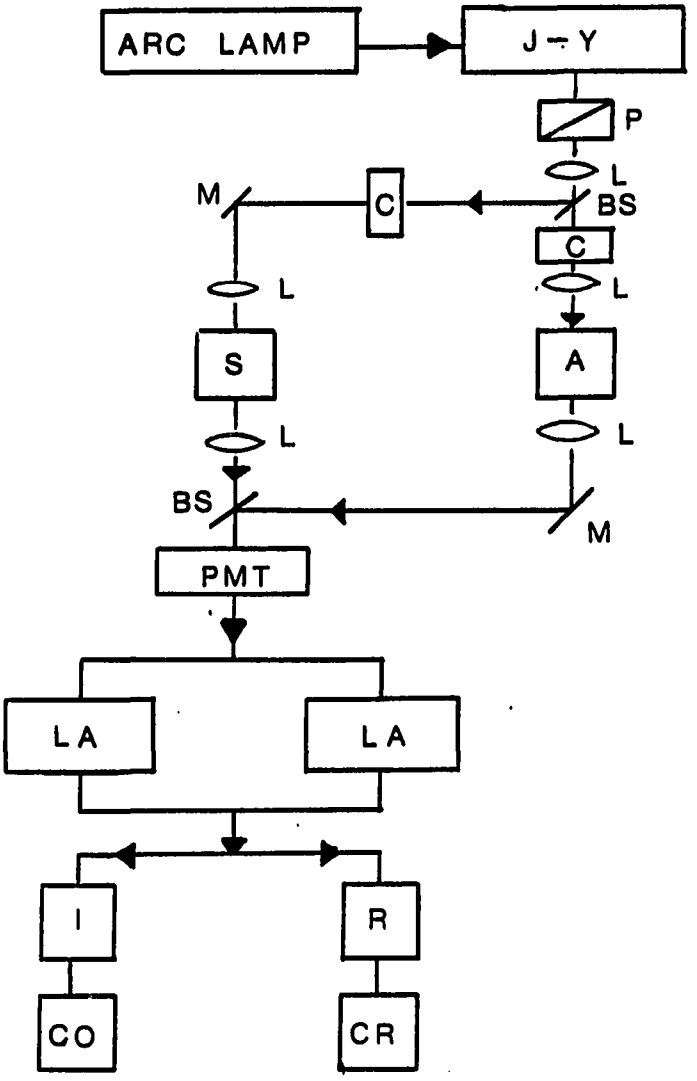

Figure 3. Experimental setup for the low temperature absorption spectra of TMCBD.
A: Attenuator BS: Beamsplitter C: Chopper CO: Computer
CR: Chart recorder I: Integrator LA: Lock-in amplifier
L: Lens M: Mirrors P: Glan-Thompson Polarizer
R: Ratiometer S: Sample PMT: Photomultiplier tube
J-Y: Jovin-Yvon monochromator

thermally cooled housing). The signals detected by the PMT were sent to two lock-in amplifiers (Ithaco model 397E0). The signals from the lock-in amplifiers were sent to a logarithmic ratiometer (Evans Associates model 4122) that provided an output proportional to the sample absorbance and was recorded on a strip chart. The signal from the lock-in amplifiers was also sent to the computer (Digital Equipment Computer Micro PDP 11/+23) through the Integrator/coupler (Ithaco model 385 E0-2) which simultaneously converts two analog voltages to digital values using a voltage-to-frequency conversion technique and integrates the signals for a selectable multiple of 60 Hz.

The low temperature single crystal fluorescence emission studies of TMCBD were performed using a XeCl excimer laser (Lambda Physik model ENG102 MSC) which produced a coherent beam at 308 nm. This 308 nm corresponds to the second excited electronic state of TMCBD. The laser beam was sent to variable beamsplitter which split the incoming laser beam for sample excitation and for reference. The sample beam was skimmed and was reduced to a smaller size by an iris. The sample laser beam excited the sample which was immersed in liquid helium in a Pope glass dewar at an angle of about 60° from the beam propagating direction to minimize laser scattering. The fluorescence was detected at right angles with two convex lenses, monochromator, PMT, and photodiode array. The 1 m McPherson scanning monochromator (model No. 2061) with holographic grating which has a transmission range of 185 nm to 650 nm (136 mm ruled width x 116 mm groove length, 2400 grooves/mm, F/7) provided a linear dispersion of 0.416 nm/mm and ~10 cm^{-1} resolution with 300 μ slit width. The dispersed signal was detected either by

photomultiplier tube (Amperex model XP-2232) or Tracor Nothern (TN 6134) blue-enhanced intensified gatable photodiode array (PDA). The fluorescence detected by the PMT was sent to a dual gated amplifier (Quanta-Ray model DGA-1) which had a fixed gatewidth of 100 μsec, converted to the voltage, then recorded on a strip chart. The signal detected by the PDA was analyzed by a Tracor Nothern (TN 6500) optical multichannel analyzer (OMA). This detector (PDA and OMA) in conjunction with 1 m monochromator allows the simultaneous acquisition of ~ 6 nm. The spectra obtained by the OMA was calibrated by recording the emission line of the iron hollow-cathode lamp. The schematic diagram of the experimental setup used for the fluorescence emission study is shown in Fig. 4.

The polarized far infrared spectra were obtained with a FT-IR (Fourier Transform Infrared spectrophotometer, IBM model IR-98) with a Cambridge Physical Science model KR-430 (KRS-5 substrate) polarizer. TMCBD crystals were mounted on the copper plate in the same manner as for the polarized absorption study and cooled by blowing liquid nitrogen vapor or by connecting copper rod between the copper plate and liquid nitrogen. Although the exact temperature of samples used in the infrared study is not known, it is assumed to be ~ 100 K.

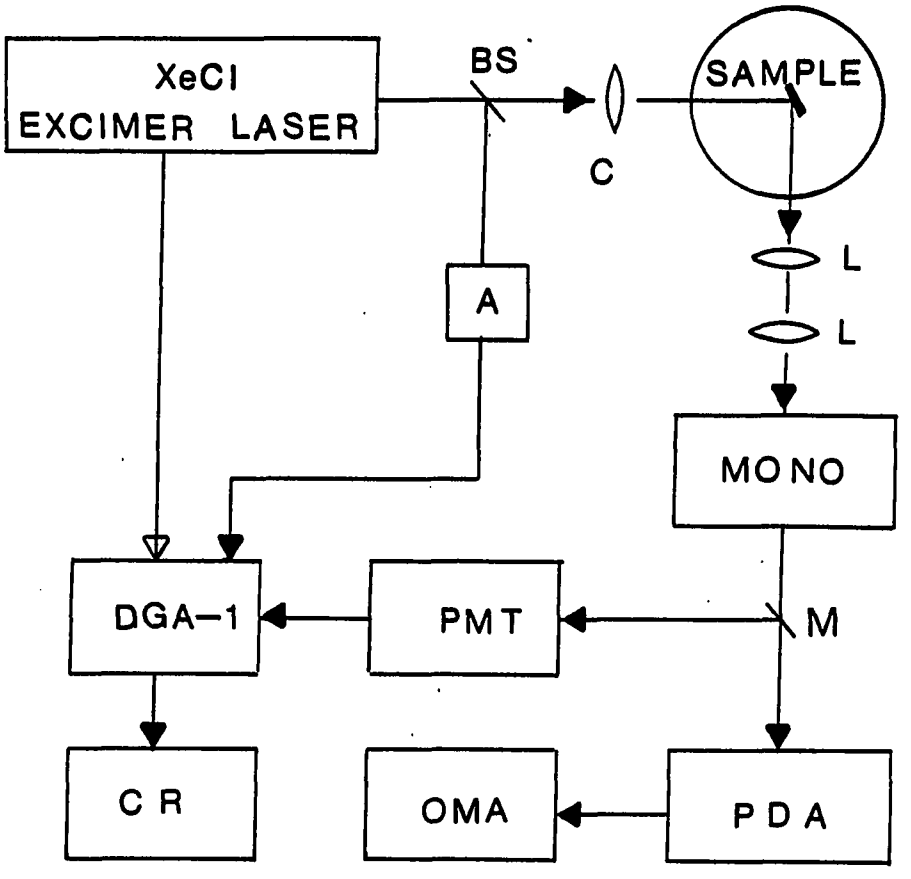

Figure 4. Schematic diagram of the experimental setup for the fluorescence spectra of TMCBD at low temperature.
A: Photodiode BS: Beam splitter C: Iris L: Lens
PMT: Photomultiplier tube DGA-1: Dual gated amplifier
MONO: Monochromator M: Mirror PDA: Photo diode array
OMA: Optical multichannel analyzer CR: Chart recorder

RESULTS

Although absorption spectra have been measured for all three crystal faces [(001), (010), (110)], we will discuss mainly the xy-polarized and z-polarized absorption spectra of (001) crystal face because little additional information is provided by the other spectra. The xy- and z- polarized absorption spectra of the (001) crystal face of TMCBD in the range 320 nm - 370 nm are shown in Fig. 5 and Fig. 6 and vibrational assignments are listed in Table 4 and 5. All of the observed absorption spectra show long progressions mainly with two intervals, 306 cm^{-1} and 523 cm^{-1}. The other progression forming mode (517 cm^{-1} mode) is observed building on a few vibronic origins and electronic origin of S_1 state. The z-polarized absorption spectrum shown in Fig. 5 shows very sharp (FWHM=1.2 cm^{-1}) band at 27133 cm^{-1} and progressions building on this band. This sharp band at 27133 cm^{-1} is assigned as a (0-0) origin band of the $S_1 \leftarrow S_0$ transition because no other band is observed in the lower energy region than the 27133 cm^{-1} and because SBWV (19) and GCN (20) also assigned this band as a (0-0) origin band in their polarized absorption studies on TMCBD. The intense bands occurring in the vicinity 3000 cm^{-1} higher in energy from the $S_1 \leftarrow S_0$ origin band in all the absorption spectra of TMCBD observed in the present study are assigned as C-H stretching vibrations. Further discussion on the progression forming modes and the C-H stretching vibrations will appear in the discussion section.

Six vibronic origins are observed in the z-polarized absorption spectra, while fifteen vibronic origins are observed in the xy-polarized

Figure 5. z-polarized single crystal absorption spectrum of TMCBD in the (001) crystal face. Sample temperature is 4.2 K. Resolution is 1.1 cm^{-1}

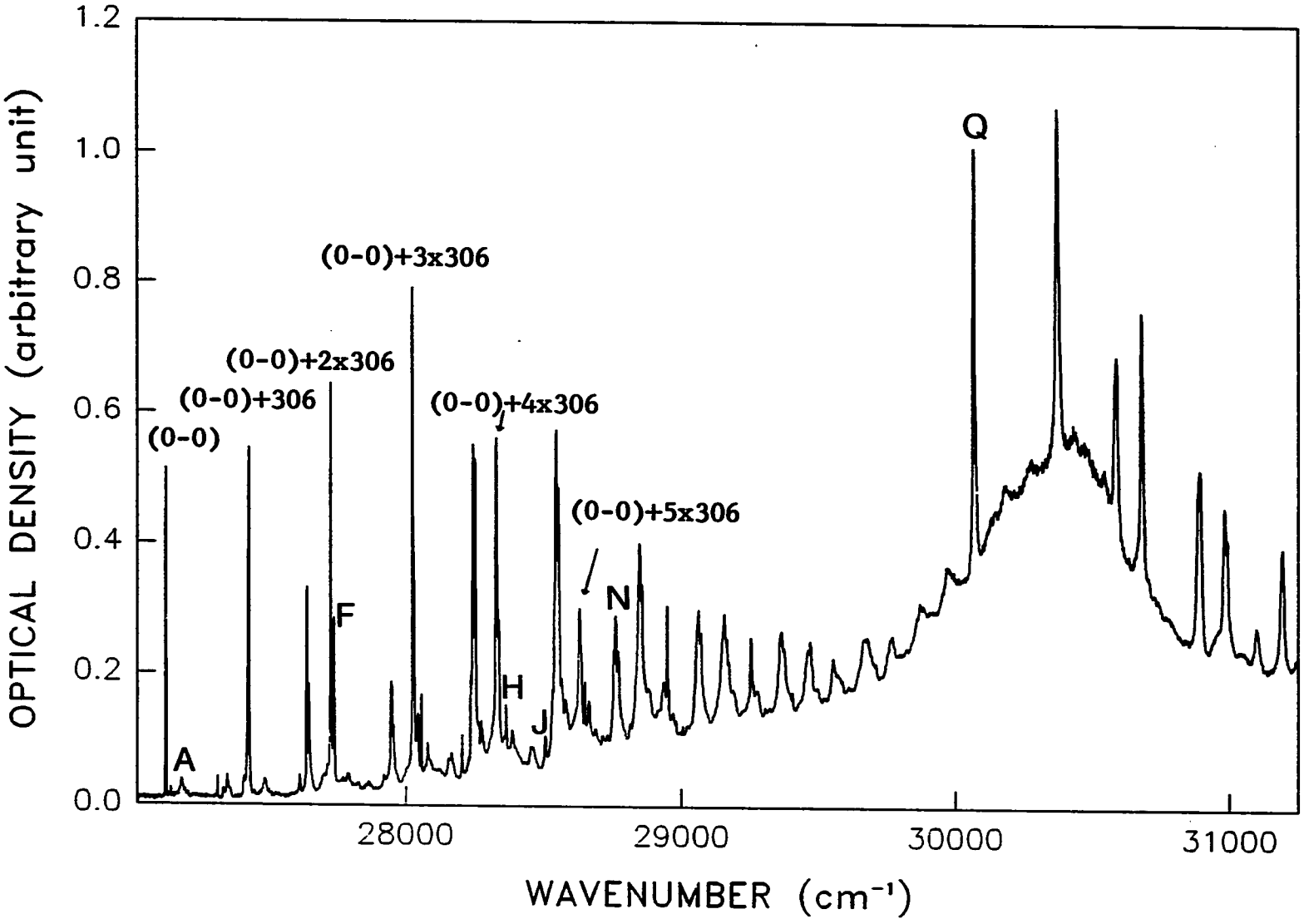
OPTICAL DENSITY (arbitrary unit)
1.2
1.0
0.8
0.6
0.4
0.2
0.0
(0-0)
(0-0)+306
(0-0)+2x306
(0-0)+3x306
(0-0)+4x306
(0-0)+5x306
A
F
H
J
N
Q
28000
29000
30000
31000
WAVENUMBER (cm⁻¹)

Table 4. Vibronic structure of TMCBD in the S_1 state observed by the z-polarized absorption spectrum of (001) crystal face

observed freq. $\Delta(cm^{-1})$	observed $\Delta\nu(cm^{-1})$	analysis	calc. $\Delta\nu'(cm^{-1})$	$(\Delta\nu-\Delta\nu')$ (cm^{-1})	labeling of vibronic origins
27133	0	0-0	0	0	0-0
27193	60	60	60	0	A
27352	219	219	219	0	
27434	301	0 + 306	306	-5	
27495	362	60 + 306	366	-4	
27650	517	0 + 517	517	0	
27656	523	0 + 523	523	0	
27735	602	0 + 2 x 306	612	-10	
27746	613	613	613	0	F
27801	668	60 + 2 x 306	668	0	
27956	823	0 + 517 + 306	823	0	
27963	830	0 + 523 + 306	829	0	
28039	906	0 + 3 x 306	918	-12	
28044	911	613 + 306	919	-8	
28057	924				
28070	937	937	937	0	I
28095	962				
28102	969				
28170	1037	0 + 2 x 517	1034	3	
28178	1045	0 + 2 x 523	1046		
28219	1086	1086	1086	0	K

Table 4. (continued)

observed freq. $\Delta(cm^{-1})$	observed $\Delta\nu(cm^{-1})$	analysis	calc. $\Delta\nu'(cm^{-1})$	$(\Delta\nu-\Delta\nu')$ (cm^{-1})	labeling of vibronic origins
28225	1092	1092			
28260	1127	0 + 517 + 2 x 306	1129	-2	
28268	1135	0 + 523 + 2 x 306	1135	0	
28280	1147				
28285	1152				
28346	1213	0 + 3 x 306	1218	-5	
28353	1220	613 + 2 x 306	1221	-1	
28378	1244	937 + 306	1243	1	
28402	1269	962 + 306	1268	1	
28477	1344	0 + 2 x 517 + 306	1340	4	
28527	1394	1086 + 306	1392	2	
28553	1420				
28566	1433	0 + 517 + 3 x 306	1435	-2	
28585	1452				
28598	1465				
28656	1523	613 + 3 x 306	1531	-8	
28674	1541	937 + 2 x 306	1549	-8	
28683	1550				
28780	1647	0 + 2 x 517 + 2 x 306	1648	-1	
28786	1653	1653			
28796	1663	0 + 2 x 523 + 2 x 306	1660	3	

Table 4. (continued)

observed freq. $\Delta(cm^{-1})$	observed $\Delta\nu(cm^{-1})$	analysis	calc. $\Delta\nu'(cm^{-1})$	$(\Delta\nu-\Delta\nu')$ (cm^{-1})	labeling of vibronic origins
28875	1742	0 + 517 + 4 x 306	1741	1	
28883	1750	0 + 523 + 4 x 306	1747	3	
28979	1846	937 + 3 x 306	1855	-9	
29091	1958	1653 + 306	1959	-1	
29102	1969	0 + 2 x 523 + 3 x 306	1969	0	
29186	2053	0 + 517 + 5 x 306	2047	6	
29283	2150	937 + 4 x 306	2161	-11	
28395	2262	1653 + 2 x 306	2265	-3	
28494	2361	0 + 517 + 6 x 306	2353	8	
29498	2365	0 + 523 + 6 x 306	2360	5	
29593	2460	937 + 5 x 306	2467	-7	
29701	2568	1653 + 3 x 306	2571	-3	
29720	2587				
29813	2680				
29912	2779				
30030	2897				
30111	2978	2978	2978	0	Q
30221	3088				
30324	3191				
30420	3287	2978 + 306	3284	3	
30479	3346				
30631	3498	2978 + 517	3495	3	

Table 4. (continued)

observed freq. $\Delta(cm^{-1})$	observed $\Delta\nu(cm^{-1})$	analysis	calc. $\Delta\nu'(cm^{-1})$	$(\Delta\nu-\Delta\nu')$ (cm^{-1})	labeling of vibronic origins
30638	3505	2978 + 523	3501	4	
30732	3599	2978 + 2 x 306	3590		
30947	3814	2978 + 523 + 306	3807	7	
31039	3906	2978 + 3 x 306	3896	10	
31050	3917				
31159	4026	2978 + 2 x 523	4024	2	
31252	4119	2978 + 523 + 2 x 306	4113	6	
31357	4224	2978 + 4 x 306	4202	22	
31466	4333	2978 + 2 x 523 + 306	4330	3	
31561	4428	2978 + 523 + 3 x 306	4419	9	

Figure 6. xy-polarized single crystal absorption spectrum of TMCBD in the (001) crystal face. Sample temperature is 4.2 K. Resolution is 1.1 cm^{-1}

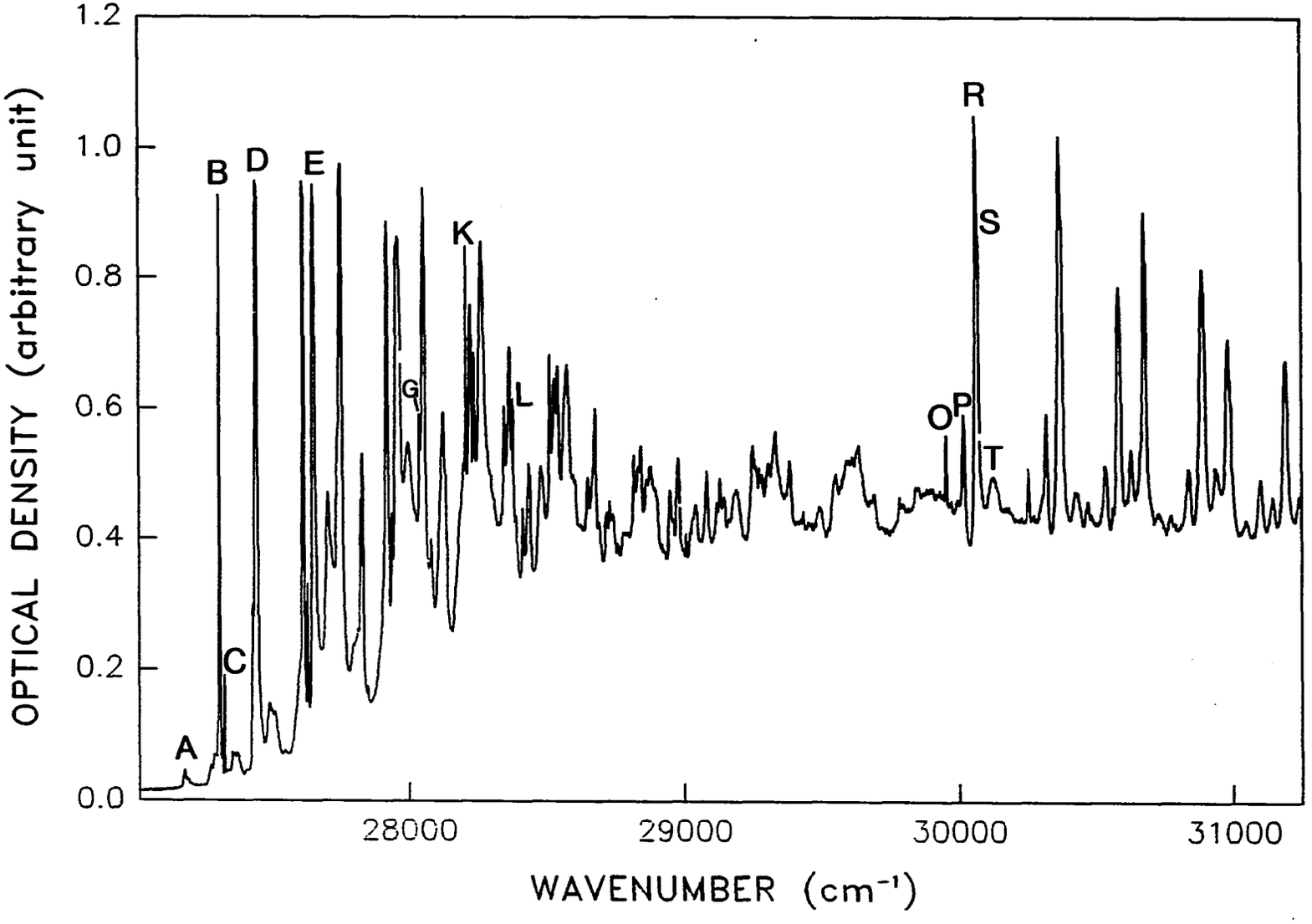
OPTICAL DENSITY (arbitrary unit)
1.2
1.0
0.8
0.6
0.4
0.2
0.0
A
B
C
D
E
G
K
L
O
P
R
S
T
28000
29000
30000
31000
WAVENUMBER (cm⁻¹)

Table 5. Vibronic structure of TMCBD in the S_1 state observed by the xy-polarized spectrum of TMCBD in (001) crystal face

observed freq. $\nu(cm^{-1})$	observed $\Delta\nu(cm^{-1})$	analysis	calc. $\Delta\nu'(cm^{-1})$	$(\Delta\nu-\Delta\nu')$ (cm^{-1})	labeling of vibronic origins
(27133)	0	0-0	0	0	0-0
27193	60	60	60	0	A
27319	186	186	186	0	B
27327	194	194	194	0	
27333	200	200	200	0	C
27441	308	308	308	0	
27453	320	320	320	0	D
27499	366	60 + 306	366	0	
27624	491	186 + 306	492	-1	
27638	505	200 + 306	506	-1	
27662	529	529	529	0	E
27714	581				
27760	627	320 + 306	626	1	
27836	703	186 + 517	703	0	
27844	711	186 + 523	709	2	
27932	799	186 + 2 x 306	798	1	
27947	814	200 + 2 x 306	812	2	
27967	834	529 + 306	835	-1	
27974	841	320 + 523 (shoulder)	843	-2	
28012	879				

Table 5. (continued)

observed freq. $\nu(cm^{-1})$	observed $\Delta\nu(cm^{-1})$	analysis	calc. $\Delta\nu'(cm^{-1})$	$(\Delta\nu-\Delta\nu')$ (cm^{-1})	labeling of vibronic origins
28052	919	919	919	0	G
28069	936	320 + 2 x 306	932	4	
28095	962	962	962	0	I
28140	1007	186 + 517 + 306	1009	-2	
28215	1083				
28224	1091	1091	1091	0	K
28239	1106	186 + 3 x 306	1104	2	
28254	1121	200 + 3 x 306	1118	3	
28280	1147	529 + 2 x 306	1141	6	
28359	1226	919 + 306	1225	1	
28379	1246	320 + 3 x 306	1238	8	
28386	1253	1253	1253	0	L
28402	1269	962 + 306	1268	1	
28430	1297				
28455	1322	186 + 517 + 2 x 306	1315	7	
28500	1367	1367	1367	0	M
28530	1397	1091 + 306	1397	0	
28548	1415	186 + 4 x 306	1410	5	
28559	1426	200 + 4 x 306	1424	2	
28591	1458	529 + 3 x 306	1447	9	
28668	1535	919 + 2 x 306	1531	4	
28697	1564	1253 + 306	1559	5	

Table 5. (continued)

observed freq. $\nu(cm^{-1})$	observed $\Delta\nu(cm^{-1})$	analysis	calc. $\Delta\nu'(cm^{-1})$	$(\Delta\nu-\Delta\nu')$ (cm^{-1})	labeling of vibronic origins
28712	1579	962 + 2 x 306	1574	5	
28737	1604	1297 + 306	1603	1	
28742	1609	1091 + 523	1614	-5	
28751	1618				
28763	1630	186 + 517 + 3 x 306	1629	1	
28782	1649	1649	1649	0	
28807	1674	1367 + 306	1673	1	
28839	1706	1091 + 2 x 306	1703	3	
28858	1725	186 + 5 x 306	1716	9	
28868	1735	200 + 5 x 306	1730	5	
28887	1754				
28904	1771	529 + 4 x 306	1753	18	
28978	1845	919 + 3 x 306	1837	8	
29001	1868				
29006	1873	1253 + 2 x 306	1865	8	
29032	1899				
29069	1936	186 + 517 + 5 x 306	1935	1	
29113	1980	1367 + 2 x 306	2022	7	
29162	2029	186 + 6 x 306	2022	7	
29176	2043	200 + 6 x 306	2036	7	
29219	2086	529 + 5 x 306	2059	27	
29281	2148	919 + 4 x 306	2143	5	

Table 5. (continued)

observed freq. $\nu(cm^{-1})$	observed $\Delta\nu(cm^{-1})$	analysis	calc. $\Delta\nu'(cm^{-1})$	$(\Delta\nu-\Delta\nu')$ (cm^{-1})	labeling of vibronic origins
29309	2178	1253 + 3 x 306	2171	7	
29340	2207				
29365	2232	186 + 517 + 5 x 306	2241	-8	
29417	2284	1367 + 3 x 306	2285	-1	
29468	2335	186 + 7 x 306	2328	7	
29587	2454	919 + 5 x 307	2449	5	
29671	2538				
29726	2593	1367 + 4 x 306	2591	2	
29995	2862	2862	2862	0	0
30058	2925	2925	2925	0	P
30107	2974	2974	2974	0	R
30115	2982	2982	2982	0	S
31071	3038	3038	3038	0	T
30301	3168	2862 + 306	3168	0	
30368	3235	2925 + 306	3231	4	
30413	3280	2974 + 306	3280	0	
30421	3288	2982 + 306	3288	0	
30475	3342	3038 + 306	3344	-2	
30519	3386	2862 + 523	3385	1	
30583	3450	2925 + 523	3448	2	
30630	3497	2974 + 523	3497	0	
30676	3542	2925 + 2 x 306	3537	5	

Table 5. (continued)

observed freq. $\nu(cm^{-1})$	observed $\Delta\nu(cm^{-1})$	analysis	calc. $\Delta\nu'(cm^{-1})$	$(\Delta\nu-\Delta\nu')$ (cm^{-1})	labeling of vibronic origins
30727	3594	2982 + 2 x 306	3594	0	
30891	3758	2925 + 523 + 306	3754	4	
30942	3809	2974 + 523 + 306	3803	6	
30989	3856				
31037	3904	2982 + 3 x 306	3900	4	
31100	3967				
31156	4023	2974 + 2 x 523	4020	3	
31197	4064	2925 + 523 +2 x 306	4060	4	
31248	4115	2974 + 523 +2 x 306	4109	6	
31303	4170				
31352	4219	2982 + 4 x 306	4206	13	
31460	4327	2974 + 523 + 3 x 306	4415	9	

absorption spectra. Since one of the vibronic origins which occurs at 60 cm^{-1} of the higher energy from the origin band of $S_1 \leftarrow S_0$ is observed in the xy-polarized (Fig. 5) as well as in the z-polarized spectra (Fig. 6), totally twenty vibronic origins are identified in the S_1 state. Further discussion of the vibronic origins will appear in the discussion section. One noticeable difference in the z-polarized spectrum compared to the other polarized absorption spectra is very broad and intense feature underneath the C-H stretching vibrations. This feature is tentatively assigned as an absorption of a photoproduct of TMCBD, i.e., dimethyl ketene or tetramethyl cyclopropanone. While only one noticeable vibronic origin was observed in the C-H stretching vibration region in the z-polarized absorption spectrum, five vibronic origin were identified in the same energy region in the xy-polarized absorption spectrum. The rest of the polarized and unpolarized absorption spectra of (001), (010), and (110) crystal faces are listed in appendix at the end of this manuscript.

The low temperature single crystal fluorescence emission spectrum of TMCBD at liquid helium temperature is shown in Fig. 7. The appearance of the fluorescence spectrum is much different from that of the polarized absorption spectra. In the fluorescence emission spectrum, the (0-0) band cannot be identified. The $S_0 \leftarrow S_1$ origin band is absent because this transition is forbidden and the fluorescence comes from the zero vibrational level in the S_1 state. Additionally, the reabsorption of the origin band prevented us from identifying the true (0-0) origin band. Therefore, the frequency of (0-0) band obtained in the z-polarized absorption spectrum is used as the energy of the

Figure 7. Single crystal fluorescence emission spectrum of TMCBD at 4.2 K

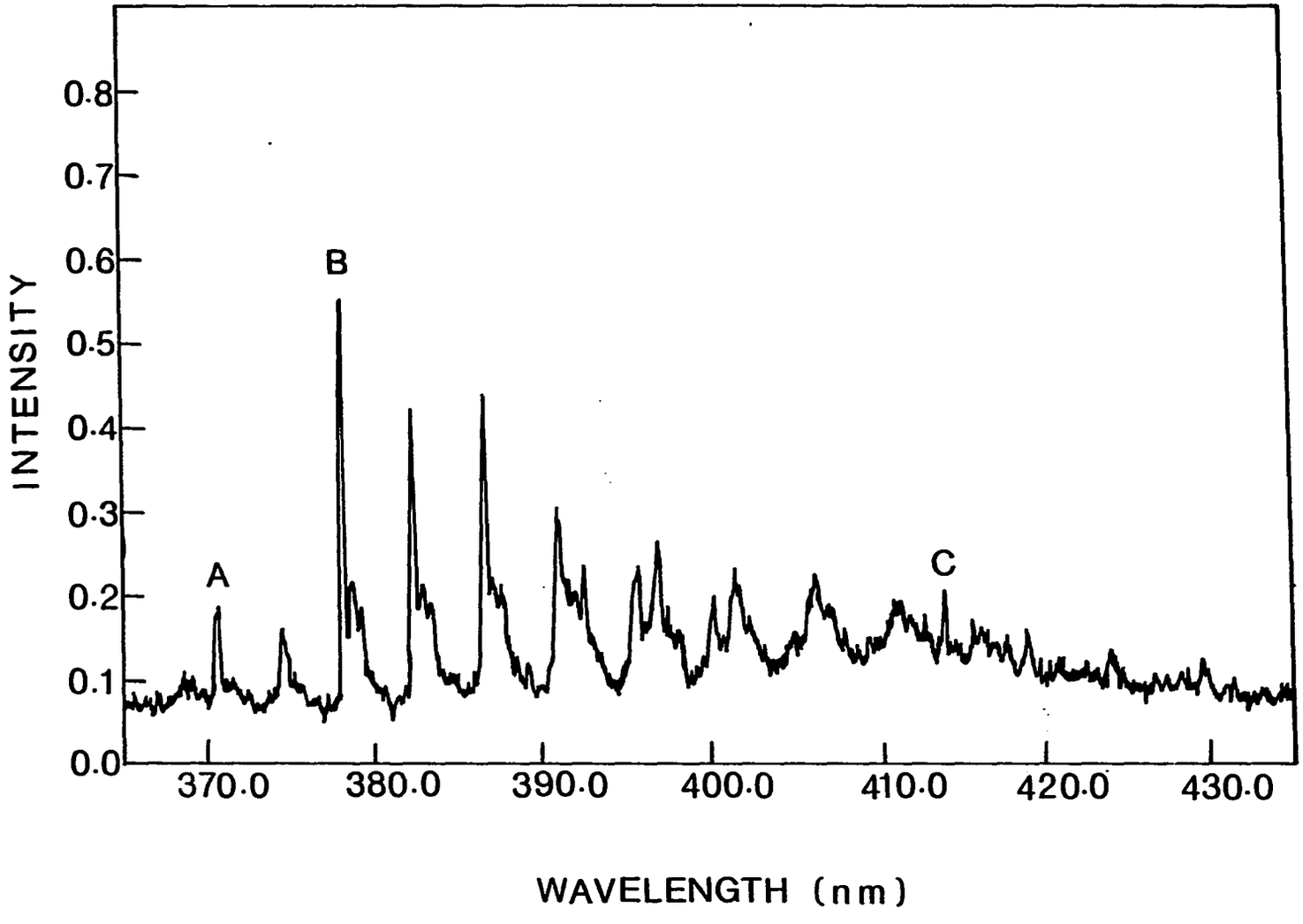
INTENSITY
0.8
0.7
0.6
0.5
0.4
0.3
0.2
0.1
0.0
A
B
C
370.0
380.0
390.0
400.0
410.0
420.0
430.0
WAVELENGTH (nm)

(0-0) band in the $S_0 \leftarrow S_1$ for the vibrational analysis in the ground state. Three vibronic origins including one vibronic origin in the C-H stretching vibrational region are identified in the fluorescence emission spectrum shown in Fig. 7. The prominent progression forming mode (290 cm^{-1}) observed in the fluorescence was correlated with the 306 cm^{-1} mode observed in the absorption spectra. Further discussion will appear later in the discussion section. The different features between the absorption spectra and the fluorescence emission spectrum will be also discussed later.

Figure 8 and Fig. 9 show the z-polarized and unpolarized infrared spectra of (001) crystal face of TMCBD, respectively. Two bands in each figure are identified as a 402 cm^{-1} and 287 cm^{-1} fundamentals. As can be seen in Fig. 8, both fundamentals are polarized in the z-direction (out-of-plane in the (001) crystal face). Since the 287 cm^{-1} is totally absorbed in the z-polarized infrared spectrum, the unpolarized spectrum, which is shown in Fig. 9, was obtained in order to get a correct frequency of the 287 cm^{-1} mode. In the xy-polarized infrared spectrum of the (001) crystal face, none of those fundamentals (402 cm^{-1} and 287 cm^{-1} modes) are observed. With the results of the polarized infrared study, it was possible to correlate the 306 cm^{-1} progression forming mode observed in the absorption spectra with the 290 cm^{-1} mode observed in the fluorescence emission spectra and with the 287 cm^{-1} fundamental observed in the polarized infrared spectra.

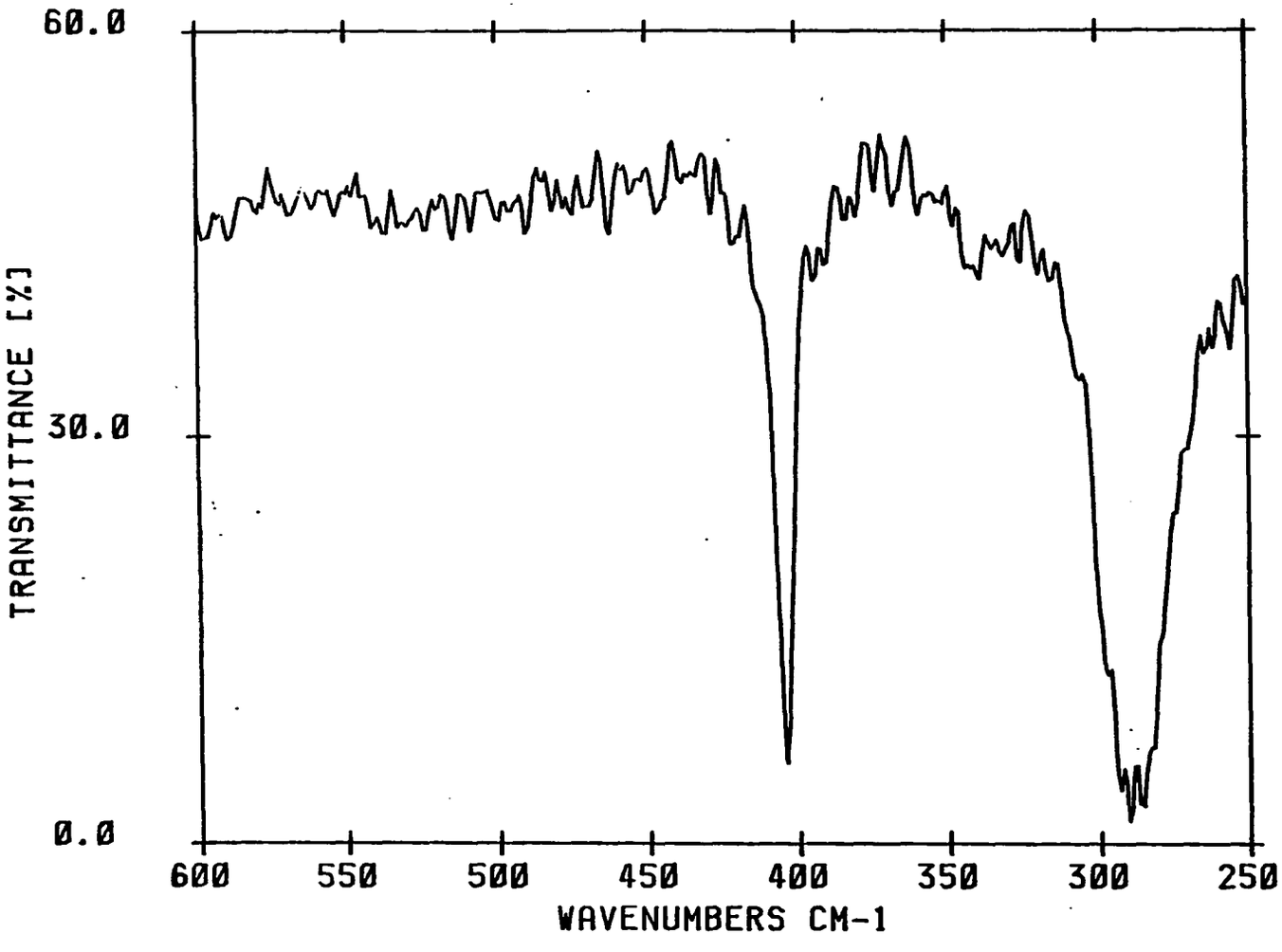

Figure 8. z-polarized infrared spectrum of TMCBD in (001) crystal face. Among three peaks in 287 cm^{-1} band, two peaks are noise

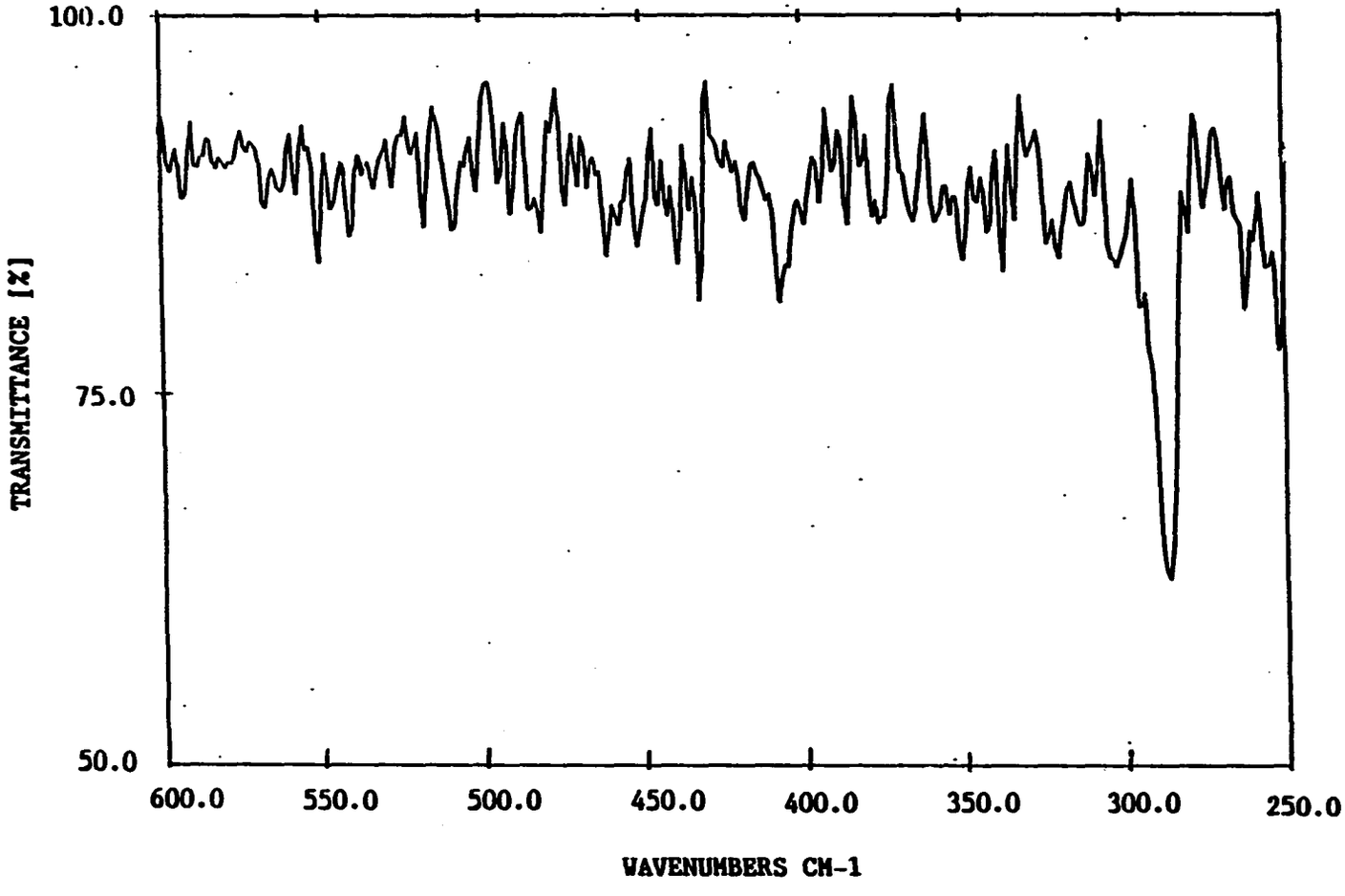

Figure 9. Unpolarized infrared spectrum of TMCBD. The correct energy of 287 cm^{-1} mode is measured by this spectrum

DISCUSSIONS

Polarized Absorption Spectra

Progression forming modes and the point symmetry group in the S_1 state

As was discussed in the introduction section, the (0-0) transition is regarded to be allowed by the crystal site group effect in the distorted symmetry (C_{2v}). There is other evidence for the change of the point symmetry group upon excitation to S_1 state. That is the presence of long progressions by the non-totally symmetric mode (b_{1u}) in the absorption spectra. Three progression forming modes (308 cm^{-1}, 525 cm^{-1}, and 1660 cm^{-1} modes) have been observed by GCN (20) in the polarized absorption spectra of TMCBD for the S_1 state. SBWV observed, however, only two progression forming modes (308 cm^{-1} mode and 526 cm^{-1} modes) in a similar study (19). Meanwhile, three progression forming modes (306 cm^{-1} mode, 517 cm^{-1} mode, and 523 cm^{-1} mode) are identified in the polarized absorption spectra for the $S_1 \leftarrow S_0$ of TMCBD in the present study. One of the progression forming modes (517 cm^{-1} mode) was not observed in the previous two studies (19,20).

Among the three progression forming modes, the characteristics of the 306 cm^{-1} (308 cm^{-1} mode in the studies by SBWV and GCN) was not correctly characterized because the previous two studies (19,20) explained this mode differently. If the 306 cm^{-1} mode is assigned as an a_g mode as GCN assigned, there is no change in the point symmetry group upon excitation to S_1 state. However, if the 306 cm^{-1} mode is assigned

as a non-totally symmetric mode (b_{1u}) as SBWV assigned, a change in the point group upon excitation to S_1 state can be assumed. For the exact assignment on the symmetry of the 306 cm^{-1} mode, a polarized infrared spectra of TMCBD was obtained in the range 250 cm^{-1} - 600 cm^{-1}. The observed infrared spectra showed that the 287 cm^{-1} mode is polarized in the z-direction. Therefore, the 287 cm^{-1} mode in the ground state is assigned as b_{1u} mode. This result proves that the 287 cm^{-1} fundamental in the ground state was incorrectly assigned in the previous two infrared studies on TMCBD by Shurvell and coworkers (26) and Nicolaisen and coworkers (25) because Shurvell and coworkers assigned the 287 cm^{-1} mode as a b_{2u} mode and Nicolaisen and coworkers assigned the same mode as a b_{3u} mode from the results of their infrared studies on TMCBD. Meanwhile, SBWV correlated the 306 cm^{-1} mode observed in the absorption spectra with the 402 cm^{-1} mode in the ground state and GCN correlated the 306 cm^{-1} mode in the S_1 state with the 298 cm^{-1} mode (a_g) in the ground state. We correlate the 306 cm^{-1} mode in the S_1 state with the 287 cm^{-1} fundamental in the ground state. The correlation between the 306 cm^{-1} progression forming mode observed in the polarized absorption spectra and the 287 cm^{-1} fundamental observed in the polarized infrared spectra was made with the results of another new experimental results obtained from low temperature single crystal fluorescence emission in the present study.

The low temperature fluorescence emission spectrum shown in Fig. 7 shows long progression with the progression interval of 290 cm^{-1} (averaged value). This 290 cm^{-1} mode is regarded as the same mode as the 287 cm^{-1} fundamental which was observed in the polarized infrared

spectra and was assigned as a b_{1u} mode. Therefore, we conclude that the 306 cm^{-1} progression forming mode observed in the polarized absorption spectra is a b_{1u} out-of-plane carbonyl wagging mode. We also conclude that the 306 cm^{-1} mode correlates with the 287 cm^{-1} mode in the ground state (290 cm^{-1} in the fluorescence emission study). This b_{1u} mode can act as a totally symmetric mode in the C_{2v} point symmetry group as shown in Table 2.

Another progression forming mode observed in the absorption spectra of TMCBD is a 523 cm^{-1} mode. This 523 cm^{-1} mode occurs building on the electronic origin as well as several vibronic origins. This 523 cm^{-1} mode also shows overtone bands building on the electronic origin as well as several vibronic origins. Therefore, the 523 cm^{-1} mode must be a totally symmetric mode. Two totally symmetric modes (585 cm^{-1} mode and 633 cm^{-1} mode) are identified in the two Raman studies (25,26) near 523 cm^{-1} in the ground state. GCN (20) correlated the 525 cm^{-1} mode (523 cm^{-1} mode in the present study) observed in the S_1 state with the 585 cm^{-1} fundamental in the ground state, while SBWV (19) correlated the same mode (525 cm^{-1} mode) with the 633 cm^{-1} mode in the ground state. Considering the assignment of these previous studies for the 523 cm^{-1} mode (19,20) and the fact that the 523 cm^{-1} mode is totally symmetric, we tentatively assign the 523 cm^{-1} progression forming mode as a totally symmetric ring breathing (or ring deformation) mode which correlates with the 585 cm^{-1} mode or 633 cm^{-1} mode in the ground state. However, since the 633 cm^{-1} mode in the ground state is correlated with the 613 cm^{-1} mode in the S_1 state as will be seen later in this manuscript, the 523 cm^{-1} progression forming mode observed in the absorption spectra is

assigned as a mode corresponding to the 585 cm^{-1} fundamental in the ground state.

The third progression forming mode observed in the polarized absorption spectra of TMCBD is a 517 cm^{-1} mode. This mode has not been identified in the previous two low temperature absorption studies (19,20) probably due to the broad bandwidth of their spectra or the high sample temperatures used (In GCN's study, the sample temperature was 77 K and the bandwidth was measured as ~ 40 cm^{-1}). This 517 cm^{-1} mode can be seen building on the electronic origin (27133 cm^{-1}), the 2978 cm^{-1} mode observed in the z-polarized absorption spectrum, and the 186 cm^{-1} mode observed in the xy-polarized absorption spectrum. The overtone of this mode (517 cm^{-1} mode) also appears building on the electronic origin as well as some vibronic origins. Therefore, the 517 cm^{-1} mode should be a totally symmetric mode, as was the case for the 523 cm^{-1} progression forming mode. There are several explanations that could account for the 517 cm^{-1} mode. One is the correlation between the 517 cm^{-1} mode in the S_1 state and one of the totally symmetric modes in the ground state. However, as was discussed previously in this manuscript, two totally symmetric modes near 517 cm^{-1} (the 585 cm^{-1} mode and the 633 cm^{-1} mode) in the ground state were already correlated with the 523 cm^{-1} and 613 cm^{-1} modes in the S_1 state. Therefore, it is not likely that the 517 cm^{-1} mode observed in the absorption spectra correlates either the 585 cm^{-1} or the 633 cm^{-1} mode in the ground state. Nevertheless, since mode mixing is large in the excited as well as in the ground state, the correlation between the 517 cm^{-1} mode in the S_1 state and any totally symmetric mode other than the 585 cm^{-1} and the 633 cm^{-1} modes in the ground state may be possible.

Another explanation is Fermi resonance in the excited state. In the ground state, the overtone of the 298 cm^{-1} fundamental can occur at ~ 596 cm^{-1} which is close to 585 cm^{-1}. Therefore, Fermi resonance between the overtone of the 298 cm^{-1} mode and the 585 cm^{-1} mode in the ground state may be possible. If there is similar Fermi resonance in the S_1 state, the overtone or the combination band of any mode (totally symmetric mode for the combination band) should occur near the other totally symmetric mode (523 cm^{-1} mode). However, no possible combination or overtone bands occurring near 523 cm^{-1} were observed in the polarized absorption spectra. Therefore, it can be concluded that Fermi resonance does not contribute to the occurrence of the 517 cm^{-1} progression forming mode in the excited state. The third possible explanation concerning the nature of the 517 cm^{-1} progression forming mode observed in the S_1 state is the occurrence of a b_{1u} mode (e.g. 402 cm^{-1} mode) in the ground state acting as a totally symmetric mode in the S_1 state (C_{2v} symmetry). According to the correlation table shown in Table 1, b_{1u} modes in the D_{2h} point symmetry group correspond to totally symmetric modes in the C_{2v} point symmetry group. Therefore, the 402 cm^{-1} mode in the ground state, which is the closest occurring b_{1u} mode relative to the 517 cm^{-1} mode of the S_1 state, can act as a totally symmetric progression forming mode (517 cm^{-1} mode) in the excited state (C_{2v} point symmetry group). However, the energy difference between the 517 cm^{-1} mode observed in the S_1 state and the 402 cm^{-1} mode observed in the ground state is too large to be considered as a correct correlation. We conclude, therefore, that the correlation between the 517 cm^{-1} progression forming mode observed in the S_1 state and any fundamental in

the ground state can be made based on the one of the reasons explained above, but the correct explanation on the characteristic of the 517 cm^{-1} mode can not be confirmed.

Since the symmetries of the 517 cm^{-1} mode and the 523 cm^{-1} mode are both totally symmetric, the 517 cm^{-1} progression interval should be observed whenever the 523 cm^{-1} progression interval is observed. However, the 517 cm^{-1} mode is observed building on the electronic origin and two vibronic origins in the S_1 state. A possible reason we did not observe the 517 cm^{-1} interval with the 523 cm^{-1} interval could be due to the broad bandwidth of vibronic origins and bands formed by progressions. For example, the bandwidth of the (0-0) band was measured as 1.2 cm^{-1} (FWHM) and that of the 517 cm^{-1} progression band building on the (0-0) band was measured as ~ 3 cm^{-1}. The bandwidth of the 186 cm^{-1} mode observed in the xy-polarized absorption spectrum was measured as ~ 4 cm^{-1} (FWHM). However, the bandwidths of several bands (e.g. 529 cm^{-1} and 2978 cm^{-1} mode) were greater than the 11 cm^{-1} (FWHM) (FWHM = ~ 12 cm^{-1} for the 529 cm^{-1} band, FWHM = 11 cm^{-1} for the 2978 cm^{-1} band). Therefore, even though the 517 cm^{-1} progression interval should be observed with the 523 cm^{-1} interval in the progression bands of the S_1 state, these two modes cannot be resolved due to the mixing of the modes in a very narrow frequency range or the broad intrinsic bandwidth of some vibronic origins. These two progression forming modes (517 cm^{-1} mode and 523 cm^{-1} mode) building on vibronic origins can be resolved only if the bandwidths of the vibronic origins or progression bands are narrow.

Herzberg-Teller vibronic coupling and assignment of vibronic origins

As was discussed in the previous section, the A_u transition in TMCBD is forbidden by the electric dipole transition selection rules and in the magnetic dipole transition selection rule. Therefore, all the bands which are observed in the absorption spectra have obtained their intensity by some other mechanism. One possibility is Herzberg-Teller vibronic coupling. In this section, a brief description of Herzberg-Teller vibronic coupling, which is an example of the breakdown of the Born-Oppenheimer approximation, will be discussed. For further description, several references are recommended (30-35).

The Born-Oppenheimer approximation (or Born-Oppenheimer principle) states that the molecular wavefunction can be written as a product of electronic and vibrational wavefunctions. Strictly speaking, this approximation is one of three currently used adiabatic approximations; Born-Oppenheimer approximation, Born-Huang approximation and the crude adiabatic approximation. The Born-Oppenheimer approximation is generally not valid in practice and can breakdown. If there is a breakdown of this approximation, there can be a mixing of electronic motions and nuclear motions, resulting in very complicated spectra. One example of a breakdown in the Born-Oppenheimer approximation is Herzberg-Teller vibronic coupling. Herzberg-Teller vibronic coupling implies that non-totally symmetric modes can mix with an electronic state (e.g., S_1 state) and if the symmetries of the mixed modes are the same as those of other higher electric dipole allowed excited electronic states, the forbidden $S_1 \leftarrow S_0$ transition can become allowed by intensity borrowing from a higher allowed electronic state.

The application of the Herzberg-Teller vibronic coupling mechanism to the case of TMCBD is discussed in the following examples. The symmetry of a 320 cm^{-1} mode is assigned as b_{2g}. This transition is not allowed by the electric dipole transition selection rules. However, the 320 cm^{-1} band shows reasonable intensity in the xy-polarized absorption spectra as shown in Fig. 6. The vibronic species of this band in the excited state is B_{2u} ($A_u \times b_{2g} = B_{2u}$). Since the y-component of the dipole moment is of B_{2u} symmetry, this transition is allowed via vibronic coupling ($B_{2u} \times B_{2u} \times A_g = A_g$) in D_{2h} symmetry and also in C_{2v} point symmetry group. Another example is the 529 cm^{-1} vibration which is assigned as b_{3u} mode. The transition to the 529 cm^{-1} vibration in the S_1 state is not allowed by the electric dipole selection rule either. However, the vibronic species of this vibration is B_{3u} ($b_{3g} \times A_u = B_{3u}$). Since B_{3u} is the x-component of the dipole moment in the D_{2h} symmetry, this transition is allowed via vibronic coupling ($B_{3u} \times B_{3u} \times A_g = A_g$) in D_{2h} symmetry and also in C_{2v} point symmetry group.

The vibrational assignment of all the observed bands are made by considering the vibronic coupling and the observed polarization of each band. The absorption spectra (xy- and z-polarized) show twenty vibronic origins in the energy region studied here. Some vibronic origins are labeled in Fig. 5 and Fig. 6, and all the vibrational assignment of the observed vibronic origins are listed in Table 6. In Table 6, some correlations between vibrational modes of the ground state and those of the excited state (S_1) are tentative. Band A is very weak and it is observed in every polarized spectrum. This band has been also observed and assigned by SBWV (19) as a band representing the transition to the

second triplet state of TMCBD or the absorption of photochemically formed dimethyl ketene. Indeed, dimethyl ketene shows absorption in this energy region (40). However, this weak band forms short progressions with a interval of 306 cm^{-1}, which is the commonly occurring progression interval in the first excited triplet state (20,36) as well as in the first excited singlet state. The infrared and Raman data obtained by Shurvell et al. (25) indicate that the 78 cm^{-1} band, which may correspond to band A in the excited state, has b_{1u} or b_{3u} symmetry. Therefore, although the characteristic of this band is not clear, we tentatively assign band A as one of the vibronic origins in the S_1 state because there is no other evidence of a second triplet state in this frequency region and because the progression bands built on the band A show the progression intervals of 306 cm^{-1}. This band is polarized in the x-, y- and z-directions.

Band B in Fig. 6 is clearly polarized in the x-direction (perpendicular to the carbonyl axis) and regarded as corresponding to the 160 cm^{-1} vibration in the ground state. Its vibronic symmetry is B_1 (in C_{2v} symmetry) which originates from B_{2g} or B_{3u} in D_{2h} symmetry. This indicates that the Herzberg-Teller active mode is either b_{2u} or b_{3g}. Infrared and Raman data (25,26) indicate that this mode has gerade (g) symmetry. Therefore, band B is assigned as a b_{3g} mode. Band E is polarized in the xy-direction as shown in Fig. 6. This band is tentatively correlated with the 661 cm^{-1} vibrational mode in the ground state because the 661 cm^{-1} fundamental of the ground state is closest lying gerade mode to the band E of the S_1 state. Although this band is polarized in the xy-direction, it has been assigned as a x-polarized b_{3g}

mode based on the intensity of this band in the x- and y-polarized spectra of (010) crystal face. The x- and y-polarized spectra of TMCBD in the (010) crystal face are shown in appendix of this manuscript.

Band C in Fig. 6, which is regarded to correlate with the 186 cm^{-1} mode in the ground state and has not been discussed in the previous two studies by SBWV (19) and GCN (20), shows predominant polarization in the x-direction. Therefore, the Herzberg-Teller active mode is either b_{2u} or b_{3g}. However, due to the ungerade (u) symmetry of 186 cm^{-1} mode (25,26), band C is assigned as b_{2u} mode, not b_{1u} or b_{3u} as mentioned in the previous studies (19,20). In contrast, band D, which is correlated with the 272 cm^{-1} mode in the ground state, is predominantly polarized in the y-direction (parallel to the carbonyl axes). Its vibronic symmetry is B_2 (in C_{2v} symmetry) which originates from B_{2u} or B_{3g} in D_{2h} symmetry. Therefore, the Herzberg-Teller active mode is either b_{2g} or b_{3u}. We assign this mode as b_{2g} based on the gerade (g) symmetry of the 272 cm^{-1} fundamental in the ground state. Bands F, H, and J observed in Fig. 5 are exclusively polarized in the z-direction (out-of-plane) and their active mode assignment is made based on infrared and Raman data (25,26). Bands G, I, K, L, and M observed in the xy-polarized spectrum are tentatively assigned as xy-polarized bands because it was difficult to distinguish the more predominant polarization even with the x- and y-polarized spectra in the (010) crystal face. These bands show comparable intensities in both x-polarized and y-polarized spectra of (010) crystal face (see appendix).

Band G (919 cm^{-1}) is assigned as a xy-polarized b_{3g} mode. However, GCN have assigned a band observed at 911 cm^{-1}, which occurs close to the

919 cm^{-1} mode observed in the present study, as a z-polarized b_{1g} mode. If these two modes (911 cm^{-1} and 919 cm^{-1}) are same mode and if the energy difference between the two modes (911 cm^{-1} mode and 919 cm^{-1} mode) is thought arising from the experimental uncertainty, then they should be xy-polarized modes because this band is clearly observed in the xy-polarized absorption spectrum (Fig. 6). No band was observed at 911 cm^{-1} with z-polarization in the present study. Band N, which was observed at 1653cm^{-1} from the origin in Fig. 5, corresponds to a symmetric carbonyl stretching mode (1855 cm^{-1} in the ground state) with an a_g symmetry. A very weak band at 1649 cm^{-1} from the origin was observed in the xy-polarized spectrum of the (001) crystal face. This band can be assigned as an asymmetric carbonyl stretching vibrational mode (1752 cm^{-1} in the ground state). Since the 1649 cm^{-1} band does not form any progression, only the 1653 cm^{-1} band was assigned as a vibronic origin. The big difference in the carbonyl stretching modes in energy between the ground and excited states has been explained previously as an indication of a C=O bond lengthening (20).

Six more vibronic origins have been observed in the frequency range 2800 cm^{-1} - 4000 cm^{-1} from the electronic origin and these will be discussed in the next section. Complete assignment of vibronic origins observed in the polarized absorption spectra of TMCBD is shown in Table 6.

C-H stretching vibrational modes or another electronic state?

Several bands with strong intensity are observed in all the absorption spectra of TMCBD in the range 2800 cm^{-1} - 4000 cm^{-1} from the origin. SBWV (19) assigned these bands as a structure which originated from the transition to a second singlet excited electronic state (S_2) because the progression intervals are different from those of the lower energy bands and because the bandwidths are slightly broader in this frequency region than those of the S_1 state (bands at lower energy region than 2800 cm^{-1}). However, GCN (20) have suggested a different interpretation of these bands. They (GCN) assigned these intense features which occur in the vicinity 3000 cm^{-1} higher in energy from the $S_1 \leftarrow S_0$ origin to vibronically induced C-H stretching vibrations of the S_1 state. Their assignment was based on the frequency shift of these bands in the absorption spectra of TMCBD-d_{12} compared to TMCBD. The present study gives experimental evidence which could support the suggestion of GCN. First, the prominent progression intervals in this energy region are 306 cm^{-1} and 523 cm^{-1} which are the same intervals as in the case of lower frequency region. Second, a weak band at 2981 cm^{-1}, which is assigned as a C-H stretching mode because the 2981 cm^{-1} mode is close in energy to the C-H stretching vibration modes, and several bands formed by a progression built on this 2981 cm^{-1} band are observed in the fluorescence emission spectrum shown in Fig. 7. Therefore, intense features occurring in the vicinity 3000 cm^{-1} higher in energy from the $S_1 \leftarrow S_0$ origin in the polarized absorption spectra are assigned as C-H stretching vibrations and their progression bands

building on each vibronic origins in this region, not a second excited electronic state.

Six vibronic origins are identified in the C-H stretching vibration region. Band Q (2978 cm^{-1}) in the z-polarized spectrum (Fig. 5) is located in energy between the doublet (2974 cm^{-1} and 2982 cm^{-1}) of the xy-polarized spectrum (Fig. 6). These three vibrational modes may originate from one fundamental of the ground state because the three bands are located very closely in energy. However, due to the different polarization, band Q is assigned as a totally symmetric mode which may correspond to the 2938 cm^{-1} vibration (a_g) in the ground state. The doublet is assigned to two separate vibronic origins. According to the infrared and Raman data (25,26), there are two very closely lying vibrational modes in the ground state, i.e., 2972 cm^{-1} mode and 2976 cm^{-1} mode. Therefore, the two vibronic origins observed at 2974 cm^{-1} and 2976 cm^{-1} in the xy-polarized absorption spectrum (see Fig. 6) are correlated with two fundamentals (2972 cm^{-1} and 2976 cm^{-1}) in the ground state. This doublet cannot be identified after the progression of two quanta because the broad bandwidth prevents resolving these two modes. A 3038 cm^{-1} band observed in Fig. 6, which is weak and broader than other C-H stretching bands, can be assigned as a combination band or a overtone band of any fundamental vibration, or even another vibronic origin band. The only possible combination of bands to get close frequency to the 3038 cm^{-1} mode is the combination of the 1367 cm^{-1} and the 1649 cm^{-1} bands. However, this combination does not exactly corresponds to the 3038 cm^{-1} band in energy. Additionally, no overtone band is observed in the energy region near the 3038 cm^{-1} mode.

Table 6. Assignment of vibronic origins

vibronic origins	$\Delta\nu(cm^{-1})$ (observed polarization)	$\Delta\nu(cm^{-1})$ ground state Ref.[25]	$\Delta\nu(cm^{-1})$ from fluorescence data	Symmetry of vibronic origins		
				From Ref. [25] Gas/soln.	From Ref. [26]	Present study
A	60(xyz)	78		b_{1u}	b_{1u}/b_{2u}	b_{1u}/b_{1u}
B	186(x)	160	158	b_{2g}/b_{3g}	b_{1g}	b_{3g}
C	200(x)	186		b_{3u}/b_{1u}	b_{1u}/b_{3u}	b_{2u}
D	320(y)	272		b_{2g}	b_{3g}	b_{2g}
E	529(y)	661	685	b_{1g}	b_{2g}	b_{2g}
F	613(z)	633		a_g	a_g	a_g
G	919(xy)	910		b_g	b_{3g}	b_{3g}
H	937(z)	963		a_g	a_g/b_{1u}	a_g
I	962(xy)	966		b_{1u}/b_{3u}	b_{3u}	b_{3u}
J	1086(z)	1044		b_{3u}/b_{1u}	b_{1u}	b_{1u}
K	1091(xy)	1059		b_{2g}/b_{3g}	b_{1g}	b_{3g}
L	1253(xy)	1257			b_{2g}	b_{2g}
M	1367(xy)	1364		b_{1u}	b_{3u}	b_{3u}
	1649(xy)	1752		b_{2u}	b_{2u}	b_{2u}
N	1647(z)	1855		a_g	a_g	a_g
O	2862(y)	2868		b_u	b_{2u}	b_{3u}
P	2925(y)	2906		b_u	b_{2g}	b_{2g}
Q	2978(z)	2938		a_g	a_g	a_g
R	2974(xy)	2972	2981	b_g	b_{3g}	b_{3g}
S	2982(xy)	2976		b_g	b_{1g}/b_{2g}	b_{2g}/b_{3g}
T	3038(xy)					b_{3g}/b_{2g}

Therefore, the 3038 cm^{-1} band is tentatively assigned as a vibronic origin which shows polarization in the xy-direction. However, it is also possible that the 3038 cm^{-1} mode is a vibronic origin or electronic origin of the second excited electronic state (S_2) because the bandwidth (~ 35 cm^{-1}) is much broader than the other C-H stretching bands. Besides, one of the photoproduct of TMCBD, i.e., dimethyl ketene, shows absorption in this energy region. Therefore, even though 3038 cm^{-1} band is assigned as a vibronic origin of the S_1 state of TMCBD, the correct assignment is still ambiguous. Bands P and Q are predominantly polarized in the y-direction as can be seen in Fig. 6 and the active Herzberg-Teller modes are assigned as b_{3u} and b_{2g}, respectively.

One of the interesting features in the z-polarized spectrum of the (001) crystal face is the broad and intense feature underneath the C-H stretching vibrations as shown in Fig. 5. This could be an indication of another hidden electronic state as mentioned by SBWV (19). However, several repetitions of the experiment gave no evidence of this broad and intense absorption. One possible explanation for this broad features underneath the C-H stretching vibrations observed in Fig. 5 is the absorption of a photoproduct of TMCBD which could be formed by long time exposure to the excitation source. Several photoproducts of TMCBD have been predicted previously (37). Among the photoproducts of TMCBD which can be formed in the singlet excited state, dimethyl ketene has been identified as a dominant photoproduct by Vala and Spafford (37). Another photoproduct which can absorb ultraviolet light in the 330 nm region, is tetramethyl cyclopropanone. However, tetramethyl cyclopropanone has been regarded as a very reactive and short lived

compound (38,39). The tetramethyl cyclopropanone has been regarded to be stable only if it is in the some specific solvent, e.g., pentane. Meanwhile, the absorption study of dimethyl ketene by Holroyd and Blacet (40) showed that there was an absorption in the range ~ 28000 cm^{-1} - 33000 cm^{-1}. However, there has been no absorption study on tetramethyl cyclopropanone probably due to the unstable characteristics of this molecule. Therefore, we conclude tentatively that the broad feature observed in the vicinity 3000 cm^{-1} higher in energy from the $S_1 \leftarrow S_0$ origin underneath the C-H stretching vibrations is an absorption of the dimethyl ketene. Nevertheless, since the carbonyl compounds, e.g., formaldehyde, show absorption in this energy region (330 nm - 350 nm) (41) it is still possible that the photoproduct may be a tetramethyl cyclopropanone.

Carbonyl wagging vibration and the double minimum potential

It has been reported that several mono-carbonyl molecules have double minimum potentials caused by the carbonyl wagging vibrational mode in the excited as well as in the ground state. This double minimum potential has been identified mainly by the presence of a anharmonic progression. SBWV (19) have suggested that the prominent progression forming mode (308 cm^{-1}, in the present case 306 cm^{-1}) corresponds to the out-of-plane carbonyl wagging mode and this mode indicates the presence of double minimum potential. However, GCN have suggested that the prominent 306 cm^{-1} band is a totally symmetric mode (20) as was discussed in the previous section. They also denied the presence of the

double minimum potential by showing the calculated results for the relative intensities of transitions originating from the v" = 0 level of the harmonic ground state by utilizing Coon et al.'s double minimum potential function (42). They suggested that if there is a double minimum potential, the maximum intensity of bands formed by a progression built on any specific vibronic origin or electronic origin with the 306 cm^{-1} progression forming mode should occur in the sixth or higher progression band.

In the present study, all the progressions are harmonic as indicated by GCN (20). However, the maximum intensity was shown at four or lower quanta progression bands not in the first or second quantum progression bands as GCN have indicated. The intensity comparison among progression bands building on vibronic origins or electronic origin can be clearly made by examining the progression bands building on the (0-0) band as an example because other progression bands formed by progression building on any vibronic origins show generally combined intensity with other modes, and therefore, it is difficult to measure the intensity of desired band only. The bands arising from progressions building on the (0-0) band show maximum intensity at the third quanta progression band as can be seen in Fig. 5. However, if both bandwidth and area of each band are considered instead of just the intensity of these bands, the relative intensities may change because the higher quanta progression bands tend to have somewhat broader bandwidths compared to the lower quanta progression bands. For example, the (0-0) band has a bandwidth of 1.2 cm^{-1} (FWHM). While the bandwidth of the third quanta progression band is ~ 5 cm^{-1} (FWHM), the bandwidth of the fourth quanta progression

band formed by the 306 cm^{-1} mode is measured as 8 cm^{-1}. Therefore, even though the intensity of the fourth quanta band formed by the 306 cm^{-1} mode is lower than that of the third quanta progression band formed by the 306 cm^{-1} mode, the bandwidth of the fourth quanta progression band is broader than that of the third quanta progression band. The band formed by progression with five quanta of 306 cm^{-1} is mixed with the progression band built on the 613 cm^{-1} vibronic origin. Therefore, for other bands formed by progression built on several vibronic origins, it is difficult to estimate the exact intensity of desired mode only because several modes are mixed into one or two bands. Nevertheless, considering the broad bandwidths of the higher quanta progression bands, the maximum intensity will be observed in the higher quanta progression bands, not in the first or second quanta as GCN (20) mentioned. Therefore, we tentatively conclude that the potential well of TMCBD in the S_1 state has double minimum and the non-totally symmetric 306 cm^{-1} progression forming mode (b_{1u}, out-of-plane carbonyl wagging vibration) is governed by the double minimum potential.

Low Temperature Fluorescence Emission Spectra and Duschinsky Effect

The single crystal fluorescence emission spectrum at 4.2 K shown in Fig. 7 has a much different appearance compared to the absorption spectra. Since the intensity of (0-0) origin transition band is regarded as very weak and the reabsorption of the origin band occurs, it is difficult to identify the exact position of the origin band in this

spectrum. Therefore, the frequency of origin band observed in the absorption spectra (27133 cm^{-1}) is used as the (0-0) band frequency, and all the vibrational assignments are made relative to this frequency.

Band A in Fig. 7 which corresponds to the band B (186 cm^{-1}) in the excited state, is assigned as a b_{3g} mode because the 186 cm^{-1} in the S_1 state has been assigned as b_{3g} mode previously in this manuscript. Band B (689 cm^{-1}) in Fig. 7, which is the most intense peak in this spectrum, is assigned as a b_{3g} mode. This 689 cm^{-1} mode may correspond to the band E in the absorption spectra (Fig. 6). However, it is difficult to understand why the frequency of this mode (689 cm^{-1}) measured by fluorescence emission spectroscopy is different from that of the possibly same mode (661 cm^{-1} mode) measured by infrared spectroscopy (25,26). Band C (2891 cm^{-1}) in Fig. 7 is assigned as a C-H stretching vibrational mode because the C-H stretching vibrations have been observed near 2870 cm^{-1} - 2980 cm^{-1} in the infrared and Raman studies (25,26). Observation of the C-H stretching vibration in the fluorescence emission spectrum confirms that the intense features in the vicinity 3000 cm^{-1} higher in energy from the $S_1 \leftarrow S_0$ origin observed in the absorption spectra are not from another excited electronic state.

All three vibronic origins forms short or long progressions with 290 cm^{-1} intervals. This 290 cm^{-1} mode has been assigned as a b_{1u} out-of-plane carbonyl wagging mode in the previous section and this mode has been correlated with the 306 cm^{-1} progression forming mode in the S_1 state. Another progression forming mode is a 970 cm^{-1} mode which might correspond to the 937 cm^{-1} or 962 cm^{-1} modes in the excited state. However, the statement that the 970 cm^{-1} mode is a progression forming

Table 7. Vibrational assignments of TMCBD observed by fluorescence emission spectra

observed freq.(cm^{-1})	relative freq.(cm^{-1})	analysis	assignment
27133	0	0	(0-0)
26975	158	158	b_{3g}(A)
26685	448	158 + 290	
26444	689	689	b_{2g}(B)
26148	985	689 + 290(+3)	
25856	1277	689 + 2 x 290(+1)	
25563	1570	689 + 3 x 290(+3)	
25474	1659	689 + 970	
25273	1861	689 + 4 x 290	
25185	1948	684 + 970 + 290	
24974	2159	689 + 5 x 290(-5)	
24899	2235	689 + 970 + 2 x 290(-3)	
24692	2441	689 + 6 x 290(-9)	
24604	2529	689 + 970 + 3 x 290	
24313	2820	689 + 970 + 4 x 290(+1)	
24152	2981	2981	b_{1g} and
23872	3261	2981 + 290(-10)	b_{2g}(C)
23574	3559	2976 + 2 x 290	
23275	3859	2976 + 3 x 290(+8)	

mode is only an assumption. Otherwise, the 1659 cm^{-1} mode could be assigned as a carbonyl stretching mode. But infrared and Raman data (25,26) have indicated that the symmetric carbonyl stretching vibration is observed at 1850 cm^{-1} and the asymmetric carbonyl stretching vibration is observed at 1750 cm^{-1}. Therefore, the only possible assignment about the nature of the 1659 cm^{-1} mode observed in the fluorescence emission spectrum is that it is a band formed by the progression building on the 689 cm^{-1} band with progression interval of 970 cm^{-1}. Assignment of vibrational bands observed in the fluorescence emission spectra is listed in Table 7.

It is difficult to say whether the relative intensity of the C-H stretching band in the fluorescence spectrum is weaker than those of absorption spectra due to the difficulty of observing the (0-0) band in the fluorescence emission spectrum. However, as mentioned at the beginning of this section, a difference in the appearance of the fluorescence spectrum and absorption spectra has been observed. Vibronic coupling is very active in the excited state with twenty vibronic origins compared to the ground state which showed only three vibronic origins and rather simple structure. This difference in vibronic activity between the S_1 state and the ground state can be explained as a Duschinsky effect (mode mixing) caused by the rotation of the normal coordinates in the excited state compared to the ground state. Duschinsky effect has been discussed for several different cases (43-48), and therefore, only brief description will be provided here.

It was first pointed out by Duschinsky (43) that the normal coordinates of excited states are in general rotated relative to those

of the ground state. This effect applies to those normal coordinates where there are two or more of a given symmetry species (irreducible point group representation). The normal coordinates Q and Q′ in the ground state and excited state respectively are related by the transformation

$$Q'_x = \sum_\alpha S_{x\alpha} Q_\alpha + \delta_x$$

where the summation is carried over all coordinates of the same symmetry as Q_x. The origin displacement, δ_x, is non-zero only for totally symmetric vibration unless a change in point group symmetry occurs upon excitation. In the case of TMCBD, where the symmetry changes from D_{2h} to C_{2v} upon excitation, the δ_x should not be neglected. This effect can modify the predicted ratio of two vibronically induced intensities so that the mirror image relationship between absorption and fluorescence is destroyed (44). Additionally, this effect makes the absorption spectra much more complicated than the fluorescence spectra of TMCBD because the rotation of the normal coordinates in the excited state can make more vibronic transitions allowed in the excited state than in the ground state. To better understand the differences in appearance between the absorption spectra and fluorescence emission spectra, more information on the potential wells of the ground state as well as the excited state are required. Furthermore, a gas state experiment for the fluorescence emission with high resolution (e.g., supersonic jet experiment) will give a better understanding the structure of the ground state of TMCBD as well as the mechanism of mode mixing.

CONCLUSION

The S_1 (A_u) ↮ S_0 (A_g) transition is forbidden in the electronic dipole selection rules and the magnetic dipole selection rules, but the (0-0) transition band shows moderate intensity in the z-polarized absorption spectrum in (001) crystal face via a crystal site group effect in the distorted symmetry (C_{2v}) from the D_{2h} symmetry upon excitation. Twenty Herzberg-Teller vibronic origins are identified in the absorption spectra and the symmetry assignments of these vibronic origins are made. Twenty vibronic origins, which are more resolved vibronic origins than the previous two studies (19,20), were resolved probably due to the high resolution experimental setup and the low temperature. However, only three vibronic origins are observed in the fluorescence emission spectra. This difference between vibronic activities of the ground state and the excited state is interpreted as a result of the Duschinsky effect caused by the rotation of the normal coordinate upon excitation.

All of the vibronic origins form progression with several modes. The 306 cm^{-1} mode (b_{1u}), the 523 cm^{-1} mode (a_g), and the 517 cm^{-1} mode (a_g) are prominent in the excited state, and the 290 cm^{-1} mode (b_{1u}) and 970 cm^{-1} mode (b_{3u}) are prominent in the ground state. The 306 cm^{-1} progression forming mode is assigned as a out-of-plane B_{1u} carbonyl wagging mode based on results of the polarized far infrared study and this mode is correlated with the 287 cm^{-1} mode (measured as 290 cm^{-1} in the fluorescence emission spectra) in the ground state. The 517 cm^{-1} progression forming mode in the absorption spectra, which is not

observed in the previous two low temperature absorption studies (19,20), is assigned as a totally symmetric mode under the C_{2v} point symmetry group as well as under the D_{2h} point group. Although it is difficult to correlate the 517 cm^{-1} mode with any fundamental in the ground state, this mode is tentatively correlated with the 402 cm^{-1} mode in the ground state. The observation of a long progression by the non-totally symmetric modes are interpreted as an indication of the geometrical structure change upon excitation. Although there have been several suggestions about the geometry of TMCBD in the excited state, the present study confirms that the geometrical structure of TMCBD in the excited state is a boat form with C_{2v} symmetry.

Intense features in the vicinity 3000 cm^{-1} higher in energy from the $S_1 \leftarrow S_0$ origin observed in the absorption spectra are assigned as C-H stretching vibrations, not a new excited electronic state, since the progression forming modes (the 517 cm^{-} mode, 523 cm^{-1} mode and the 306 cm^{-1} mode) are the same in this frequency region as those of the lower energy region. Additionally, the observation of the C-H stretching mode at 2981 cm^{-1} in the fluorescence spectra confirms this assignment. The broad and intense feature underneath the C-H stretching vibrations observed in the z-polarized absorption spectrum of (001) crystal face (Fig. 5) is understood as an absorption of a possible photoproduct of TMCBD, i.e., dimethyl ketene or tetramethyl cyclopropanone.

Although the difference in vibronic activities between the ground state and the excited state is understood as a result of Duschinsky effect, ab initio calculations for the potential surface of the excited state as well as the ground state and the polarized infrared studies on

TMCBD-h_{12} and TMCBD-d_{12} should be performed to understand better the exact cause of the difference in the vibronic activity upon excitation. Furthermore, the polarized infrared study on TMCBD and its deuterated molecule (TMCBD-d_{12}) is desired to make more accurate assignment on the vibronic origins.

REFERENCES

1. E. M. Kosower, J. Chem. Phys. 38, 2813 (1963).
2. D. C. Moule, Can. J. Phys. 47, 1235 (1969).
3. R. F. Witlock and A. B. F. Duncan, J. Chem. Phys. 55, 218 (1971).
4. H. E. Howard-Lock and G. W. King, J. Mol. Spectrosc. 36,53 (1970).
5. W. D. Chandler and L. J. Goodman, J. Mol. Spectrosc. 35, 232 (1970).
6. M. Baba and I. Hanazaki, J. Chem. Phys. 81, 5426 (1984).
7. G. W. Suter, Urs. P. Wild, and K. Shaffner, J. Phys. Chem. 90, 2358 (1986).
8. M. Baba, J. Chem. Phys. 83, 3318 (1985).
9. D. C. Moule and A. D. Walsh, Chem. Rev. 75, 67 (1975).
10. T. M. Dunn and A. H. Francis, J. Mol. Spectrosc. 50, 14 (1974).
11. J. Goodman and L. E. Brus, J. Chem. Phys. 69, 1064 (1978).
12. E. P. Peyroula and R. Jost, J. Mol. Spectrosc. 121, 177 (1987).
13. G. TerHorst and J. Kommandeur, Chem. Phys. 44, 287 (1979).
14. D. J. Pasto, D. M. Chipman, and N. Z. Huang, J. Chem. Phys. 86, 3990 (1982).
15. R. D. Gordon, J. Phys. Chem. 86, 4525 (1982).
16. H. Veenvlift and D. A. Wiersma, Chem. Phys. 2, 69 (1973).
17. R. E. Ballard and C. H. Park, Spectrochim. Acta 26A, 43 (1970).
18. J. P. Byrne and I. G. Ross, Aust. J. Chem. 24, 1107 (1971).
19. R. Spafford, J. Baiardo, J. Wrobel, and M. Vala, J. Am. Chem. Soc. 98, 5217 (1976).
20. R. D. Gordon, M. Caris, and D. G. Newman, J. Mol. Spectrosc. 60, 130 (1976).

21. J. R. Swenson and R. Hoffman, Helv. Chim. Acta 53, 2331 (1970).

22. D. O. Cowan, R. Gleiter, J. A. Hashmall, E. Heilbronner, and V. Hornung, Angew. Chem. internat. Edit. 10, 401 (1971).

23. R. Spafford, J. Baiardo, J. Wrobel, and M. Vala, J. Am. Chem. Soc. 98, 5225 (1976).

24. D. J. Fasto, D. M. Chipman, and N. Z. Huang, J. Phys. Chem. 86, 3990 (1982).

25. F. O. Nicolaisen, O. F. Nielsen, and M. Vala, J. Mol. Struct. 13, 349 (1972).

26. H. F. Shurvell, R. D. Gordon, R. H. Hester, and R. B. Girling, Spectrochim. Acta 40A, 615 (1984).

27. P. H. Friedlander and J. M. Robertson, J. Chem. Soc. 3083 (1956).

28. M. C. Riche and M. M. Janot, C. R. Acad. Sci. Paris Ser. C. 275, 543 (1972).

29. C. D. Shirrell and D. E. Williams, Acta Cryst. B30, 245 (1974).

30. G. Fisher, Vibronic Coupling (Academic Press, London, 1984).

31. G. Herzberg and E. Z. Teller, Z. Phys. Chem.(Leipz.) 21, 410 (1933).

32. G. Orlandi and W. Siebrand, J. Chem. Phys. 58, 4513 (1973).

33. A. C. Albrecht, J. Chem. Phys. 33, 156 (1960).

34. P. A. Geldof, R. P. H. Rettschnick, and G. J. Hoytink, Chem. Phys. Lett. 10, 549 (1971).

35. T. Azumi and K. Matsuzaki, Photochem. Photobiol. 25, 315 (1977).

36. M. Vala, J. Wrobel, and R. Spafford, Mol. Phys. 27, 1241 (1974).

37. M. Vala and R. Spafford, J. Photochem. 8, 61 (1978).

38. I. Heller and R. Srinivasan, J. Am. Chem. Soc. 87, 1144 (1965).

39. P. A. Leemakers, G. F. Vesley, N. J. Turro, and D. C. Neckers, J. Am. Chem. Soc. 86, 4213 (1964).

40. R. A. Holroyd and F. E. Blacet, J. Am. Chem. Soc. 79, 4830 (1957).

41. R. C. Miller and E. K. C. Lee, Chem. Phys. Lett. 33, 104 (1975).

42. J. B. Coon, N. W. Naugle, and R. D. Mckenzie, J. Mol. Spectrosc. 20, 107 (1966).

43. F. Duschinsky, Acta Physicochim. 7, 551 (1937).

44. J. A. Warren, Ph.D. Dissertation, Iowa State University, 1985.

45. F. Metz, M. J. Robey, E. W. Schlag, and F. Dorr, Chem. Phys. Lett. 51, 8 (1977).

46. B. Sharf and B. Hornig, Chem. Phys. lett. 7, 132 (1970).

47. G. J. Small, J. Chem. Phys. 54, 3300 (1971).

48. J. A. Warren, J. M. Hayes, and G. J. Small, Chem. Phys. 102, 313 (1986).

SUMMRY AND CONCLUSION

It has been shown, so far, in this dissertation that electronic spectroscopy is a desirable spectroscopic method for the study on vibronic structures of the excited state as well as ground state of polyatomic molecules. The spectra obtained by laser induced fluorescence (LIF) are well resolved, and therefore, they provide rich information on the vibronic structures of the excited state. Although dispersed fluorescence spectra of some p-alkyl substituted phenols are not well resolved, some necessary information on the ground state are observed. The observation of isomers for p-alkyl substituted phenols in these studies assures that electronic spectroscopy can be used as a method of detecting isomers. The observation of hydrogen bonded species in the fluorescence excitation spectra is another example of potential application of electronic spectroscopy for the study of hydrogen bonds.

The single crystal polarized absorption studies and fluorescence studies on TMCBD at low temperature provided high resolution spectra with many vibronic bands. This information on TMCBD can not be obtained by a gas phase experiment or by a solution phase experiment with high resolution at the present stage. Therefore, if the gas or solution phase electronic spectroscopy does not give enough information, the single crystal spectroscopy can be used as a primary or a complementary methods for the study of electronic energy structures in polyatomic molecules. Additionally, the polarized study provided a firm symmetry assignment of the vibrational modes in the excited state.

Future work

The electronic spectroscopy in a supersonic jet on large molecules such as chlorophyll, proteins, and amino acids, is an active project and will become more active project in the near future, if laser desorption techniques can be utilized to vaporize large samples. In particular, studies on the electronic structure and conformational isomers of tyrosine are hoped to do. These experiments will provide more information on the vibrational structures and electronic structures of large molecules without the interferences from solvents or matrices.

The application of the supersonic jet spectroscopy on TMCBD has not succeeded at the present time. However, it will be possible to get information on this molecule in the gas phase with high resolution, if the two color multiphoton ionization spectroscopy in a supersonic jet is used. This two color experiment was to be performed by using outputs of the Nd:YAG pumped dye laser and the ArF excimer laser. However, time synchronization of these two lasers and the pulse of the molecular beam from the pulsed valve was difficult due to the drift and zitter of both lasers. If the time synchronization problem can be solved, the photoionization of TMCBD can be accomplished with two lasers. If this experiment is successful, other di-carbonyl or mono-carbonyl molecules can be studied and more information on the vibronic structures and the photochemistry of these molecules will be obtained.

Phosphorescence is another method useful for studying low fluorescent carbonyl compounds, e.g., TMCBD, in the gas phase. Several studies on low fluorescent polyatomic molecules by sensitized

phosphorescence technique in a supersonic jet have been reported (22,23). Therefore, if these techniques (two color multiphoton ionization and sensitized phosphorescence) can be utilized, non-fluorescent or merely fluorescent carbonyl $n\pi^*$ transitions can be studied in the gas phase with high resolution and without solvent or matrix effect.

REFERENCES FOR GENERAL INTRODUCTION

1. J. M. Hayes and G. J. Small, Anal. Chem. 55, 565A (1983).
2. A. Kantrowitz and J. Grey, Rev. Sci. Instrum. 22, 328 (1951).
3. G. B. Kiastakowsky and W. P. Slichter, Rev. Sci. Instrum. 22, 333 (1951).
4. R. E. Smalley, B. L. Ramakrishna, D. H. Levy, and L. J. Wharton, J. Chem. Phys. 61, 4363 (1974).
5. D. V. Brumbaugh, J. E. Kenney, and D. H. Levy, J. Chem. Phys. 78, 3415 (1983).
6. Y. Sugahara, N. Mikami, and M. Ito, J. Phys. Chem. 90, 5619 (1986).
7. T. R. Rizzo, Y. D. Park, and D. H. Levy, J. Chem. Phys. 85, 6945 (1986).
8. Y. D. Park, T. R. Rizzo, L. A. Peteanu, and D. H. Levy, J. Chem. Phys. 84, 6539 (1986).
9. J. Grotemeter, U. Bosel, K. Walter, and E. W. Schlag, J. Am. Chem. Soc. 108, 4233 (1986).
10. H. V. Weyssenhoff, H. L. Selzle, and E. W. Schlag, Z. Naturforsch, 409, 674 (1985).
11. J. A. Warren, J. M. Hayes, and G. J. Small, Chem. Phys. 102, 313 (1986).
12. J. A. Warren, J. M. Hayes, and G. J. Small, Chem. Phys. 102, 323 (1986).
13. J. B. Hopkins, D. E. Powers, and R. E. Smalley, J. Chem. Phys. 72, 5039 (1980).

14. R. Tembreull, T. M. Dunn, and D. M. Lubman, Spectrochim. Acta 42A, 899 (1986).

15. M. Fujii, T. Kakinuma, N. Mikami, and M. Ito, Chem. Phys. Lett. 127, 303 (1986).

16. J. W. Hager, D. R. Demmer, and S. C. Wallace, J. Phys. Chem. 91, 1375 (1987).

17. R. Tembreull and D. M. Lubman, Anal. Chem. 59, 1003 (1987).

18. R. Tembreull and D. M. Lubman, Anal. Chem. 59, 1082 (1987).

19. D. Dogherty, P. Brint, and S. P. McGlynn, J. Am. Chem. Soc. 100, 5597 (1978).

20. R. D. Gordon, M. Caris, and D. G. Newman, J. Mol. Spectrosc. 60, 130 (1976).

21. R. Spafford, J. Baiardo, J. Wrobel, and M. Vala, J. Am. Chem. Soc. 98, 5217 (1976) ; J. Am. Chem. Soc. 98, 5225 (1976).

22. A. Goto, M. Fujii, N. Mikami, and M. Ito, J. Phys. Chem. 90, 2370 (1986).

23. S. Kamei, S. Tatsuya, N. Mikami, and M. Ito, J. Phys. Chem. 90, 5615 (1986).

ACKNOWLEDGEMENT

I would like to express my thanks to a number of peoples who aided me in the performance of various stage of this research. I am particularly grateful to my research advisor, professor Gerald J. Small, for his expert guidance throughout this research. The work described in this thesis could not have been completed without his helpful advice, his clear insight in the field, and patient discussions.

I am greatly indebted to Dr. John M. Hayes for his valuable advice and guidance in the experimental procedures as well as data analysis. I also owe thanks to other members of the group, particularly Dan Zamzow, Kevin Gillie, and Dr. R. Scott Cooper who helped me in the laboratory. An additional thanks to Dr. John M. Hayes, Dr. R. Scott Cooper, and Kevin Gillie who helped me in the proofreading this thesis.

I would also like to offer my thanks to Mike Kenney, Bryan Isaac, Steve Johnson, Dr. Ryszard Jankowiak, Deming Tang, and In-Ja Lee for their friendship during my graduate study.

Additionally, I would like to thank Iowa State University and the Ames Laboratory-USDOE for funding and support during this work.

More importantly, I would like to sincerely thank to my parents, Seok-Hoon and Nap-Heui, for their encouragement and financial support throughout my education. I would also like to thank to my sons, Tae-yeon and Tae-yun, who have brought me many happy times.

Finally, my sincere thanks and love to my wife, Sookja, for the encouragement, support, her patience, and, most of all, her love.

APPENDIX

The following figures are unpolarized single crystal absorption spectra of TMCBD in three different crystal faces [(001), (010), (110)] and polarized absorption spectra of TMCBD in (010) and (110) crystal faces. The polarized absorption spectra are the x-and y-polarized absorption spectra in (010) crystal face and parallel and perpendicular polarized spectra of (110) crystal face of TMCBD.

Figure 10. Unpolarized single crystal absorption spectrum of TMCBD in the (001) crystal face. Sample temperature is 4.2 K. Resolution is 1.1 cm^{-1}

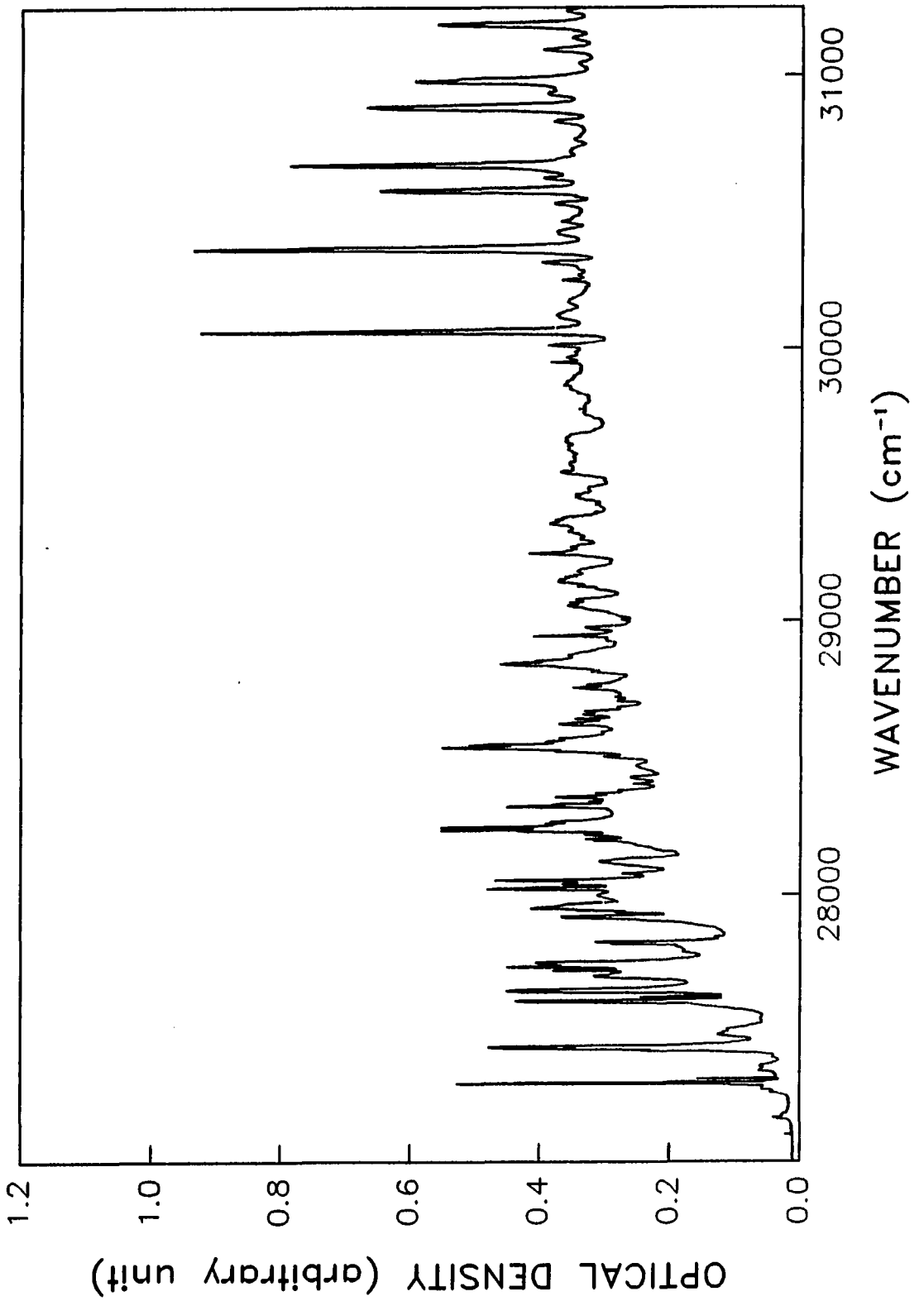
OPTICAL DENSITY (arbitrary unit)
1.2
1.0
0.8
0.6
0.4
0.2
0.0
28000
29000
30000
31000
WAVENUMBER (cm⁻¹)

Figure 11. x-polarized single crystal absorption spectrum of TMCBD in the (010) crystal face. Sample temperature is 4.2 K. Resolution is 1.1 cm^{-1}

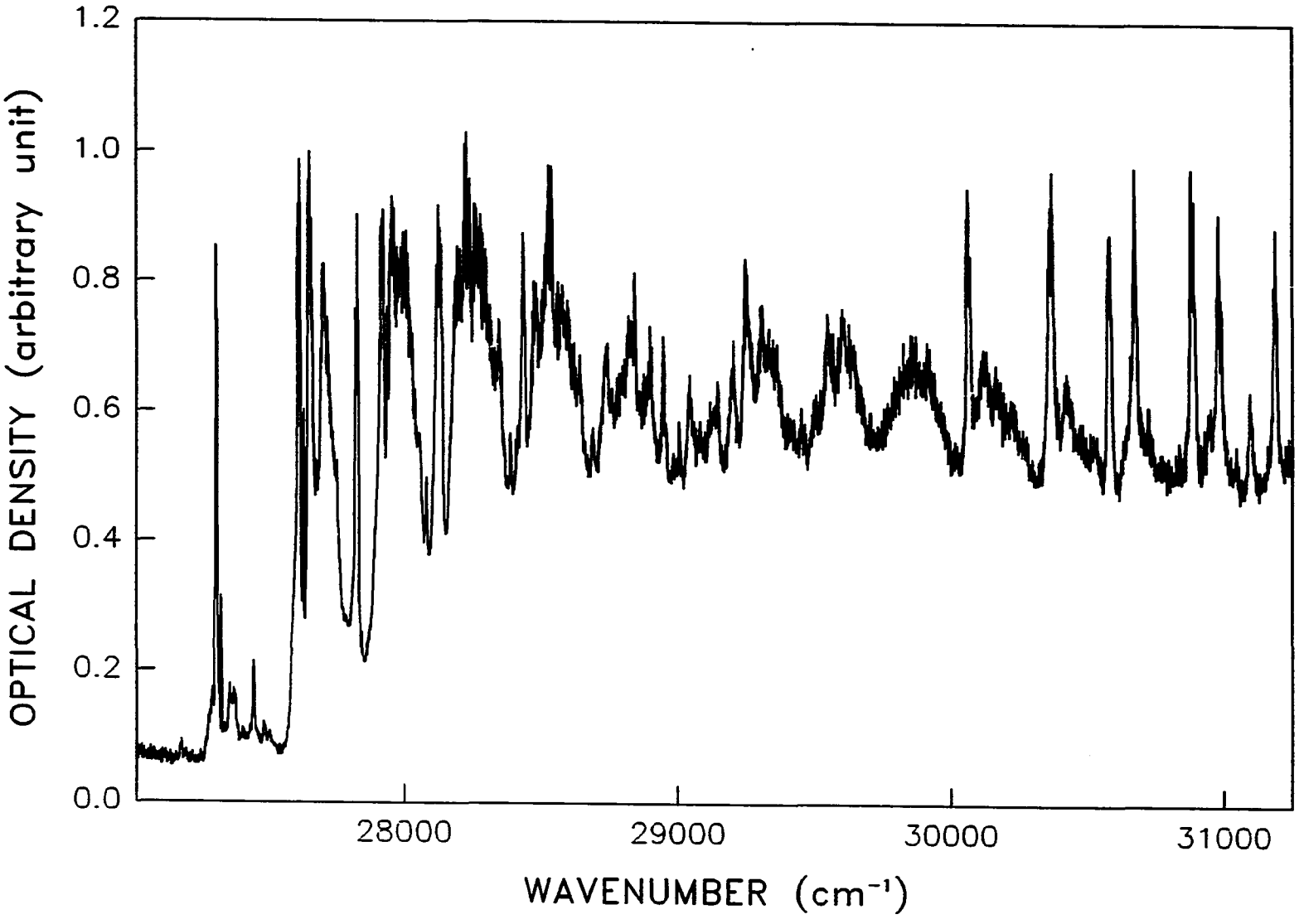
OPTICAL DENSITY (arbitrary unit)
1.2
1.0
0.8
0.6
0.4
0.2
0.0
28000
29000
30000
31000
WAVENUMBER (cm⁻¹)

Figure 12. y-polarized single crystal absorption spectrum of TMCBD in the (010) crystal face. Sample temperature is 4.2 K. Resolution is 1.1 cm^{-1}

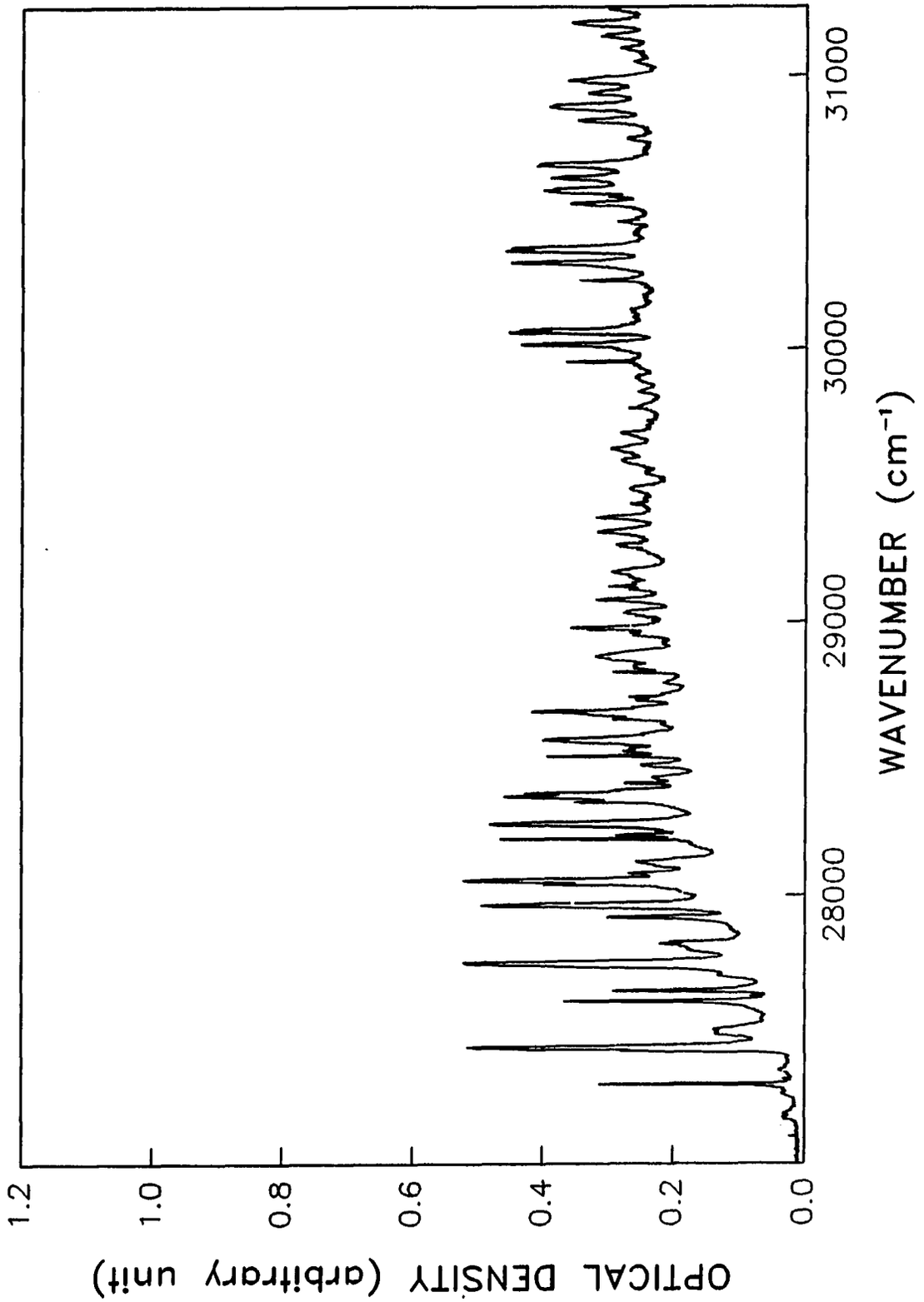
OPTICAL DENSITY (arbitrary unit)
1.2
1.0
0.8
0.6
0.4
0.2
0.0
28000
29000
30000
31000
WAVENUMBER (cm⁻¹)

Figure 13. Unpolarized single crystal absorption spectrum of TMCBD in the (010) crystal face. Sample temperature is 4.2 K. Resolution is 1.1 cm^{-1}

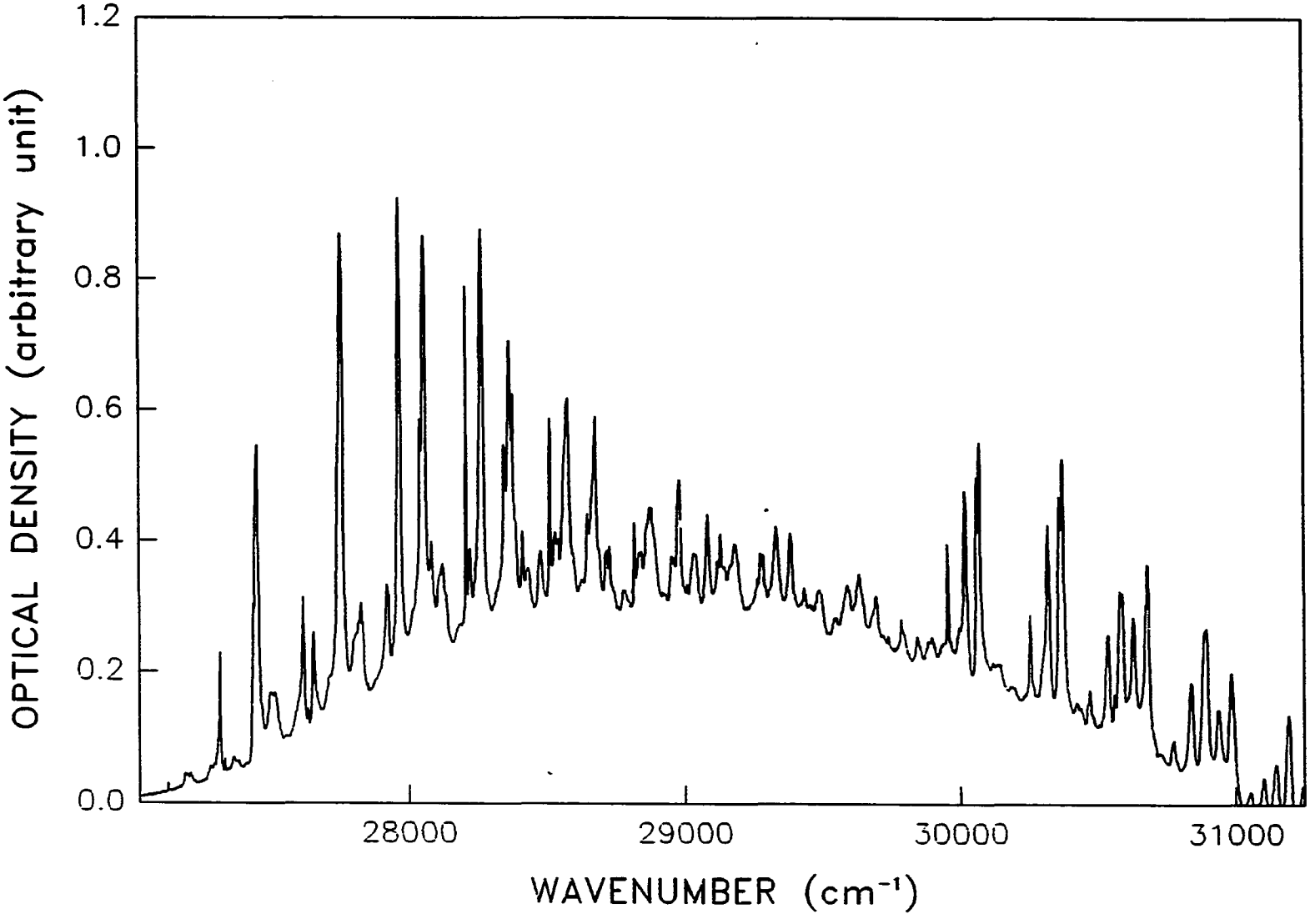
OPTICAL DENSITY (arbitrary unit)
1.2
1.0
0.8
0.6
0.4
0.2
0.0
28000
29000
30000
31000
WAVENUMBER (cm⁻¹)

Figure 14. Parallel polarized to the extinction direction single crystal absorption spectrum of TMCBD in the (110) crystal face. Sample temperature is 4.2 K. Resolution is 1.1 cm^{-1}

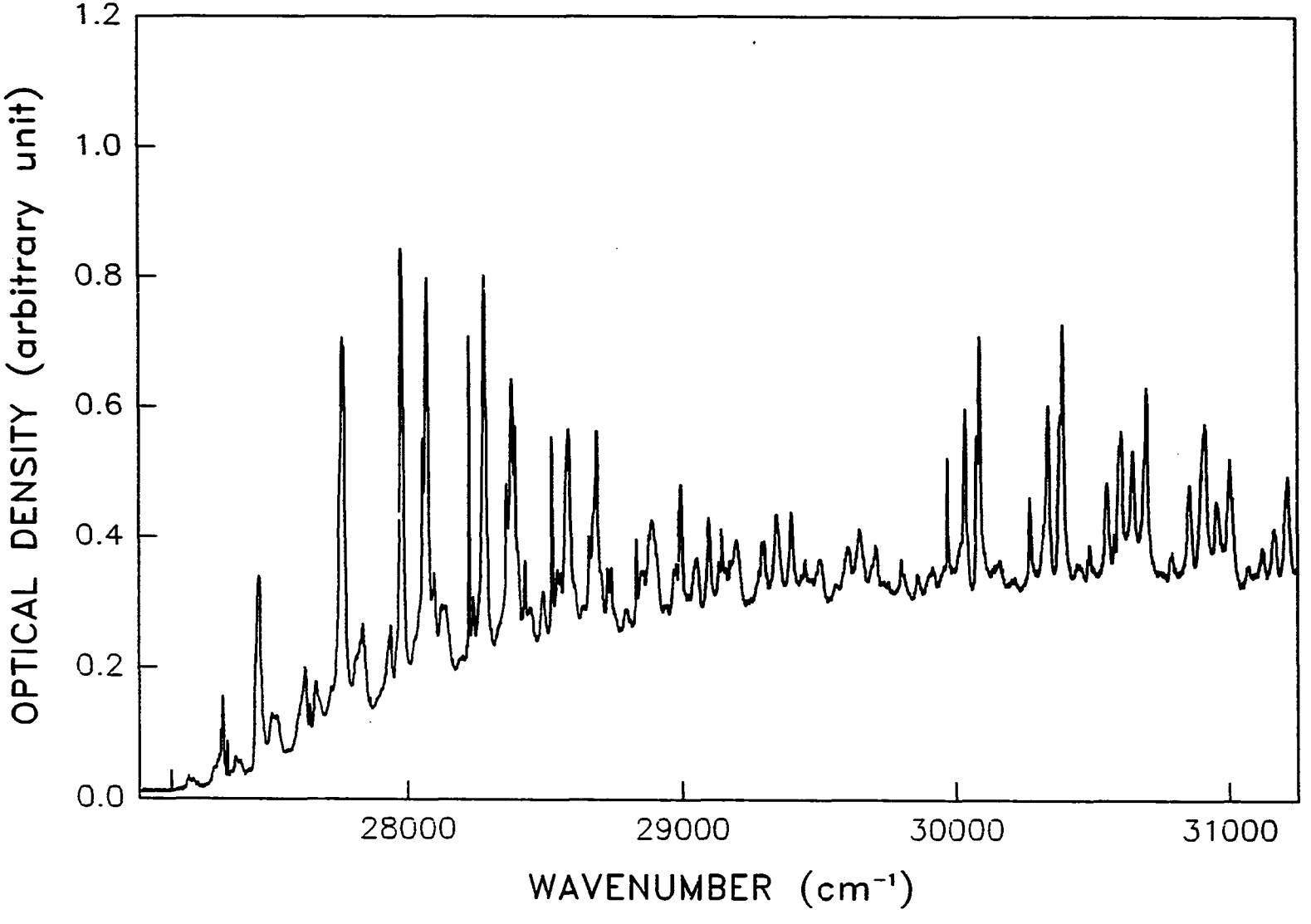
OPTICAL DENSITY (arbitrary unit)
1.2
1.0
0.8
0.6
0.4
0.2
0.0
28000
29000
30000
31000
WAVENUMBER (cm⁻¹)

Figure 15. Perpendicular polarized to the extinction direction single crystal absorption spectrum of TMCBD in the (110) crystal face. Sample temperature is 4.2 K. Resolution is 1.1 cm^{-1}

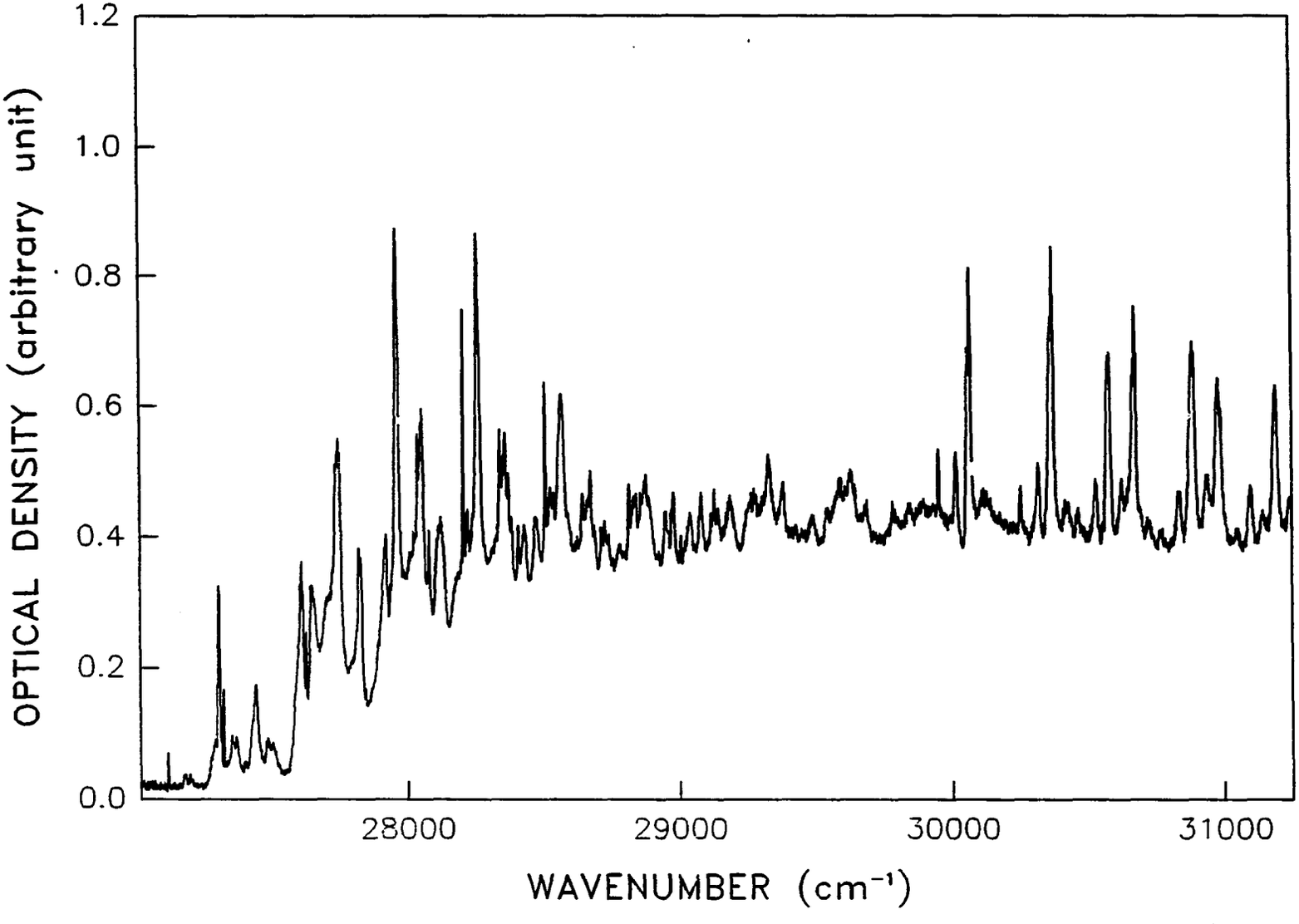
OPTICAL DENSITY (arbitrary unit)
1.2
1.0
0.8
0.6
0.4
0.2
0.0
28000
29000
30000
31000
WAVENUMBER (cm⁻¹)

Figure 16. Unpolarized single crystal absorption spectrum of TMCBD in the (110) crystal face. Sample temperature is 4.2 K. Resolution is 1.1 cm^{-1}

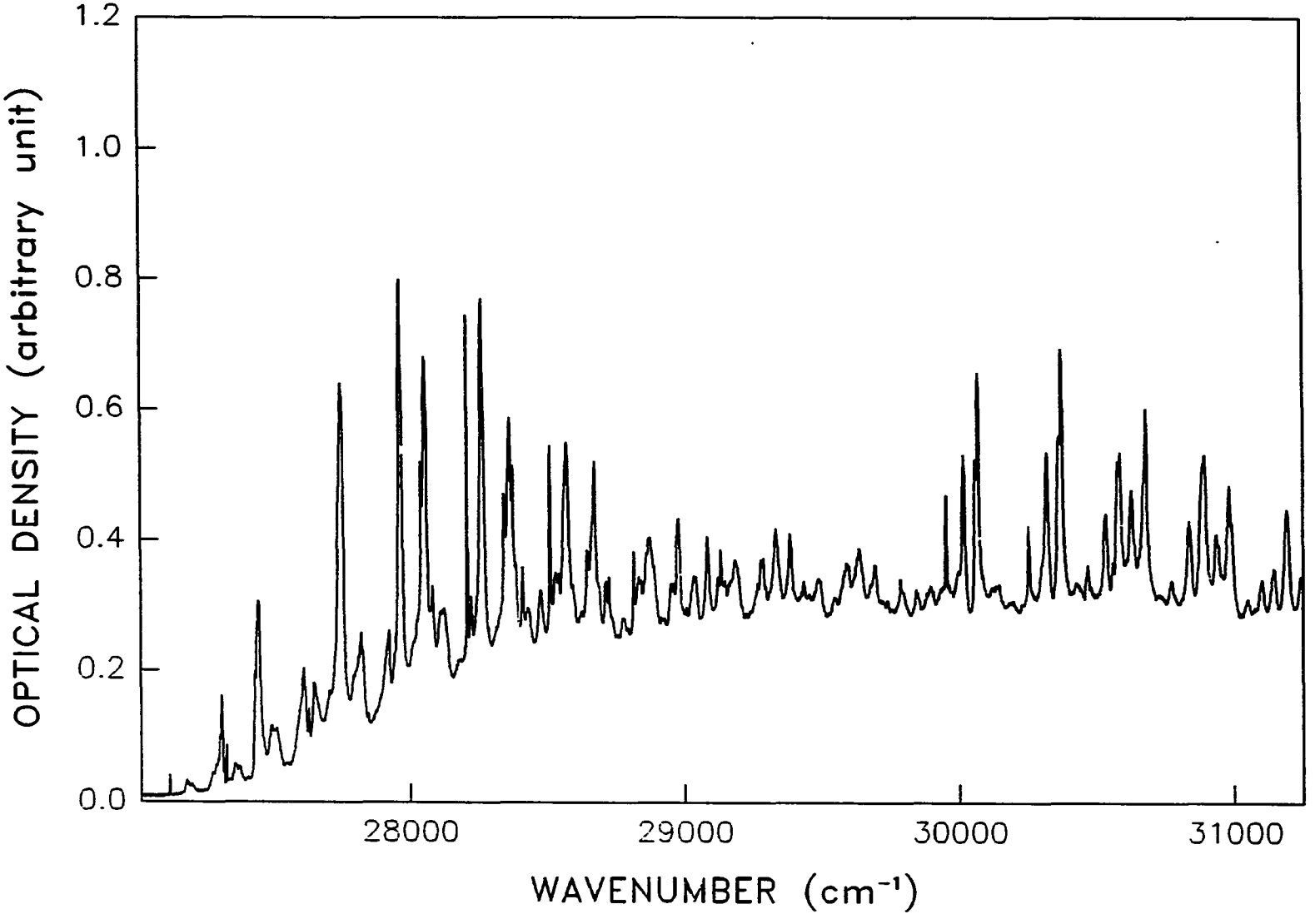
OPTICAL DENSITY (arbitrary unit)
1.2
1.0
0.8
0.6
0.4
0.2
0.0
28000
29000
30000
31000
WAVENUMBER (cm⁻¹)